

---

# SPR 755 – Investigation and Assessment of Effective Patching Materials for Concrete Bridge Decks

---

*Sponsoring Agencies:*

South Carolina Department of Transportation



Federal Highway Administration



*Principal Investigators:*

Dr. Prasad Rangaraju  
Glenn Department of Civil Engineering  
Clemson University

April 2025

1. Report No. FHWA-SC-25-01	2. Government Accession No.	3. Recipient's Catalog No.	
4. Title and Subtitle <i>Investigation and Assessment of Effective Patching Materials for Concrete Bridge Decks</i>		5. Report Date <i>April 2025</i>	
		6. Performing Organization Code	
7. Author(s) <i>Prasad Rangaraju</i>		8. Performing Organization Report No.	
9. Performing Organization Name and Address <i>Clemson University 306 South Palmetto Blvd. Clemson, SC, 29634-0911</i>		10. Work Unit No. (TRAIS)	
		11. Contract or Grant No. <i>SPR No. 755</i>	
12. Sponsoring Agency Name and Address <i>South Carolina Department of Transportation PO Box 191 Columbia, SC 29202-0191</i>		13. Type of Report and Period Covered <i>Draft Final Report Sept 1 2020 – Dec 31, 2023</i>	
		14. Sponsoring Agency Code	
15. Supplementary Notes <i>Mr. James Roberts (Graduate Student), Mr. Adam Biehl (Graduate Student), Dr. Mohannad Naser (Co-PI)</i>			
16. Abstract <i>Periodic maintenance of bridge decks through patching repairs is an essential strategy to maintain an effective transportation network. However, poor performance of patched sections needs to be studied to develop appropriate material selection methodology and proper construction practices to achieve durable repairs. The principal objective of this study was to evaluate a range of cementitious rapid-set patching materials for use as repair materials on bridge decks and develop a set of criteria to allow for selection of appropriate repair materials depending on environmental exposure conditions and compatibility with substrate concrete. For this purpose, a set of representative rapid-set patching materials based on different active binder chemistries were selected. Their hydration behavior along with mechanical and transport properties were evaluated across a range of environmental exposure conditions. In addition, the impact of surface preparation of the substrate concrete on the bond with the repair material, and the impact of vibration on the bond of repair material with substrate were also planned in this investigation. However, these studies could not be completed due to difficulty in securing field test sites in a timely manner. The principal findings from this study suggest that the success of achieving an effective repair with prebagged repair materials and plant-batched repair mixtures depend on key factors such as the sensitivity of repair materials performance to ambient temperature and quality of substrate surface in terms of texture and moisture saturation level.</i>			
17. Key Word <i>Rapid Set Patching Materials, Bond Strength, Compatibility of Materials, Shrinkage, Surface Preparation</i>		18. Distribution Statement <i>No restrictions.</i>	
19. Security Classif. (of this report)  Unclassified.	20. Security Classif. (of this page)  Unclassified.	21. No. of Pages  96	22. Price

## Disclaimer

---

The contents of this report reflect the views of the author who is responsible for the facts and the accuracy of the data presented. The contents do not necessarily reflect the official views of the South Carolina Department of Transportation or Federal Highway Administration. This report does not constitute a standard, specification, or regulation.

The State of South Carolina and the United States Government do not endorse products or manufacturers. Trade or manufacturer's names appear herein solely because they are considered essential to the object of this report.

## Acknowledgments

---

The research conducted for this report was funded by the South Carolina Department of Transportation (SCDOT) under SPR Project No. 755. We express thanks to the steering committee members including Mr. David Rogers (Chair), Mr. Merrill Zwanka, Mr. Caleb Gunter, Ms. Temple Short, Mr. Rodrick Tucker, Mr. Blake Gerken (FHWA), Mr. Daniel Cook, Mr. Sean Futch and Mr. Terry Swygert. Furthermore, support for analytical testing provided by National Brick Research Center is appreciated. Also, thanks are expressed to material suppliers who provided the Portland cement, rapid set patching materials and chemical admixtures needed for this study.



## Executive Summary

---

As the transportation infrastructure in the US continues to age and deteriorate over time, the need for timely maintenance to properly rehabilitate and extend the design service life of these structures is growing [1,2]. Currently, the South Carolina Department of Transportation (SCDOT) specifies the use of plant-produced ready-mix concrete for large bridge-deck patching projects. However, this is not always practical, especially in jobs that do not require large amounts of patching or in situations where patching of deteriorated portions of concrete bridge decks must be conducted in a rapid manner to maintain the serviceability. In this regard, the use of pre-bagged, rapid set patching materials that are amenable to on-site batching and mixing with excellent bond characteristics and accelerated cure rates are desirable. While the development of a qualified set of alternate repair materials is essential, it is also important to develop a process to select these rapid set patching materials, based on the nature of the distress and the ability of the patching materials to adequately meet the requirements under ambient environmental conditions.

There are currently numerous pre-bagged repair materials that are readily available on the market. Many of these materials are specially designed to achieve high performance and exhibit various attributes intended for specific applications. However, the material components are often proprietary in nature, and the performance specifications provided are often based on controlled lab settings, restricting the knowledge of how these different materials will perform in any given application with different exposure conditions. Additionally, engineers are often forced to make cost-efficient decisions without the proper insight into the makeup of these materials; or how the performance of the repair material will be affected by the environment; and their compatibility performance as a composite material with existing substrate concrete mixes. All these factors likely affect the overall performance and longevity of the patching repairs and can ultimately be the cause of rapid deterioration before the repair has met its intended design service life. Considering these concerns, the focus of the present study was to evaluate the performance of selected bagged rapid set patching materials (RSPMs) and plant-batched concrete mixtures in a range of environmental conditions.

In this investigation a total of 9 different bagged rapid-set patching repair materials were selected. Of these five products were based on formulations where Portland cement was used with other admixtures (PC1 through PC5). The remainder of the products consisted of patching materials with calcium aluminate cements (CAC), calcium sulfo-aluminate cements (CSA) and magnesium oxide-based cements (MgO).

For larger repair projects that require large volumes of repair materials, plant-batched Portland cement concrete mixtures are employed. Often, these concrete mixtures contain a range of chemical admixtures such as set-accelerators, high-range water reducers, shrinkage reducing admixtures, air-entraining admixtures and others to positively affect the flow, setting, early-age strength gain, shrinkage and other behaviors. However, the durability performance of these

concrete mixtures as repair and overlay materials has been questioned due to premature failures observed on some projects (Personal Communication – David Rogers, SCDOT). In this investigation plant-based patching mixtures prepared with Portland cement in combination with different set-accelerators were investigated. These set-accelerators compositions captured several chloride and non-chloride-based accelerators as well as nucleation-based accelerators, referred to as physical accelerators in this study. The impact of these set-accelerators at low- and high-dosages on the performance of patching mixtures was investigated at a range of temperatures. In addition, the impact of these set-accelerators on the performance of patching mixtures prepared with both Type III and Type/II Portland cements were investigated.

Compatibility of properties between repair materials and substrate concrete is essential for a durable repair [3]. However, a mismatch of mechanical and electro-chemical performance properties between the repair materials and substrate concrete can directly contribute to accelerated damage of the patched area [4]. Properties such as compressive, flexural, tensile, and bond strength, elastic and shear moduli, Poisson's ratio, coefficient of thermal expansion, chloride migration resistance and electrical resistivity, all of which are important in assuring a durable repair were studied in this research [5–7]. In addition, the hydration behavior of repair materials (using isothermal calorimetry) and their stiffening/hardening behavior (Vicat needle penetration and ultrasonic pulse velocity testing) at early ages, and compressive strength of these materials across a range of ambient temperatures (10°C, 23°C and 40°C) were investigated. The specific test temperatures were selected to simulate ambient temperatures at different times of the year and its impact on the performance of the repair materials.

Results from this in-depth study show that the performance of both bagged and plant-based patching mixtures depended on several factors at the time of mixing and placement, as well as on quality of surface preparation of the patching area.

Experimental testing on bagged Rapid-Set Patching Materials (RSPMs) yielded several conclusions about their effectiveness and usability:

- **Binder performance:** The chemistry of the binders, i.e., whether they are based on PC, CSA, CAC-or MgO affected their hydration behavior and their sensitivity to environmental factors such as temperature. While PC, CSA and CAC-based repair materials showed comparable performance across various tests, MgO-based RSPM showed slower early-age reactions requiring closer monitoring.
- **Temperature sensitivity:** Setting time and compressive strength of different RSPMs were highly affected by ambient environmental conditions, i.e. temperature, with significant variability in some RSPMs across the temperatures investigated, i.e., 10°C, 23°C and 40°C.
- **Bond strength:** The moisture condition of substrate concrete affected the bond behavior of RSPMs depending on which test method was employed. Use of substrate concrete in dry condition showed better bond performance of RSPMs in slant-shear test, while

saturated surface-dry condition of substrate concrete yielded better bond performance in pull-off test method.

- **Shrinkage:** Several RSPMs showed early-age shrinkage exceeding tensile strain capacity, showing tendency to crack, and this behavior was further affected by the ambient temperature.
- **Durability:** RSPMs generally demonstrated mechanical compatibility with substrate concrete. Surface and bulk electrical resistivity and chloride migration testing showed good to moderate correlation, however, the results depended on specific RSPMs. Also, compared to substrate concrete, the transport properties of RSPMs varied widely suggesting potential to impact long-term durability through microcell corrosion
- **Pulse velocity:** Ultimate pulse velocity remains unaffected by accelerators, but higher dosages significantly influence post-dormant velocity changes.

The following conclusions about the effectiveness and usability of accelerated plant-based concrete mixtures are drawn from experimental testing conducted:

- **Setting time:** Both chemical and physical set accelerators reduce setting time for Type I/II and Type III cements, with greater acceleration observed in Type I/II cements.
- **Water-to-cement ratio:** Higher ratios (0.42) enhance the effectiveness of set accelerators, while lower ratios (0.33) reduce their impact.
- **Heat flow:** Higher accelerator dosages boost heat flow during the acceleration phase but show limited impact on final hydration heat.
- **Dormant period:** Chemical accelerators decrease or maintain dormant periods, whereas physical accelerators increase or maintain them depending on specific composition.
- **Pulse velocity:** Ultimate pulse velocity remains unaffected by accelerators, but higher dosages significantly influence post-dormant velocity changes.
- **Compressive strength:** Minimal impact at low temperatures; increased strength at higher temperatures.
- **Restrained shrinkage:** Accelerators shorten the time to crack and reduce tensile strain capacity, heightening the risk of cracking in patched sections. Results indicate that the use of the set accelerators, while accelerating the rate of reaction, do not accelerate the rate of tensile strain capacity gain, thus resulting in earlier failures. This is further supported by the fact that the heat of hydration at the time to cracking was comparable across all accelerators and the control specimens.
- **Temperature effects on shrinkage:** At low temperatures, cracking is delayed for chemical accelerators and significantly delayed for physical accelerators.

The main conclusions from this study indicate that ambient temperature can have a significant impact on setting and hardening behavior at early ages, which in turn can have a profound impact on long-term mechanical performance of patching materials. Results from Vicat needle testing and Ultrasonic pulse velocity (UPV) testing showed significant differences in setting and the

hardening behavior of patching materials as a function of temperature at the time of placement and curing. Also, high ambient temperature exposure during setting can rapidly increase the rate of exothermic heat production, but the cumulative heat produced over time can be lower indicating an overall negative effect. It was determined that use of repair materials in hot-weather applications without proper conditioning of the mix constituents can lead to rapid stiffening and result in poor consolidation, thus degrading the performance and durability of the patch. Findings from this study show a good correlation between surface resistivity of a patching material and its chloride migration coefficient while the correlation with bulk resistivity showed moderate correlation. Selected repair materials showed a vast range of electrical resistivity values, which if used in unison with a low resistivity substrate concrete could potentially result in initiation of a macro-cell corrosion of rebar and lead to deterioration in areas surrounding the patched area.

Overall, it is important to establish threshold performance criteria as a function of ambient temperature for bagged RSPMs and plant-based accelerated concrete mixtures for patching purposes. Different set accelerators can result in different performances of plant-based concrete patching mixtures and therefore appropriate selection of set accelerators for the intended repair purposed should be based on relevant properties of the concrete mixtures such as its setting time, bond strength, and heat of hydration.

# Table of Contents

---

Disclaimer.....	iii
Acknowledgments.....	iv
Executive Summary.....	v
Table of Contents.....	ix
List of Figures.....	xii
List of Tables.....	xiv
1. Introduction.....	1
2. Literature Review.....	5
2.1. Bridge Deck Deterioration Mechanisms.....	5
3. Experimental Plan.....	9
2.1. Materials.....	9
2.1.1. Portland Cement.....	9
2.1.2. Fine Aggregate.....	10
2.1.3. RSPM.....	10
2.1.4. Set Accelerators.....	10
2.1.5. Reference Substrates.....	11
2.2. Mixing Procedures.....	12
2.3. Experimental Methods.....	12
2.3.1. Setting Time.....	12
2.3.2. Isothermal Calorimetry.....	12
2.3.3. Ultrasonic-Pulse Velocity (UPV).....	13
2.3.4. Compressive Strength.....	13
2.3.5. Slant Shear Bond Strength.....	13
2.3.6. Pull-Off Bond Strength.....	13
2.3.7. Shrinkage Ring Test.....	14
2.3.8. Coefficient of Thermal Expansion (CoTE).....	14
2.3.9. Resonate Frequency.....	14
2.3.10. Surface/Bulk Resistivity.....	14
2.3.11. Chloride Migration.....	14

3.	Evaluation of RSPMs .....	15
3.1.	Objective .....	15
3.2.	The Influence of Binder Type on RSPMs Performance in Fresh and Hardened State ....	15
3.2.1.	Setting Time .....	15
3.2.2.	UPV .....	16
3.2.3.	Compressive Strength.....	18
3.2.4.	Slant-Shear Bond Strength.....	19
3.2.5.	Pull-Off Bond Strength.....	20
3.2.6.	Shrinkage Ring Test.....	21
3.2.7.	CoTE.....	22
3.2.8.	Resonate Frequency .....	22
3.2.9.	Surface/Bulk Resistivity .....	23
3.2.10.	Chloride Migration.....	24
3.3.	The Role of Environmental Temperature on the Early Age Performance of RSPMs.....	25
3.3.1.	Setting Time .....	25
3.3.2.	Isothermal Calorimetry.....	28
3.3.3.	UPV .....	30
3.3.4.	Compressive Strength.....	32
3.3.5.	Shrinkage Ring Test.....	34
4.	Evaluation of Accelerated Batched Concrete Mixtures.....	36
4.1.	Problem Statement.....	36
4.2.	Objective .....	36
4.3.	Results.....	37
4.3.1.	Setting Time .....	37
4.3.2.	Isothermal Calorimetry.....	47
4.3.3.	UPV .....	52
4.3.4.	Compressive Strength.....	56
4.3.5.	Shrinkage Ring Test.....	57
5.	Conclusions and Recommendations .....	60
5.1.	Conclusions .....	60
5.2.	Recommendations.....	62

References .....	64
Appendix A: RSPM Summary Sheets .....	66
Appendix B: Field Visits.....	77
District One – Columbia, SC .....	77
District Three – Greenville/Spartanburg.....	79
District Five – Florence/Myrtle Beach.....	82
Appendix C: Provision Specification for Qualifying Cementitious Rapid Set Patching Materials .....	85

## List of Figures

---

Figure 1: Condition of Bridges in South Carolina [9].....	2
Figure 2: South Carolina NHS bridges deck area by year built/reconstructed [9] .....	3
Figure 3: Failed patching materials on bridge deck on I-77 causing large potholes.....	4
Figure 4: Particle Size Distribution of Portland Cements and Sand.....	9
Figure 5: The Early Age UPV of PC-based RSPMs at 73 °F.....	17
Figure 6: The Early Age UPV of CAC, CSA, and MgO-based RSPMs at 73 °F.....	18
Figure 7: Compressive Strength of the RSPM at 73 °F.....	19
Figure 8: The Slant-Shear Bond Strength of RSPMs with SSD and Dry Substrates at 73 °F.....	20
Figure 9: The Pull-Off Bond Strength of RSPMs with SSD and Dry Substrates at 73 °F.....	21
Figure 10: The Coefficient of Thermal Expansion of 91-Day RSPM Samples Cured at 73 °F.....	22
Figure 11: Bulk and Surface Resistivity of 91-Day RSPMs Samples Cured at 73 °F.....	24
Figure 12: The Setting Time of PC-based RSPMs as a Function of Environmental Temperature.....	26
Figure 13: The Setting Time of CAC and CSA-based RSPMs as a Function of Environmental Temperature .....	27
Figure 14: The Setting Time of the MgO-based RSPM as a Function of Environmental Temperature.....	27
Figure 15: The Influence of Temperature on the Heat Flow of (a) PC-1, (b) PC-2, (c) PC-3, (d) PC-4, (e) PC-5, (f) CAC-1, (g) CAC-2, (h) CSA-1, (i) CSA-2, and (j) MgO-1.....	29
Figure 16: The Influence of Temperature on the Development of the Early Age Ultrasonic Pulse Velocity on (a) PC-1, (b) PC-2, (c) PC-3, (d) PC-4, (e) PC-5, (f) CAC-1, (g) CAC-2, (h) CSA-1, (i) CSA-2, and (j) MgO-1.....	31
Figure 17: Influence of Elevated Temperature on RSPM Casting.....	32
Figure 18: The Compressive Strength at 50 °F Compared to the Compressive Strength at 73 °F for RSPMs.....	33
Figure 19: The Compressive Strength at 104 °F Compared to the Compressive Strength at 73 °F for RSPMs.....	34
Figure 20: Vicat Needle Setting Time for Type I/II Cement at Normal Consistency at 73 °F .....	38
Figure 21: Vicat Needle Setting Time for Type III Cement at Normal Consistency at 73 °F.....	39
Figure 22: Influence of temperature on setting time of Type III cement at w/c = 0.33 .....	41
Figure 23: Influence of temperature on setting time of Type III cement at w/c = 0.36 .....	43
Figure 24: Influence of temperature on setting time of Type III cement at w/c = 0.42 .....	46
Figure 25: Hydration kinetics for Cl accelerator at 73 °C (w/c = 0.42).....	48
Figure 26: Hydration kinetics for NCl accelerator at 73 °C (w/c = 0.42).....	49
Figure 27: Hydration kinetics for NCl-1 accelerator at 73 °C (w/c = 0.42).....	49
Figure 28: Hydration kinetics for XS-55 accelerator at 73 °C (w/c = 0.42).....	50
Figure 29: Hydration kinetics for XS-44 accelerator at 73 °F (w/c = 0.42).....	51
Figure 30: Hydration kinetics for SU accelerator at 73 °F (w/c = 0.42).....	52
Figure 31: Ultrasonic wave velocity for different accelerators at w/c = 0.33 (73 °F).....	53
Figure 32: Ultrasonic wave velocity for different accelerators at w/c = 0.36 (73 °F).....	54
Figure 33: Ultrasonic wave velocity for different accelerators at w/c = 0.42 (73 °F).....	55
Figure 34: Ultrasonic wave velocity for different accelerators at 50 °F (w/c = 0.42).....	56
Figure 35: Compressive strength of cement pastes at a temperature of 73 °F and w/c = 0.42 (S/C=1.5) .....	57
Figure 36: Compressive strength of cement mortar at a temperature of 50 and 73 °F and w/c = 0.42 (S/C = 1.5).....	57
Figure 37: Influence of accelerator type and dosage on the restrained shrinkage and cracking time of mortar with S/C = 1.5 at 73 °F (w/c = 0.42).....	58
Figure 38: Influence of accelerator type and dosage on the restrained shrinkage and cracking time of mortar with S/C = 1.5 at 50 °F (w/c = 0.42).....	59



## Appendix B

Figure B-1: The exposed surface of deteriorating patching materials (a) patch 1 (b) patch 2 (c) patch 3 (d) patch 3 (e) patch 5 (f) patch 6.....	78
Figure B-2: (a) Bridge Substructure and Supports (b) Bridge Pavement Surface with Alligator Cracking (c) Thermal Gradient of Pavement Surface in the Morning (d) Thermal Gradient of Pavement Surface in the Evening .....	79
Figure B- 3: Pavement Surface of the Bryant Road Bridge over I-85 .....	80
Figure B-4: (a) Deteriorated Patch on I-26 over Lake Bowen (b) Thermal Imaging of Deteriorated Patch on I-26 over Lake Bowen.....	80
Figure B-5: (a) Pavement Surface on Fairforest Bridge Road (b) Side Profile of Patching (c) Thermal Imaging of Pavement Surface (d)Deteriorated Shoulder with Corrosion .....	81
Figure B-6: (a) Patched Pavement Section with Corrosion (b) Alligator Cracking along Patched Area (c) Patched Section with Corrosion Staining (d) Uneven and Cracked Patch.....	82
Figure B-7: (a) Corrosion through Pavement Surface (b) Corrosion Adjacent to Patched Section (c) Section to Expose Corroded Rebar.....	83
Figure B-8: (a) Pavement Surface of US 17 over Sampit River (b) Potential RSPM Incompatibility with Subsequent Repairs.....	84

# List of Tables

---

Table 1: Inventory of Bridge Assets in South Carolina [8].....	1
Table 2: ICRI CSP Surface Preparation Methods [17] .....	7
Table 3: Oxide Composition and Bogue's Phase Composition of Portland Cements Used .....	9
Table 4: RSPMs Sample IDs and Water Dosage Per Weight of RSPM.....	10
Table 5: Set Accelerators Physical and Chemical Properties .....	10
Table 6: Accelerator Dosages .....	11
Table 7: 5000-psi Reference Concrete Mixture Proportions.....	11
Table 8: Setting Time of the RSPMs at 73 °F.....	16
Table 9: The Time to Crack and Average Strain Rate from Restrained Shrinkage Ring Testing at 73 °F.....	21
Table 10: Results from Resonate Frequency Testing of 91-Day RSPMs Samples Cured at 73 °F.....	23
Table 11: Chloride Migration Coefficients for 91-Day RSPMs Samples Cured at 73 °F.....	25
Table 12: Time to Cracking and Strain Rate from Restrained Shrinkage Ring Testing on RSPMs at 50, 73, and 104°F .....	35
Table 13: Percentage difference in setting time and $T_i$ to $T_f$ interval with temperature change from 50 to 73 °F for Type III cement at $w/c = 0.33$ .....	41
Table 14: Percentage difference in setting time and $T_i$ to $T_f$ interval with temperature change from 50 °F to 73 °F for Type III cement at $w/c = 0.36$ .....	45
Table 15: Percentage difference in setting time and $T_i$ to $T_f$ interval with temperature change from 50 to 73 °F for Type III cement at $w/c = 0.42$ .....	47

## Appendix A

Table A-1: Framework of RSPM Summary Sheets .....	66
Table A-2: PC-1 Summary Sheet .....	67
Table A-3: PC-2 Summary Sheet .....	68
Table A-4: PC-3 Summary Sheet .....	69
Table A-5: PC-4 Summary Sheet .....	70
Table A-6: PC-5 Summary Sheet .....	71
Table A-7: CAC-1 Summary Sheet.....	72
Table A-8: CAC-2 Summary Sheet.....	73
Table A-9: CSA-1 Summary Sheet .....	74
Table A-10: CSA-2 Summary Sheet .....	75
Table A-11: MgO-1 Summary Sheet.....	76

# 1. Introduction

---

## 1.1 Background

South Carolina Department of Transportation (SCDOT) maintains the 4<sup>th</sup> largest highway network in the country consisting of 41,358 centerline miles (90,605 lane-miles) of paved roads with 8,451 bridges with an average age of about 40 years. These structures include over 1,000 large culverts, defined as bridges with a span greater or equal to 20 ft. SCDOT inspects all bridges which are located on public roads. The SCDOT maintained bridges are categorized as shown in **Table 1**. With such a large network, the SCDOT is challenged to maximize available funds to maintain its network in the best condition possible for commuters, business owners and traveling public.

Table 1: Inventory of Bridge Assets in South Carolina [8]

Functional Class	Count	Bridge Deck Area (Square Feet)
NHS	1,765	39,508,348
Federal Aid	3,875	24,950,318
Off System	2,811	7,716,380
Total	8,451	72,175,046

The SCDOT network also facilitates an annual vehicle-miles traveled (VMT) of about 131.7 billion [8]. Given this tremendous VMT magnitude, the SCDOT monitors progress in maintaining and preserving bridges using a set of metrics such as percentage of state-owned bridges classified as substandard, structurally deficient, functionally obsolete and load restricted. These metrics are compared to the agency's goals and targets to evaluate the effectiveness and efficiency of resource allocation and utilization processes. The basis for these metrics follows an NBI scale of 0 – 9, wherein a bridge is considered in poor condition if its deck, substructure or superstructure rates 4 or below. A bridge is considered as in good condition if all its components are rated 7 or above. The condition of SCDOT bridges is outlined in **Figure 1** [9]



Figure 1: Condition of Bridges in South Carolina [9]

Maintaining such a large network of bridges is a difficult task knowing that the average age of our bridge infrastructure is 40 years old and that only 42.37% of all bridges in SC have decks in good condition bridges, while the rest are in fair or poor condition (48.30% and 9.33%, respectively). As such, maintaining a healthy and functional transportation infrastructure is of utmost importance not only to the public and businesses within the state of South Carolina, but to the whole nation as well.

**Figure 2** shows the age of the NHS bridge inventory by deck area in South Carolina [9]. Based on the 2017 NBI dataset shown in the FHWA report (2018), 48% of bridges by count and 30% by deck area were built or reconstructed from the 1960's to 1970's during the construction boom related to the development of the Interstate Highway System. About 35% of the bridges by count and 11% by deck area built or reconstructed prior to the 1970's were concrete bridges. A sizable proportion (40% by count and 23% by deck area) of this particular inventory is 45 years old or

older. In other words, these bridges have either exceeded or will soon exceed their originally anticipated design service life of 50 years.

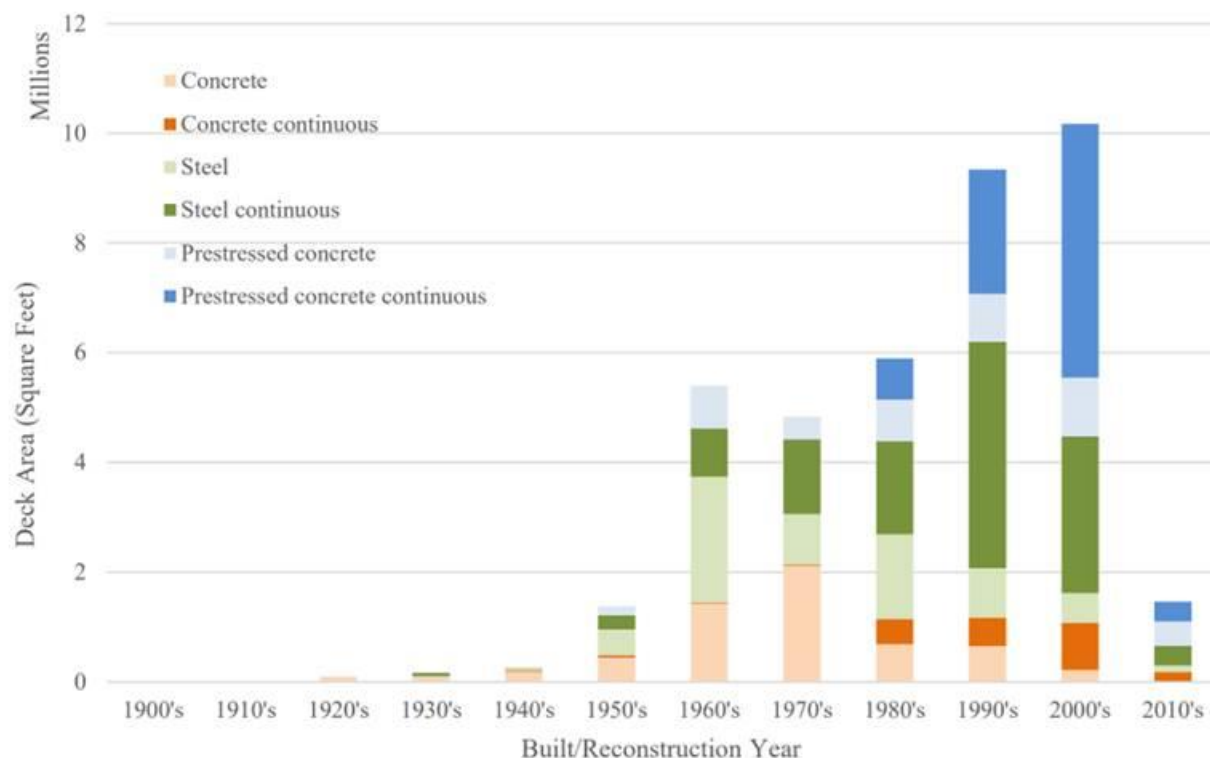


Figure 2: South Carolina NHS bridges deck area by year built/reconstructed [9]

The recent Transportation Asset Management report by the SCDOT reported that the average annual funding level required to maintain bridge systems in SC at a desired percentage of poor bridges for each system over the next ten years would be approximately: \$75 million for NHS bridges (4.0% poor); \$70 million for federal aid bridges (9.5% poor); and \$55 million for off-system bridges (7.4% poor).

Among all the bridge components, i.e. deck, substructure and superstructure, the bridge deck is the most vulnerable to deterioration over time and hence it needs periodic maintenance. The reason for deck being more susceptible to deterioration than other structural elements can be attributed to the following: (1) deck bears all of the traffic loading directly; and (2) deck presents a large surface area-to-volume ratio of concrete over which the actions of environment are impacted upon, such as exposure to deicing salts, exposure to wetting/drying and freezing/thawing conditions, loss of cover over the reinforcement with time due to a combination of load-aggravated deterioration mechanisms such as spalling, delamination, etc. resulting in more aggressive corrosion of reinforcement and other mechanisms. Also, it is important to note that the bridge deck is the most likely component of the bridge structure that also suffers from lack of good construction practices. For instance, maintaining adequate cover depth over reinforcement and high-quality cover

(without any cracks) throughout a bridge deck is not only extremely important in maintaining the service life of the deck, but is an equally challenging task. Further, improper curing of the deck at the time of construction can result in premature cracking and deterioration. All these stressors will result in the failure of the bridge deck (cracking and spalling) more often than other components of the bridge.

One of the strategies employed in repairing bridge decks that have not significantly deteriorated to warrant complete replacement, is the use of patching materials to repair the deck; thereby extending its service life. Depending on the location of the bridge and the traffic volumes involved, the patching of the spalls and potholes is often accomplished using rapid setting patching materials. However, the field performance of the patching materials has not always been good, and in some situations, it was found to be rather poor. **Figure 3** shows a case in point on a bridge deck on Interstate I-77 where large potholes in the bridge deck, that have been repeatedly patched, failed causing significant damage to vehicles.



Figure 3: Failed patching materials on bridge deck on I-77 causing large potholes

Considering the on-going premature failures of patching materials on bridge decks, it is essential to develop an understanding of factors that cause premature failure of patching materials along with identifying and determining properties of patching materials that render them suitable for repair applications. In addition, appropriate construction practices need to be identified and applied in the field to ensure durable repair. This research study focuses on conducting a field study of failed bridge patching repairs, evaluating commonly used repair materials based on different compositions and identifying factors that are likely to affect the quality and longevity of repaired sections.

## 2. Literature Review

---

The following section summarizes a review of the current literature regarding the various types of bridge deck deterioration mechanisms, the preparation of a bridge deck patch, and the different types of bridge deck patching materials.

### 2.1. Bridge Deck Deterioration Mechanisms

The deterioration of bridge decks in the form of spalling and cracking is caused due to several different reasons ranging from improper construction practices to use of concrete with inadequate mechanical and durability properties. Improper construction practices can include, but are not limited to, improper design and detailing of the deck, i.e. lack of adequate cover over steel reinforcement, inappropriate placement of steel reinforcement in the deck, or use of concrete with inadequate workability and inadequate curing of concrete after placement in the deck [3,7,10,11].

Materials-related distresses in bridge decks arise due to numerous reasons that can include the following: use of concrete with inadequate mechanical properties and/or inadequate durability to perform under the environmental exposure conditions, cracking induced by excessive shrinkage in concrete, potential incompatibility between properties of different elements of concrete bridge deck, such as differences in coefficients of thermal expansion, moduli of elasticity, etc. [12–15].

Often, failures in bridge decks occur within patching materials that were used to repair an existing damage in bridge deck. The reasons for failure in patched sections can range from improper surface preparation of the patching area within substrate deck to use of repair materials that are inherently incompatible with the substrate concrete in the deck, in terms of differences in coefficient of thermal expansion, elastic moduli, shrinkage characteristics and others. Improper preparation of patching area can include: (a) lack of sufficient texture within the patching area to develop bond with repair material (b) inadequate moisture conditioning of the substrate surface (i.e. lack of saturated-surface dry conditions), (c) lack of straight edges on the section to be patched, resulting in feathered edges, i.e., insufficient thickness of the patched area. Also, repair materials are often formulated to achieve high early-performance to ensure a short window of operation in the field due to traffic demands.

### 2.2. Surface Preparation of Patching Area

The type of patching repair and the materials used for the repair on a bridge deck are a function of the extent of damage in the bridge deck, the nature of the distress, environmental exposure conditions, traffic demands and other considerations. Patching repairs are generally classified as either a partial-depth repair or a full-depth repair. Partial-depth repairs are applied where the damaged sections in the bridge decks are relatively small and isolated areas. Full-depth repairs are warranted when the damaged areas of bridge deck constitutes a significant proportion of the entire deck surface, and the use of partial depth repair will likely not yield a durable repair for an

expected service life. Also, in a full-depth repair scenario the entire thickness of the affected portion of the bridge deck is replaced with repair material; often this involves a plant-batched Portland cement concrete mixture. While in a partial-depth repair, only a limited thickness of the bridge deck in the affected area is replaced with repair material. It is therefore important in partial depth repairs that the concrete within the affected area of bridge deck be prepared by not only removing affected concrete to sufficient depth within the deck, but also precisely defining the boundaries of the affected concrete to achieve a well-defined polygon with straight edges.

The bond performance of a repair is not only a function of the chemical reactions between the repair and the substrate matrices, but also a function of the physical properties and the quality of the substrate surface [16]. Therefore, surface preparation of the patching area in the bridge deck is considered as an important aspect in achieving a successful bond between the repair and the substrate surfaces. While several performance attributes defining the quality of the substrate concrete and repair materials are defined, there are few standards that exist for defining the quality and the level of surface preparation needed for patching repairs in the construction industry. Currently, the ICRI (International Concrete Repair Institute) produces CSP (concrete surface profile) chips representing different levels of roughness ranging from 1-10 as shown in **Table 2**[17]. Each level has a recommended preparation methodology to achieve a similar level of roughness. However, these chips are limited in the overall range of surface roughness and provide no basis for the effect of micro-texture, as the chips are silicone profiles. For example, the use of hydro-demolition for surface preparation or removal of unsound concrete can result in larger craters/pits with increased height differentials than is seen on the ICRI level 10 chip. Therefore, there are surface preparation methods whose resulting profiles fall outside of the range of those recommended by ICRI.



Table 2: ICRI CSP Surface Preparation Methods [17]

<b>ICRI CSP Recommended Preparation Methods</b>	
<b>1</b>	Acid Etched
<b>2</b>	Grinding Disc
<b>3</b>	Light Shot-Blast
<b>4</b>	Light Scarification
<b>5</b>	Medium Shot-Blast
<b>6</b>	Medium Scarification
<b>7</b>	Heavy Abrasive Shot-Blast
<b>8</b>	Scabbled
<b>9</b>	Heavy Scarification
<b>10</b>	Handheld Concrete Breaker + Abrasive Shot

### 2.3 Rapid Set Patching Materials (RPSM)s

A wide variety of RSPMs are available for use on bridge decks, all with different chemical compositions and varying fresh and hardened properties. Some of the predominant formulations of RSPMs are based on mortar and/or concrete mixtures with binders composed of (a) Portland Cement with special chemical admixtures for set-control behavior, (b) high-alumina cements, (c) calcium sulfo-aluminate cements, (d) magnesium oxide cements, (e) polymer emulsions and others [18]. While there are several others, product literature from commercial RSPMs show these to be some of the more commonly used materials for repairs on bridge decks. It should be noted that if the underlying reason for a bridge deck deterioration is not addressed and eliminated, the use of any type of repair material will not likely result in a durable repair.

Portland cement concrete patching materials use conventional ordinary Portland cement as its binding agent. OPC concrete used as a repair material is beneficial as it is widely available and provides an economic solution. Often, OPC binder is used in combination with several admixtures such as water-reducers, viscosity modifying agents, set-accelerators, corrosion inhibitors, and supplementary cementitious materials to allow a contractor to positively influence setting behavior and hydration reactions and to gain specified strength-levels in a short period of time.

Repair materials with high alumina cements often are formulated in combination with Portland cement for their rapid set and strength-gain behavior. While the high levels of calcium aluminates present in these binder systems are responsible for the high heat of hydration produced during the exothermic reaction of these repair materials and early-age strength gain, the Portland cement provides long-term strength and durability. The high-alumina cement can also mitigate shrinkage cracking due to formation of expansive ettringite in the matrix, while also providing better resistance to aggressive sulfates in the environment [19].

Repair materials based on calcium sulfoaluminate (CSA) cements are widely used as patching materials on bridge deck owing to their rapid strength development, and excellent durability against aggressive chemical environments, shrinkage and other environmental exposure conditions such as freeze-thaw [19,20]

A range of repair materials based on magnesium-based binders are also used as rapid set patching materials [21] These formulations include magnesium phosphate cements, magnesium oxychloride (MOC) cements, magnesium oxysulfate (MOS) cements among other magnesium-based formulations. Each of these formulations exhibits high early-strength and excellent bond characteristics, however some cements such as MOCs tend to exhibit poor resistance to moisture ingress.

Polymer modified concretes, such as Latex-Modified Concretes (LMC), are also used in full-depth or partial-depth patching repairs of concrete in bridge decks. LMC is a widely used material for patching and bridge deck overlays due to its durability, bond strength, and rapid curing properties. It is a composite material that combines traditional concrete with latex polymers, enhancing its performance in demanding environments. However, application of LMC demands a complex application process that requires skilled labor to prepare the substrate surface. Additionally, LMC is much more expensive than cement-based patching materials, and can be prone to shrinkage cracking, if not properly cured.

Another category of polymer modified concretes covers polymer impregnated concretes where conventional Portland cement concrete is impregnated with a low viscosity monomer and is polymerized in-situ. This improves the durability and resistance to harmful agents when compared to OPC concrete.

### 3. Experimental Plan

The experimental program for this research was broken into two halves focused on the usage of accelerated batch mixtures and RSPMs, respectively. Work between the two sections occurred simultaneously. This section describes the materials, mixing procedures, and methods used to complete the two halves of the study.

#### 2.1. Materials

The following materials were utilized to complete the accelerated batch mixtures and RSPMs portions of the studies. Not all materials were utilized for both portions of the study.

##### 2.1.1. Portland Cement

ASTM C150 Type III cement was used for a major part of this study to characterize the hydration kinetics and early properties of the accelerated batch mixtures. However, for comparison purposes, a limited study with ASTM Type I/II cement was also conducted. In this study, both Type I/II and Type III cement were produced from the same batch of clinker unless specified otherwise. The oxide composition of Type III and Type I/II cement are shown in **Table 3**. Furthermore, the particle size distribution of the cement is shown in **Figure 4**. The Type III Cement had a specific surface area of 520 m<sup>2</sup>/kg and a mean particle size of 10.3 microns. The Type I/II Portland Cement had a specific surface area of 400 m<sup>2</sup>/kg and a mean particle size of 14.8 microns.

Cement Type	SiO <sub>2</sub> (%)	Al <sub>2</sub> O <sub>3</sub> (%)	Fe <sub>2</sub> O <sub>3</sub> (%)	CaO (%)	MgO (%)	SO <sub>3</sub> (%)	Na <sub>2</sub> O (%)	K <sub>2</sub> O (%)	TiO <sub>2</sub> (%)	C <sub>3</sub> S (%)	C <sub>2</sub> S (%)	C <sub>3</sub> A (%)	C <sub>4</sub> AF (%)
III	20.52	4.85	3.41	63.45	1.27	3.67	0.118	0.491	0.265	54.4	17.8	7.1	10.4
I/II	19.89	4.89	3.33	63.31	1.26	2.95	0.136	0.487	0.268	53.6	15.7	7.1	10.0

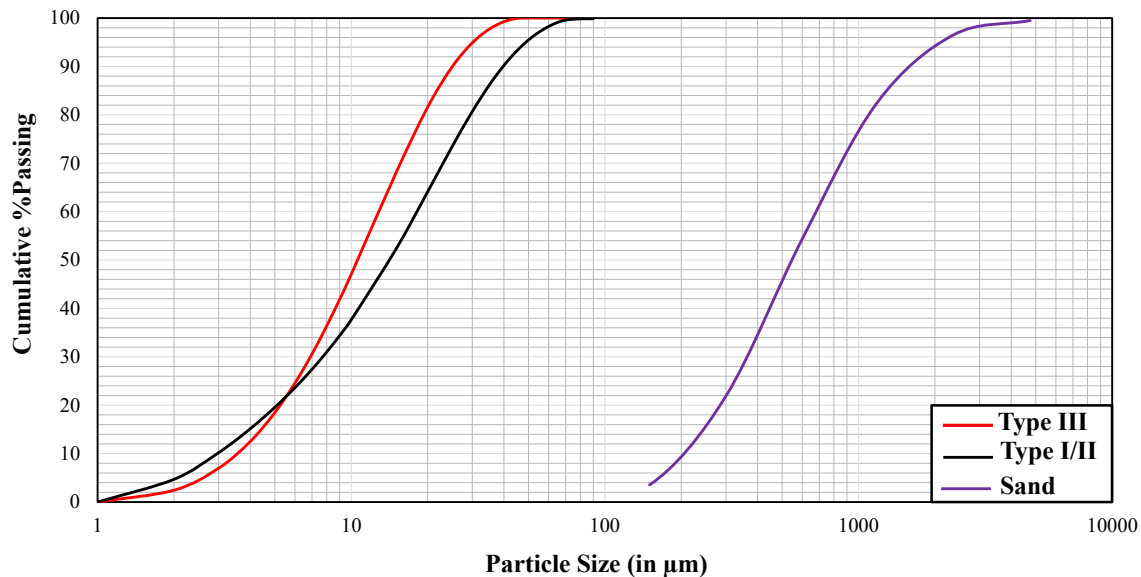


Figure 4: Particle Size Distribution of Portland Cements and Sand

### 2.1.2. Fine Aggregate

A well-graded sand with a maximum particle size of 2.36mm was used in mortar mixtures with set accelerators. The particle size distribution of the sand is also included in **Figure 4**. The sand had a specific gravity of 2.65 and absorption of 1.09%.

### 2.1.3. RSPM

The RSPMs selected for this project came from a variety of manufacturers and while all materials fall under the same classification, they employ differing cement types and additives. This study will designate the differing RSPMs by their cement type. RSPMs including ordinary Portland cement only are designated by PC-#, RSPMs including a mixture of ordinary Portland cement and calcium aluminate cement are designated by CAC-#, RSPMs including a mixture of ordinary Portland cement and calcium sulfoaluminate cement are designated by CSA-#, and RSPMs containing magnesium oxide cement only are designated by MgO-#. A table including the full list of patching materials and the recommended water dosage rates are included in **Table 4**. The recommended water dosage rates is the weight of water to include to a designated weight of RSPM.

Sample ID	PC-1	PC-2	PC-3	PC-4	PC-5	CAC-1	CAC-2	CSA-1	CSA-2	MgO-1
Water Dosage (Mass %)	6.2%	7.1%	10.3%	8.6%	6.5%	8.9%	8.8%	11.1%	9.9%	8.2%

### 2.1.4. Set Accelerators

The set accelerators used in this study were commercially manufactured chloride-based, non-chloride based, C-S-H nano particle-based and a shotcrete accelerator. The physical properties and chemical composition of the accelerators are given in **Table 5**. These accelerator were chosen to provide a variety of set accelerator mechanisms and degrees of acceleration.

Accelerator	Specific Gravity	Solid Content	Chemical Makeup
Chloride Based (Cl)	1.31	37%	Calcium Chloride ( $\text{CaCl}_2$ )
Non-Chloride Based 1 (NCl)	1.17	53%	Sodium Nitrate, Sodium Thiocyanate, and Methyl-Diethanolamine
Non-Chloride Based 2 (NCl-1)	1.12	--	Calcium Nitrate and Sodium Thiocyanate
C-S-H Based 1 (XS 55)	1.12	33%	C-S-H Nanoparticles, Sodium Thiocyanate, Silicic Acid, and Calcium Salts
C-S-H Based 2 (XS 44)	1.12	36%	C-S-H nanoparticles, Triisopropanolamine

Shotcrete Accelerator (SA)	1.42	45%	Aluminum Sulfate, Glycerol, Diethanolamine
----------------------------	------	-----	---

The dosage of the accelerators is generally divided into low and high dosages unless otherwise specified. The accelerator content for low and high dosages by weight of cement (bwoc) are given in **Table 6**. The dosages used in this study are based upon the manufacturer’s recommendation except for the chloride-based accelerator, which is based on ACI 318 specification. The water content was adjusted for all the test methods based on the solids content of the admixture.

Table 6: Accelerator Dosages

Accelerator	Dosage (% bwoc)	
	Low	High
Cl	0.52	2.62
NCl-1	0.58	2.60
NCl-2	0.58	2.60
CSH-1	0.58	2.60
CSH-2	0.26	1.00
SA	5.0	10.0

#### 2.1.5. Reference Substrates

As a reference for durability testing a 5000-psi concrete bridge deck mixture was analyzed alongside the accelerated batched concrete and RSPMs. The 5000-psi mixture had a 3-inch slump and utilized a #789 coarse aggregate. The mixture proportions for the reference concrete are listed in **Table 7**.

Table 7: 5000-psi Reference Concrete Mixture Proportions

Water - Cement Ratio	0.35
Sand - Cement Ratio	1.3
Fine Agg. – Coarse Agg. Ratio	0.63
HRWR Dosage per 100 lbs Cement	0.5%
VMA dosage per 100 lbs Cement	0.2%

Additionally, to reduce the variability of pull-off testing standardized concrete testing blocks were ordered from TACM (Technical Applications for Concrete Materials) to act as the substrate material for the patching overlays. The surfaces were prepared before testing to an ICRI surface preparation level of one, three, and seven.

## 2.2. Mixing Procedures

Two mixing procedures were used for the tests conducted during this study. The first procedure was for the setting time, ultrasonic pulse velocity, isothermal calorimetry, compressive strength, bulk resistivity, chloride migration and resonant frequency test. The first mixing procedure used a 5-quart Hobart planetary mixer and followed ASTM C305-20 for mixing mortar, except for the RSPMs. For the RSPMs instead of the interval where sand was added, an extended mixing period on low speed was conducted (30s). The second procedure was used for the restrained shrinkage ring, slant-shear bond strength, pull-off bond strength, and coefficient of thermal expansion tests due to the higher batch volume. The second mixing procedure utilized a 50-quart capacity counter-current pan mixer and followed the procedure outlined by the RSPM provider. This typically entailed a mixing time between 3-8 minutes at a low speed.

To accurately test the influence that temperature plays on the accelerated batched concrete and RSPMs, all mixture components and mixing water were preconditioned to their respective testing temperature (50, 73, and 104°F) for 24±1 hours in an environmental chamber (±0.5°F precision) under sealed conditions. The RSPMs and mixing water were removed from the environmental chamber directly before mixing to minimize temperature variation. For samples tested at 104°F that stiffened before mixing concluded work was not completed, as the accelerated batch concrete or RSPM was deemed to unsuitable for application.

## 2.3. Experimental Methods

The following methods were utilized to complete the study. Not all methods were used for both the accelerated batch mixtures and RSPMs sections of the study.

### 2.3.1. Setting Time

Setting time of the repair materials was performed in accordance with ASTM C191-21 Method B and ASTM C807-21. As some of the bagged patching mixtures contain large aggregate particles, the samples were first sieved at 4.75 mm and tested for normal consistency as specified in ASTM C807-21. This is to ensure that the stiffness and material behavior is consistent after larger aggregates are removed, thus altering the water demand of the system based on the recommended dosages provided by the manufacturers. Setting time for initial and final set times were determined for a needle penetration depth of 35mm and 5mm respectively. In addition to the previously mentioned experimental controls the Vicat test also included an isolated water bath and water chiller/circulator to allow for temperature testing, however the temperature range is limited from 50-73°F, therefore a secondary refrigerated bath circulator was modified and used for 104°F testing. All binder materials and mixing water were conditioned to the appropriate temperatures using an environmental chamber.

### 2.3.2. Isothermal Calorimetry

An assessment of the hydration kinetics and heat of hydration (HoH) of the accelerated batch mixtures and RSPMs was performed in compliance with ASTM C1679-22 and ASTM C1702-23.

Tests were performed at 50, 73 and 104°F to study the impact of temperature exposure on the rates of heat release and overall reactivity of the material. Individual sample sizes were 100g of freshly mixed material, that was sampled from a one kg binder mix with the appropriate water dosages based on the manufacturer's recommendations. The samples were monitored for 168 hours.

#### *2.3.3. Ultrasonic-Pulse Velocity (UPV)*

Ultrasonic-Pulse Velocity (UPV) testing was done in accordance with ASTM C597-22. The test setup consists of a silicone mold with a cylindrical hole for the sample (40mm diameter), where the transmitter and the receiver are inserted into the opposite ends of the silicone mold. The maximum particle size for the test setup was 4.75mm and larger particles were sieved out to minimize interference. Tests were conducted at 50, 73 and 104°F temperature exposures in an environmental chamber ( $\pm 0.5^\circ\text{F}$  and  $50 \pm 5\%$  RH). Pulse wave velocities were then measured once per minute for 24 hours to monitor the stiffening and initial hardening of the sample. The required sample size is approximately 200g of freshly mixed material, which was sampled from a 1000g mix to ensure homogeneity.

#### *2.3.4. Compressive Strength*

The compressive strength of the plant-produced accelerated concrete and RSPMs was performed in accordance with ASTM C109-24 on 2" cubes and ASTM C39M-21 on 3"x6" cylinders, respectively. Samples were cast and tested at variable ambient temperatures of 50, 73 and 104°F to understand the impact of environmental temperature on early age material performance. Material conditioning and curing was done using an environmental chamber. Samples were tested at an age of 0.25, 0.5, 1, 3 and 7-days.

#### *2.3.5. Slant Shear Bond Strength*

The bond strength was assessed on RSPM using the slant/shear method in accordance with ASTM C882M-20. Samples were cut at a 30° angle from vertical and 10mm from the base of the cylinder. The smooth saw-cut surfaces acted as a control, while other surface preparations were performed on the bond interface surface to study the effect of surface area/roughness interaction on bond performance. The half-cylinders were placed back into the 3"x6" cylinder molds in both dry and SSD (Saturated Surface Dry) conditions to test impact of substrate conditions on bonding ability. The repair materials were then cast on top of the substrate half-cylinder and cured for seven days then tested for bond strength.

#### *2.3.6. Pull-Off Bond Strength*

Bond strength was also assessed using the Pull-Off method, performed in accordance with ASTM C1583M-20. RSPMs were applied to the surface of the TACM substrate (SSD state) and left to cure for four days. Failure in either cementitious material alone suggests that the bond between the two is stronger than the tensile capacity of the failed material. Bond failures between the substrate and repair material were used to calculate the bond strength.

#### *2.3.7. Shrinkage Ring Test*

Shrinkage testing of the accelerated batch mixtures and RSPMs was conducted in accordance with ASTM C1581M-18a, except that the outer ring was removed once the strain exceeded 15 microstrain or once 24 hours elapsed, as some accelerated batch mixtures and RSPMs set rapidly and experienced significant amounts of autogenous shrinkage. Mixing followed the alternative mixing procedure for larger sample sizes. Samples were exposed to temperatures of 50, 73 and 104°F in an environmental chamber. The test continued until the sample cracked or 28 days elapsed.

#### *2.3.8. Coefficient of Thermal Expansion (CoTE)*

The CoTE was tested on triplicate 91-day or older RSPM samples per AASHTO T336. Samples were cast in laboratory conditions and stored in a curing room until they eclipsed 28 days of curing. The samples were then cut to a height of  $7 \pm 0.2$ " and added inserted into the CoTE test setup and evaluated.

#### *2.3.9. Resonate Frequency*

Resonate frequency testing was performed on 91-day RSPM samples in accordance with ASTM C1259-21, ASTM E1876-22 and ASTM C215-19. The test was used to determine the dynamic young's modulus, dynamic shear modulus and Poisson's ratio via impulse excitation of vibrations. Samples were cast in laboratory conditions and stored in a curing room until they eclipsed 91 days of curing. The samples were then dried to remove surface moisture and evaluated.

#### *2.3.10. Surface/Bulk Resistivity*

Testing of surface and bulk resistivity was completed on triplicate 91-day RSPM samples in accordance with AASHTO T358-19. Samples were cast in laboratory conditions and stored in a curing room until they eclipsed 28 days of curing. The samples were then dried to remove surface moisture and evaluated for both surface and bulk resistivity.

#### *2.3.11. Chloride Migration*

Chloride Migration testing was done in accordance with the NORDTEST Method NT BUILD 492. Samples were cast in laboratory conditions and stored in a curing room until they eclipsed 91 days of curing. The samples were then cleaned and left to fully dry before vacuum impregnated with a fully saturated calcium hydroxide (CH) solution 24 hours prior to testing. After which, the testing to determine the depth of chloride ingress was undertaken.



## 3. Evaluation of RSPMs

---

### 3.1. Objective

The objective of this portion of the study was to evaluate common RSPMs to identify the appropriate environmental conditions, substrate performance, and present deterioration mechanisms to ensure an effective and long-lasting patch. To achieve this effectively testing focused on evaluating the mechanical/durability performance of the RSPMs at 73°F and the early age performance of the RSPMs at 50, 73, and 104°F. The results from these tests were used to generate the recommendations in the conclusions section and the RSPM summary sheets in **Appendix A: RSPM Summary Sheets**.

### 3.2. The Influence of Binder Type on RSPMs Performance in Fresh and Hardened State

The proper assessment of RSPMs is critical to the effective utilization and selection of RSPMs based upon project conditions. However, the utilization of multiple binder types when formulating RSPMs results in vastly different fresh and hardened properties. To better understand how these binder types influence the fresh and hardened properties of RSPMs an assessment is completed on the setting time, early age stiffness, compressive strength, slant-shear bond strength, pull-off bond strength, restrained shrinkage, coefficient of thermal expansion (CoTE), electrical resistivity, and chloride permeability of PC, CSA, CAC, and MgO-based RSPMs. Conclusions and recommendations are generated both for specific RSPMs and larger binder types.

#### 3.2.1. Setting Time

The setting time of a given RSPM is a critical parameter for categorization, as an extended setting time requires additional lane closure time. Conversely, too short of a setting time limits the ability of the concrete placement crew to consolidate the concrete, potentially resulting in premature deterioration effectively. General experience indicates that RSPMs should provide at least a 15-minute window before the initial set to ensure proper construction and a final set no longer than one hour to ensure quick reopening to traffic [7]. Testing on the selected RSPMs (**Table 8**) indicated that only five RSPMs (PC-2, PC-4, PC-5, CAC-1, and CSA-1) had initial and final sets within that time window. Most failed samples did not fall within that window setting before fifteen minutes elapsed, with only MgO-1 setting after the designated final set time threshold. The premature or delayed setting of these RSPMs does not exclude them from use but requires that placement crews have premature knowledge about the RSPM to ensure that concrete batches are not more than what can be cast during the open window of the RSPM.

Further analysis of the binder types as a function of passing or falling outside the preferred setting window does not indicate that certain binder types are preferable or result in a faster/slower setting time, except for MgO-based RSPMs which appear to indicate an extended setting time generally but have a limited sample size and could be reduced based upon mixture formulation changes. Otherwise, all other binder types had approximately 50% of their RSPMs inside the setting time window and 50% outside of the window. The variability in meeting the window indicates that the

ability to achieve a designated setting time is a function of RSPM additive, chemical admixture, and water content rather than binder type. Furthermore, all binder types can be tuned to be set either earlier or later depending on manufacturer preference, which is important when discussing the influence of temperature on setting behavior later.

Table 8: Setting Time of the RSPMs at 73°F

Sample ID	Initial Setting Time (min)	Final Setting Time (min)	Interval (min)
PC-1	10	13	2
PC-2	18	32	14
PC-3	7	8	1
PC-4	16	17	2
PC-5	25	29	4
CAC-1	17	28	11
CAC-2	5	6	2
CSA-1	16	24	8
CSA-2	3	5	3
MgO-1	188	193	5

### 3.2.2. *UPV*

The early-age development of stiffness in cementitious systems is best characterized by monitoring the ease of transmitting ultrasonic waves through a sample, which is expressed as pulse velocity. By monitoring the change in pulse velocity as a function of time, the ultimate stiffness and setting time are determinable. However, this portion of the study will predominately utilize ultrasonic pulse velocity as a relative measure to provide insights into how the development of stiffness will influence the practical usage of these RSPMs.

The results from ultrasonic testing on PC-based RSPMs are shown in **Figure 5**. These results indicate that PC-based RSPMs generally experience a rapid change in pulse velocity, which generally onsets approximately 15 minutes after casting and ends approximately an hour after casting. After this, a significantly slower but positive change in velocity is observed, indicating a slowing but not termination of cement hydration. These results correlate well with DOT requirements for setting behavior, as a stiffer RSPM will better withstand the reopening of traffic and mitigate the risk of rutting and damage. The only PC-based RSPM that did not exhibit a rapid stiffening between 15-60 minutes after casting was PC-5. Instead, a slight increase in stiffness was observed between hours zero to two and then a rapid stiffening between hours two and three. This delay in stiffness could result in deterioration if traffic is reopened prematurely.

Lastly, when observing the peak pulse velocity for the RSPMs, a general range between 4000-5000 m/s is observed. These stiffness values are slightly larger than those observed for ordinary Portland cement concrete and mortars previously tested in this lab (3000-3500 m/s). Overall, this could indicate some incompatibility with the substrate, as overly stiff patches could resist

deformation from the surrounding pavement and cause cracking. However, as RSPMs are generally utilized for partial depth repairs, this may be a secondary consequence.

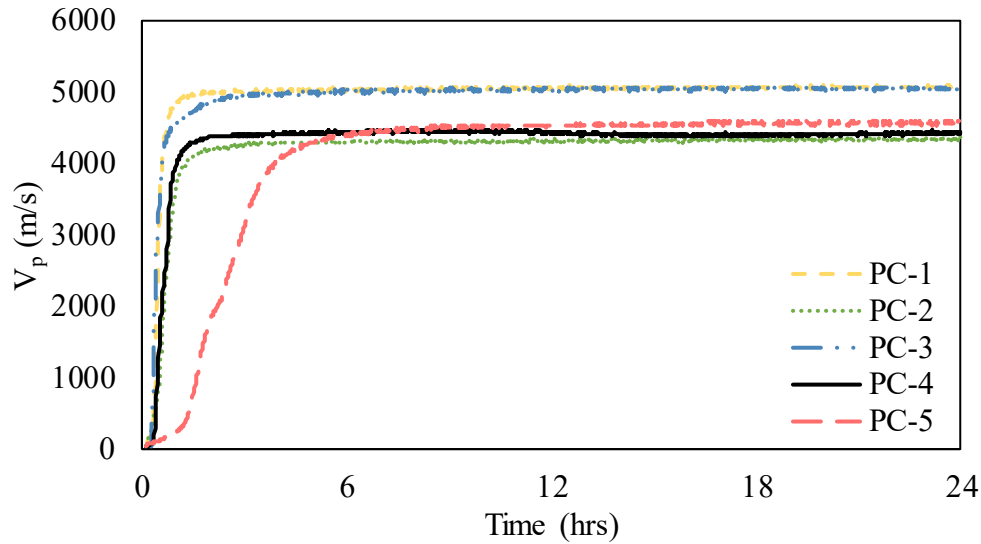


Figure 5: The Early Age UPV of PC-based RSPMs at 73°F

The results from ultrasonic testing on the CAC, CSA, and MgO-based RSPMs are shown in **Figure 6**. The stiffening behavior of the CAC and CSA-based RSPMs was like the PC-based RSPMs. However, CAC-1 experienced a slightly delayed stiffening rate compared to the other CAC, CSA, and PC-based RSPMs, with rapidly stiffening over 30 minutes to two hours after mixing. The main difference between the CAC and CSA-based RSPMs and the PC-based RSPMs is the peak pulse velocity range, where peak pulse velocity generally falls between 3500 and 4500 m/s. This better correlates to pulse velocities observed in ordinary Portland cement concretes and mortars, decreasing the likelihood of incompatibility.

Test results from testing with the MgO-based RSPM demonstrate the retarded setting behavior of the MgO-based RSPM. MgO-1 did not experience a period of rapid acceleration as the other RSPM utilized in this project. Instead, a more gradual acceleration was observed between the one-hour and twenty-four-hour periods. This testing proves that caution should be taken when working with MgO-based RSPMs, as reopening to traffic will require delay compared to the other RSPMs. Notably, the peak pulse velocity of the MgO-1 sample was not lower than the other RSPMs, achieving a 24-hour pulse velocity of 3721 m/s. This corresponds well with ordinary Portland cement concrete and mortars and could demonstrate better compatibility when large loads that could cause deformation are present.

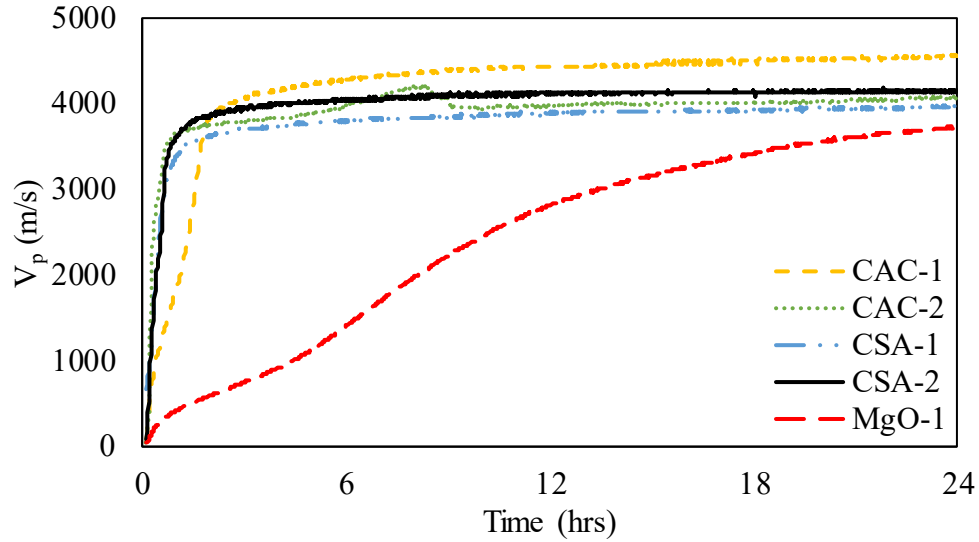


Figure 6: The Early Age UPV of CAC, CSA, and MgO-based RSPMs at 73°F

### 3.2.3. Compressive Strength

Results from compressive strength testing on the RSPMs are shown in **Figure 7**. Developing adequate compressive strength is key to RSPM withstanding traffic loads. ASTM C928-20 requires a one-day and seven-day compressive strength of 2000 and 4000 psi, respectively, for its lowest strength grade. For its highest strength grade, 5000-psi compressive strength is required for one and seven days. Testing indicated that all samples passed the thresholds for the lowest grade classification, and MgO-1 was the only sample to fail to pass the highest-grade classification (4768 psi in one day). Furthermore, testing at 0.25 and 0.5 days demonstrates the differing rates of reaction of the patching materials, with most gaining strength quite rapidly, except for CAC-2 and MgO-1, having relatively low 0.25-day compressive strengths. Overall, compressive strength development is not an issue for any specific binder type, as the ultimate compressive strength of all systems significantly surpasses those required by ASTM. Further testing could investigate how RSPMs of excessive strength respond to loading, as the compressive strength of some RSPMs would approximately double or triple the strength of a 4000-psi concrete but does not appear significant to the current study.

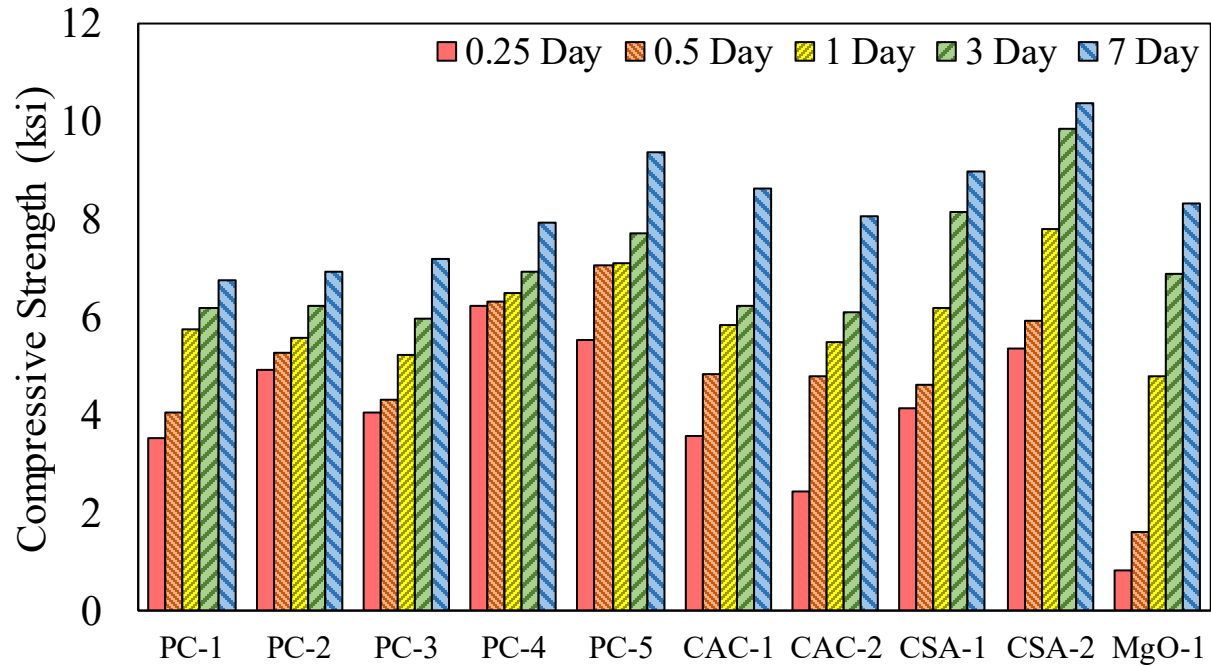


Figure 7: Compressive Strength of the RSPM at 73°F

#### 3.2.4. Slant-Shear Bond Strength

The bond strength of the RSPMs was evaluated utilizing the slant-shear bond strength test, with variable substrate saturation to observe how the pretreatment of the surface influences the quality of the bond to the pavement. The results from the bond testing are shown in **Figure 8**. ASTM C948-20 requires a seven-day bond strength of 1500 psi for all grades of patching materials. Testing indicated that most RSPMs achieved this bond level in an SSD and a dry state. However, the dry substrates generally achieved a higher bond strength than the SSD substrates. Samples CSA-1 for the SSD and dry state failed, as did the dry substrate for MgO-1. These results indicate that CSA-1 should not be utilized, as accelerated delamination and deterioration are possible. However, this is not a decreased performance as a function of binder type, as CSA-2 achieved the highest slant-shear bond strength of all the selected RSPMs.

Furthermore, based on the general performance of the RSPMs, dry substrates are preferred over SSD. The reduced bond strength is potentially due to the reduction of effective macro/microtexture along the substrate surface due to the surface moisture. However, the preparation of the pavement surface could provide a significantly more impactful influence on the slant-shear bond strength, as indicated by literature, where 20-25% increases in performance were observed with increasing surface preparation. Furthermore, experience and observations from the field visits highlighted the importance of surface preparation in ensuring a strong and durable bond to a substrate.

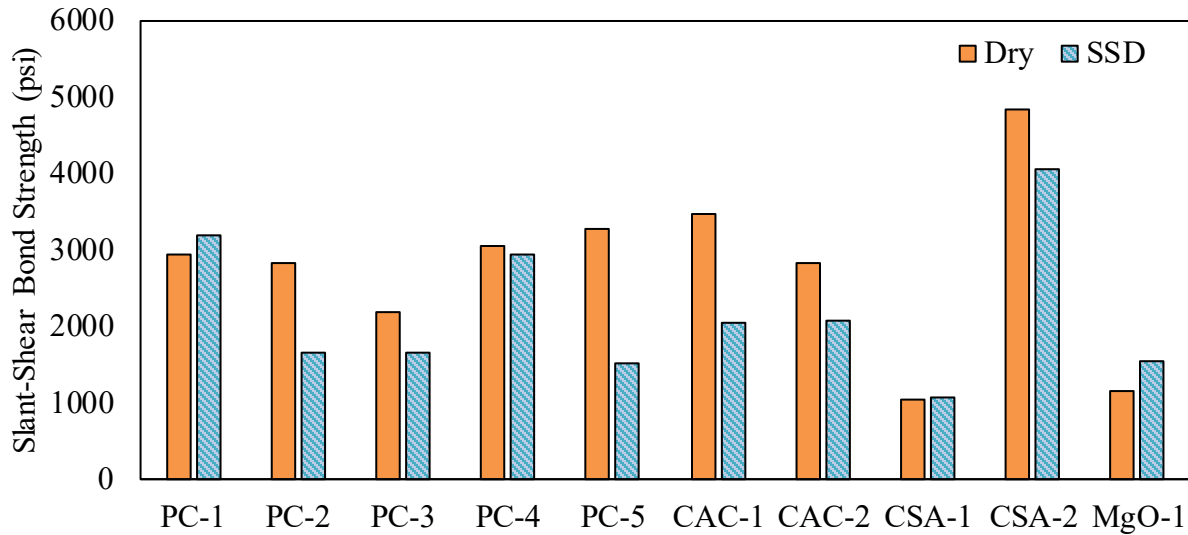


Figure 8: The Slant-Shear Bond Strength of RSPMs with SSD and Dry Substrates at 73°F

### 3.2.5. Pull-Off Bond Strength

In conjunction with slant-shear bond strength testing, pull-off bond strength tests were also conducted to investigate a second mode of bond strength. Pull-off bond strength is significantly less influenced by surface preparation and is more highly influenced by the inherent bond strength and stickiness of the RSPM. General RSPM guidelines from ASTM do not specify a pull-off bond strength, but SCDOT high friction surface treatment guidelines outline a 250-psi pull-off bond strength or failure in the substrate to pass inspection. This report will utilize 250 psi as its internal pull-off bond strength threshold. Furthermore, testing will investigate the influence of substrate saturation by testing SSD and Dry substrates in parallel.

**Figure 9** displays the pull-off bond strength testing results conducted on dry and SSD substrates. Importantly, PC-3 could not be tested due to the weak bond to the substrate, resulting in delamination when coring the sample for testing. As such, PC-3 is not recommended as the bond strength appears unsuitable for in-site application. Further analysis of the test results indicates that multiple patching materials demonstrate inadequate bond strength with PC-2 dry, PC-5 dry, CAC-1 dry, CAC-2 SSD and dry, and CSA-1 SSD and dry falling below the 250-psi threshold. The lower strength of the dry substrates relative to the SSD substrate for pull-off bond strength is potentially due to the lower degree of hydration caused by moisture being taken from the RSPM to saturate the dry substrate. Based upon the percent increase in performance for pull-off bond strength testing relative to the decrease in performance in slant-shear bond strength testing, the usage of SSD substrates is recommended. To offset the decrease in slant-shear bond strength, surface preparation could be utilized to increase performance, as previously discussed during the slant-shear bond strength results section.

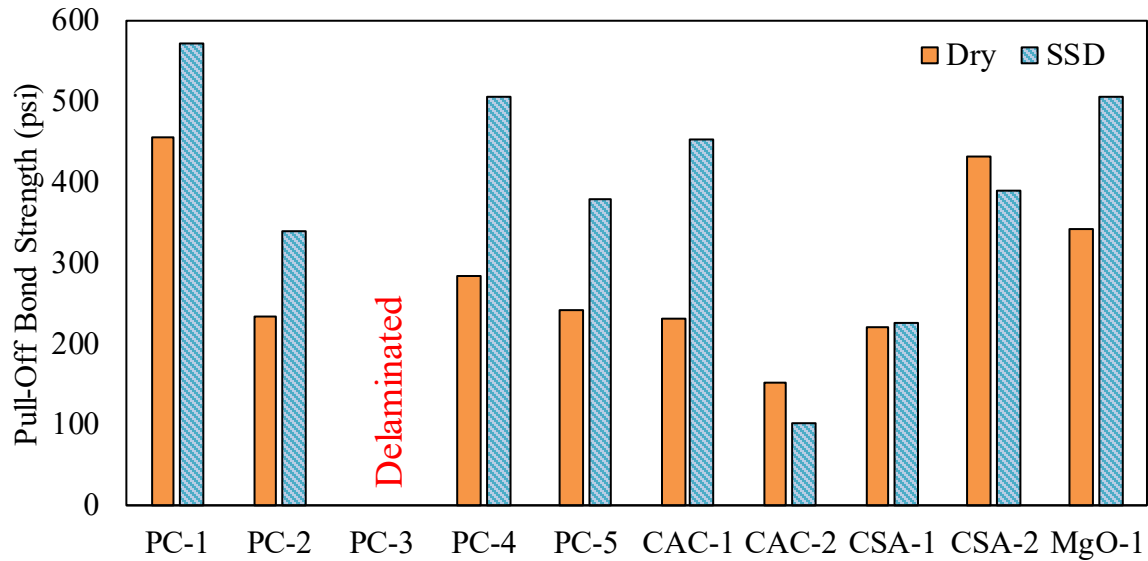


Figure 9: The Pull-Off Bond Strength of RSPMs with SSD and Dry Substrates at 73 °F

### 3.2.6. Shrinkage Ring Test

The shrinkage of the RSPMs was evaluated utilizing the restrained shrinkage ring test, as the restrained shrinkage ring test combines the effects of shrinkage and tensile strain capacity to provide a measure of shrinkage and durability. Test results collected from the shrinkage ring testing include time to crack and the strain rate and are shown in **Table 9**. Testing generally indicated a low durability for the RSPMs, as the fast-setting times corresponded to a higher initial shrinkage when the tensile stress and strain capacity were not fully developed. Analysis indicated that multiple samples tested failed before seven days elapsed (PC-1, PC-2, PC-4, CAC-1, CAC-2, CSA-1, and MgO-1) and had high strain rates (>15 psi/day). General guidelines would indicate that due to the below seven-day time to crack that a high potential for cracking is present. Therefore, significant caution should be taken when working with these RSPMs as improper patch shapes could easily result in cracking and failure of the patch. However, not all RSPMs failed with PC-3, PC-5, and CSA-2 exhibiting longer times to crack with lower strain rates, as such they may provide better performance and be less likely to crack under less-than-ideal geometries. Overall, binder type does not appear to be a significant factor in reducing the chance of cracking, as RSPMs within existing binder types provided drastically different performances.

Table 9: The Time to Crack and Average Strain Rate from Restrained Shrinkage Ring Testing at 73 °F

	PC-1	PC-2	PC-3	PC-4	PC-5	CAC-1	CAC-2	CSA-1	CSA-2	MgO-1
Time to Crack (Days)	1.75	0.25	>28	4.25	22.25	1.5	0.1	4.5	>28	4.25
Strain Rate (psi/day)	34.4	142.7	1.3	20.4	4.5	59	990.2	5.2	3.17	10.5

### 3.2.7. CoTE

The CoTE was evaluated and compared to the CoTE of ordinary Portland cement (OPC) concrete samples to determine the compatibility of the RSPMs to Portland cement concrete pavements. Testing on OPC concrete resulted in COTE ranging from  $5.2\text{--}5.7 \times 10^{-5}$  in/in/°F, whereas the CoTE for the RSPMs ranged from  $6.2\text{--}7.7 \times 10^{-5}$  in/in/°F. In effect, resulting in a deviation of the RSPMs from the OPC concrete from 110-147%. In practice, this would at worst result in a differential expansion of 0.15 inches over a 100-foot span during a temperature change of 50°F or a stress of the development of 125 microstrain over the same 100-foot span during a temperature change of 50°F assuming full restraint. This level of stress should not result in cracking and indicates that the CoTE for the selected RSPMs is compatible with the substrate. Furthermore, the role of binder type appeared to be a secondary factor for the characterization of material CoTE, with all binder types resulting in comparable CoTE values. The full results for the CoTE testing are shown in **Figure 10**.

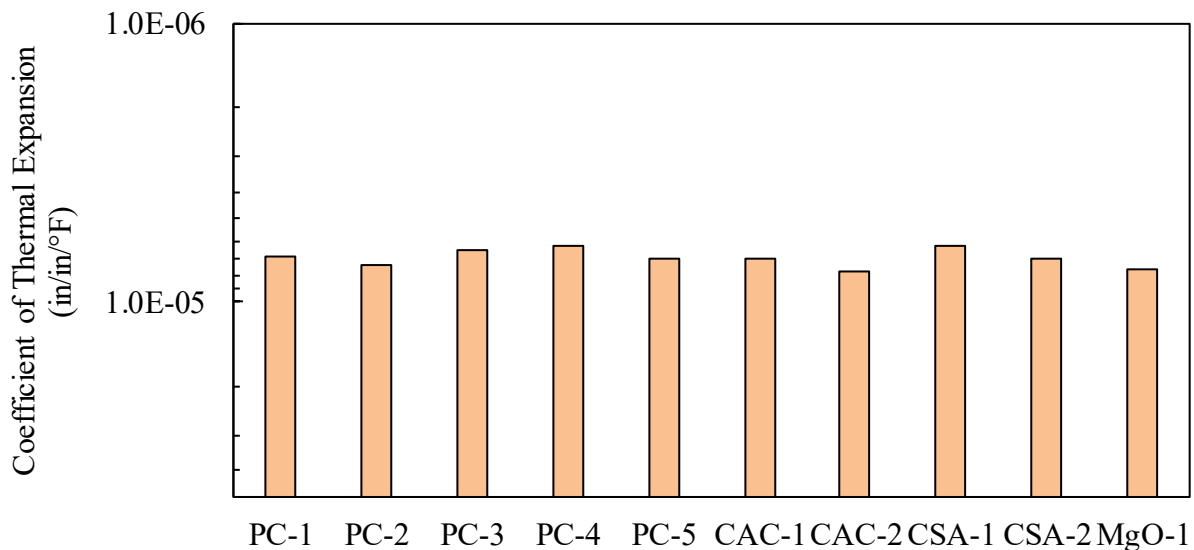


Figure 10: The Coefficient of Thermal Expansion of 91-Day RSPM Samples Cured at 73°F

### 3.2.8. Resonate Frequency

An investigation of the Poisson's ratio, dynamic modulus of elasticity, and dynamic shear modulus was conducted using the resonate frequency test. Tests results were compared to a control OPC concrete sample, which demonstrated a Poisson's ratio of 0.18, dynamic modulus of elasticity of  $6.66 \times 10^6$  psi, and a dynamic shear modulus of  $2.83 \times 10^6$  psi. Test results from resonate frequency testing on the RSPMs are shown in **Table 10**. Test results on Poisson's ratio of the RSPMs indicated a small range of deviation from 0.15-0.23, which only deviates slightly from the control Poisson's ratio of 0.18. Minimizing the difference between the substrate and RSPMs Poisson's ratio is critical as traffic loads could result in the development of longitudinal stresses that could result in delamination of the RSPM. However, the likelihood of failure due to incompatibility due to load-based deformation appears more likely from normal or shear stresses. The dynamic modulus of elasticity of the RSPMs varied from  $3.55\text{--}7.44 \times 10^6$  psi, which results in RSPMs with



dynamic modulus of elasticity as low as 53% of the control and as high as 108% of the control. Generally, indicating that the RSPMs are less stiff than the control OPC concrete. In practice, this would result in greater deformation from the RSPMs than the control substrate and thereby the buildup of stress at the interface between the substrate and the RSPM. In practice, assuming a 500-psi load is being applied a differential strain buildup of approximately 75 microstrain, which would again not result in failure. Similarly, testing on the dynamic shear modulus showed a range of 54-114% of the control ( $1.53\text{-}3.23 \times 10^6$  psi) and would demonstrate a differential strain buildup of approximately 150 microstrain, which should not result in failure. Overall, load/thermal deformation-based testing measures indicated that the RSPMs were compatible with the control substrates and is of secondary consequence when evaluating the effectiveness of the RSPMs.

Table 10: Results from Resonate Frequency Testing of 91-Day RSPMs Samples Cured at 73°F

	E (psi)	G (psi)	Poisson (-)	Specific Gravity (-)
PC-1	7.16E+06	3.12E+06	0.15	2.34
PC-2	6.51E+06	2.72E+06	0.20	2.27
PC-3	6.15E+06	2.56E+06	0.20	2.15
PC-4	6.46E+06	2.67E+06	0.21	2.31
PC-5	6.42E+06	2.67E+06	0.20	2.31
CAC-1	7.44E+06	3.23E+06	0.15	2.35
CAC-2	5.85E+06	2.46E+06	0.19	2.26
CSA-1	3.55E+06	1.53E+06	0.16	2.12
CSA-2	5.66E+06	2.31E+06	0.23	2.25
MgO-1	4.83E+06	2.00E+06	0.21	2.14

### 3.2.9. Surface/Bulk Resistivity

Lastly, testing on the resistance to chloride ingress was completed using electrical resistivity and chloride migration test results. Testing on the electrical resistivity of the RSPMs was conducted to assess the resistance of chloride ingress relative to the control substrates. Testing of the control substrates resulted in bulk and surface resistivity readings varying from 10-50  $\text{k}\Omega \cdot \text{cm}$ , generally indicating a low to very low risk of chloride penetration. The test results for the RSPMs are shown in **Figure 11**. The surface and bulk resistivity of the RSPMs was highly variable, but not heavily dependent on the binder type, as multiple binder types provided high and low electrical resistances. Samples PC-4 and CSA-1 provided the lowest electrical resistance, which would indicate an elevated risk to chloride ingress and should result in caution when utilizing these RSPMs in locations subject to elevated chloride levels. Alternatively, the highest electrical resistivity values were shown in the PC-5 and CAC-2 samples, which maxed the electrical resistivity meter at 1000  $\text{k}\Omega \cdot \text{cm}$  and would indicate a negligible risk of chloride ion penetration. However, these RSPMs should still be used with caution, as their high electrical resistivity relative to the controls could result in the formation of a galvanic corrosion cell due to the large difference in electrical resistivity, potentially causing the further corrosion of reinforcement. Caution should be taken when splicing these RSPMs onto locations where rebar corrosion has already begun. Overall,

testing would indicate that PC-1, PC-2, PC-3, CAC-1, CSA-2, and MgO-1 would provide the best resistance to chloride ingress while still minimizing the risk of the formation of a galvanic corrosion cell and are therefore recommended when corrosion is a factor when assessing a potential patch location.

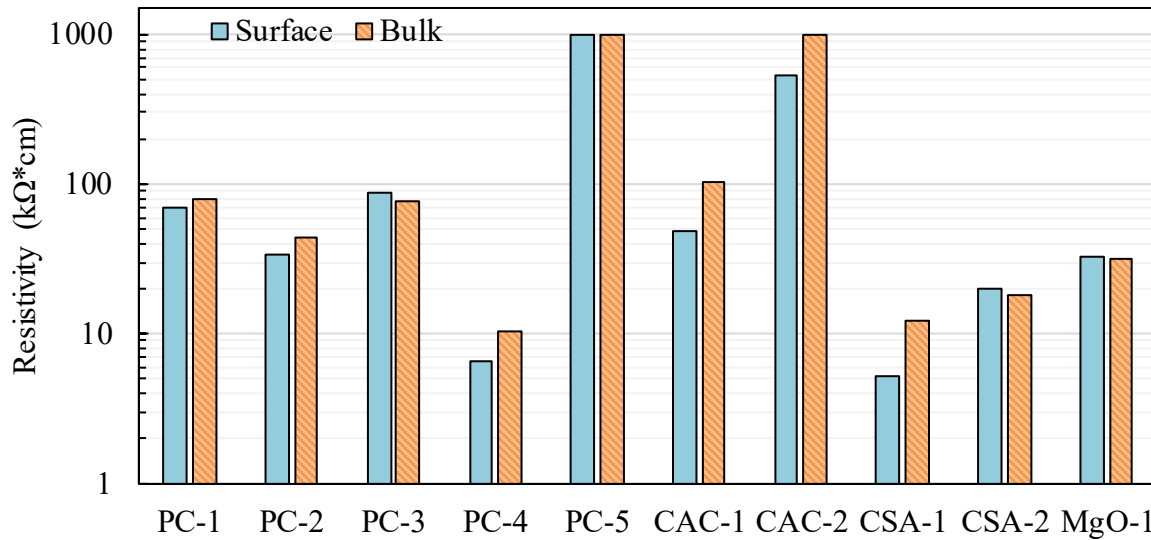


Figure 11: Bulk and Surface Resistivity of 91-Day RSPMs Samples Cured at 73°F

### 3.2.10. Chloride Migration

In support of the electrical resistivity testing chloride migration testing was completed on the RSPMs to further categorize the effectiveness of the patching materials and provide a better analysis of the high resistivity RSPMs. As expected, PC-5 and CAC-2 demonstrated the lowest chloride migration rates, indicating that the risk of chloride penetration-based corrosion is negligible. Furthermore, testing indicated that the resistance to chloride migration for PC-5 was orders of magnitude greater than the alternative RSPMs, with a chloride migration coefficient of  $1.8 \times 10^{-13} \text{ m}^2/\text{s}$ . Whereas, CAC-2 had a chloride migration coefficient of  $6.7 \times 10^{-11}$ , which while greater than the average was still two orders of magnitude lower than PC-5. Overall, testing would indicate that the chloride permeability of the RSPMs is lower than the substrate concrete, apart from PC-4 and CSA-1. Indicating that most RSPMs can better resist the ingress of chlorides and should reduce the risk of chloride-based corrosion when properly implemented.

Table 11: Chloride Migration Coefficients for 91-Day RSPMs Samples Cured at 73°F

Materials	Cl Migration (m <sup>2</sup> /s)
PC-1	1.1E-09
PC-2	3.1E-09
PC-3	7.7E-10
PC-4	1.5E-09
PC-5	1.8E-13
CAC-1	2.3E-10
CAC-2	6.7E-11
CSA-1	1.5E-09
CSA-2	4.1E-10
MgO-1	2.1E-09

### 3.3. The Role of Environmental Temperature on the Early Age Performance of RSPMs

Temperature is a key parameter when completing a concrete construction project, temperature strongly influences the rate of reaction and initial rheology of a concrete mixture [10,12]. To control the initial temperature of a concrete mixture materials are frequently preconditioned to approximately 73°F or optimized by including warmer/colder batch water to ensure the mixture is approximately 73°F. The control of the curing temperature occasionally extends past the initial fresh mixture via the usage of insulated formworks, curing blankets, and shades to reduce the variability and achieve the mechanical performance required of the final product. Unfortunately, RSPMs are not always cast considering the temperature as pavement patches generally open less than 24 hours after casting. This includes the RSPMs not being at the appropriate temperature during mixing as well as after casting. This section of the report focuses on the influence of temperature on RSPMs to determine which RSPMs can best respond to suboptimal environmental conditions.

This section of testing evaluates the setting behavior and initial strength gain of the previously mentioned RSPMs at temperatures of 50°F, 73°F, and 104°F. Testing includes Vicat setting time, isothermal calorimetry, UPV, compressive strength, and restrained shrinkage ring testing.

#### 3.3.1. Setting Time

The setting time of the RSPMs at variable temperatures is shown in **Figure 12** to **Figure 14**. The RSPMs generally showed a setting time less than 3 hours, the first time for compressive strength testing in ASTM C928-20. The only exception to the sub three hour setting time was for the MgO-1 sample at 50°F which set eight hours after casting. Testing generally observed that the setting from shortest to longest was 104°F to 73°F to 50°F. PC-2 was the only exception and is potentially a testing variability issue.

Testing on PC-based RSPMs is shown in **Figure 12**. Testing demonstrated that the PC-based RSPMs at 104°F displayed rapid setting times, ranging from 1-11 minutes to initial set and 2-17 minutes to final set. The short period before setting makes the proper placement and consolidation

of PC-based RSPMs in field unlikely and would generally make these patching materials unsuitable for hot weather conditions. At lower temperatures the range of setting times varies much greater with the initial setting times at 73°F ranging from 7-25 minutes and the final setting times ranging from 8-32 minutes. Providing a more manageable casting window, but still unsuitable for certain RSPMs (PC-1 and PC-3). Finally, testing at 50°F displays one of the primary advantages of the PC-based RSPMs as certain RSPMs maintain a final setting time of less than 30 minutes (PC-2, PC-4) allowing for the easy placement of the RSPM without worrying about an extended setting window limiting the reopening of the pavement to traffic. Overall, PC-based RSPMs provide a varied response that is generally able to adapt to project/environmental constraints but are limited at elevated temperatures.

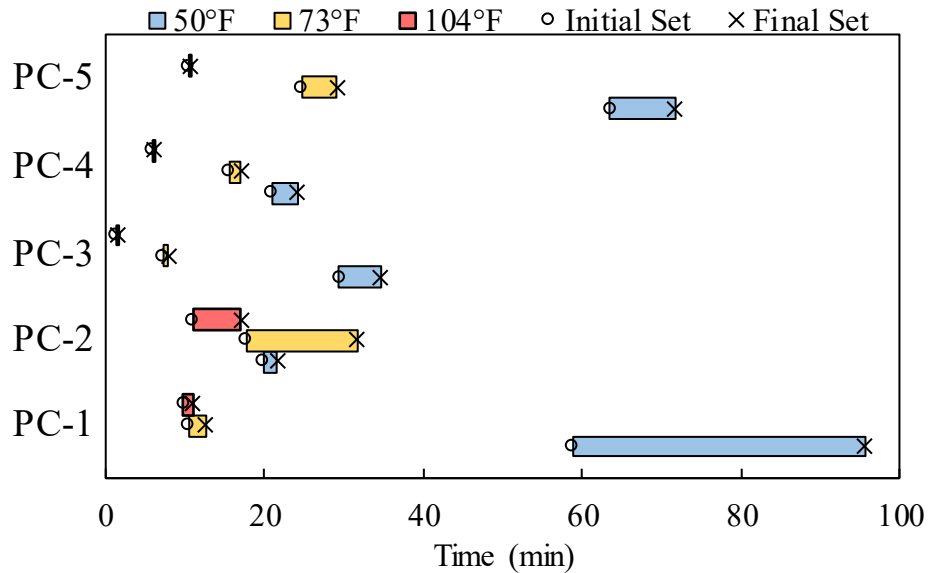


Figure 12: The Setting Time of PC-based RSPMs as a Function of Environmental Temperature

**Figure 13** displays the results for the CAC and CSA-based RSPMs. Relative to the PC-based RSPMs CAC-based RSPMs comparable initial and final setting times, with one RSPM matching the faster setting PC-based RSPM and another matching the slower setting PC-based RSPMs. Alternatively, the CSA-based RSPMs generally displayed slightly shorter setting times but were comparable to the PC and CAC-based RSPMs. CAC and CSA-based RSPMs appear tentatively capable of handling the full range of 50°F (CSA-2 and CAC-2), 73°F (CSA-1, CAC-1), and 104°F (CAC-1) without sacrificing performance. The suitability of these RSPMs is tentatively acceptable, but depends upon the other setting, shrinkage, and strength testing mentioned in the coming results.

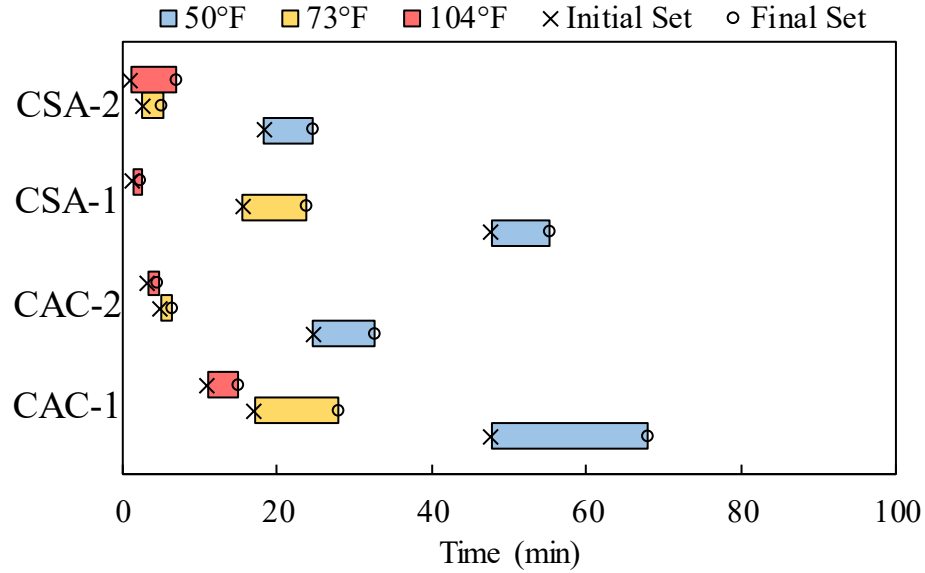


Figure 13: The Setting Time of CAC and CSA-based RSPMs as a Function of Environmental Temperature

The performance of the MgO-based RSPM is shown in **Figure 14**. Testing indicated that the setting behavior of the MgO-based RSPMs is significantly retarded compared to the PC, CAC, and CSA-based RSPMs, as the MgO-1's 104°F testing more closely aligned with the slowest setting other RSPMs at 50°F. MgO-1 appears suitable only for conditions where an extended setting time window is necessary, and traffic does not need to reopen shortly after casting. Furthermore, caution should be given when MgO-1 is used at lower temperatures as the final setting time occurs approximately 8.5 hours after the initial casting. Other suitable products should perform adequately at a significantly shorter time.

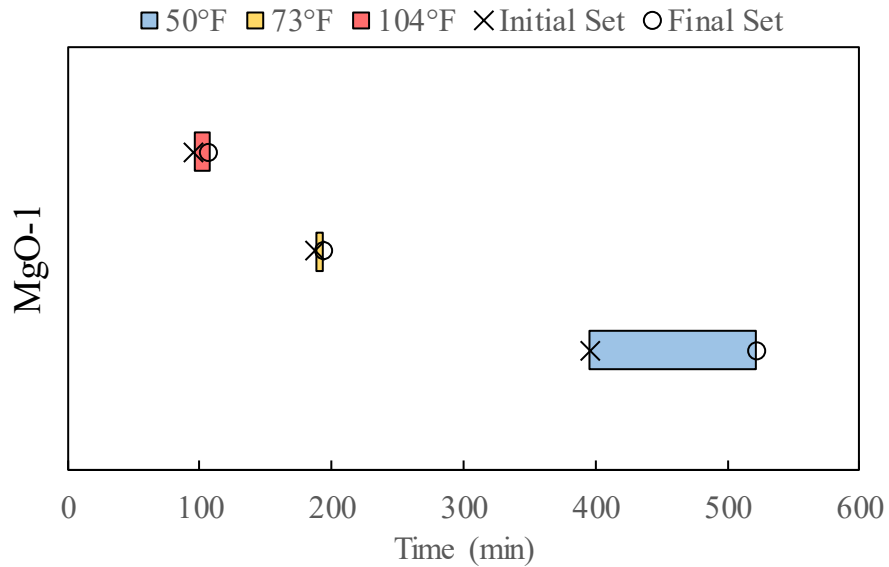


Figure 14: The Setting Time of the MgO-based RSPM as a Function of Environmental Temperature

### 3.3.2. Isothermal Calorimetry

The heat flow of the RSPMs at variable environmental temperatures is shown in **Figure 15a-j**. The cumulative heat of hydration was not calculated for these RSPMs, as the heat flow for most RSPMs exceeded the maximum range of the isothermal calorimeter resulting in inaccurate heat of hydration data. Furthermore, temperature equilibrium was unstable during the main heat release phase as a plurality of tests run experienced most of their release during the first 75 minutes after casting. Test results provide a relative comparison of the heat flow produced by each RSPM and indicate the duration of heat release. The relative order of the maximum heat flows as a function of temperature is 104°F being the fastest, 73°F being in the middle, and 50°F being the slowest. However, some tests demonstrated the peak heat flow for 50°F occurring before 73°F, which may be due to the type of accelerating admixtures utilized for those respective RSPMs.

For PC-based RSPMs (**Figure 15a-e**). The peak heat flows demonstrated a mix of performances as a function of temperature. While all RSPMs at 104°F demonstrated peak heat flows before the first hour after mixing the behavior was not the same at 50°F and 73°F. For PC-1 and PC-2 the time to peak heat flow was approximately equivalent occurring roughly three hours after initial casting. Alternatively, for PC-3, PC-4, and PC-5 the time to peak heat flow at 73°F was during the first hour after casting and the 50°F time to peak heat flow was highly variable with PC-5 exhibited a peak heat flow approximately 3 hours after casting and PC-3 and PC-4 exhibiting a peak heat flow approximately an hour after casting. Overall, testing on PC-based RSPMs indicates a rapid heat release shortly after casting comparable to the rapid setting times discussed previously. Care should be taken to ensure that thermal incompatibility and cracking will not occur because of the heat release from the RSPM.

The performance of the CAC, CSA, and MgO-based RSPMs relative to the PC-based RSPMs was comparable to the results previously discussed for the setting time of the RSPMs. CAC and CSA-based RSPMs exhibited performances comparable to the PC-based RSPMs with one CAC and CSA-based RSPM exhibiting behavior comparable to the slower reacting PC-based RSPM and one CAC and CSA-based RSPM exhibiting behavior comparable to the faster reacting PC-based RSPMs. Lastly, testing on the MgO-based RSPM demonstrated a greatly retarded peak heat flow relative to the PC-based RSPMs at all temperatures. For the MgO-based RSPM the heat flow did not yet reach ambient levels at 24-hours and required a longer 36-hour test duration, granted MgO-1 did achieve its peak heat flow at approximately 18-hours inside the typical test duration. Overall, tests results indicated similar recommendations to the setting time results with certain RSPMs appear more suitable for 50°F, 73°F, and 104°F testing, with the binder type being a secondary variable in most cases.

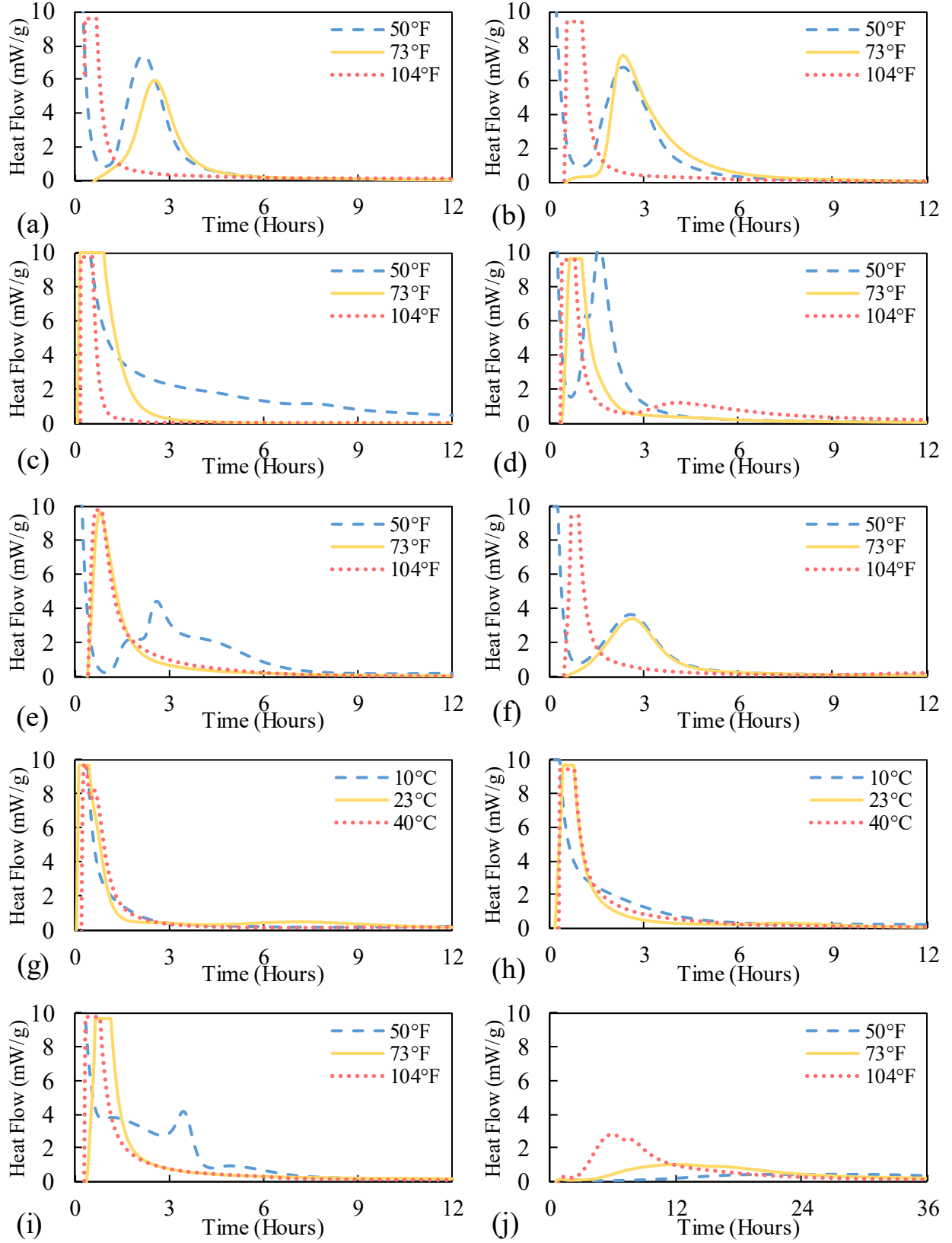


Figure 15: The Influence of Temperature on the Heat Flow of (a) PC-1, (b) PC-2, (c) PC-3, (d) PC-4, (e) PC-5, (f) CAC-1, (g) CAC-2, (h) CSA-1, (i) CSA-2, and (j) MgO-1

### 3.3.3. UPV

The early age development of mixture stiffness was evaluated via UPV testing to monitor the setting of the RSPMs as a function of temperature. The results of the UPV testing are shown in **Figure 16a-j**. The order of temperature reaching their terminal pulse velocity was 104°F first, 73°F second, and 50°F third for all RSPMs. This matches the results from isothermal calorimetry and indicates that as expected increasing temperature results in a faster rate of reaction for all binder types. Furthermore, the terminal pulse velocity magnitude either experienced minimal variation between the different temperatures or were generally ordered with 73°F being the highest, 104°F being the second highest, and 50°F being the lowest. This ordering is potentially due to the delay in hydration causing the lower temperature samples to not stiffen fully as well as the greater number of internal defects of the higher temperature samples due to worse rheology. There were some exceptions to this order, with PC-3, CAC-2, and CSA-2 having an order of 73°F, 50°F, and 104°F. This is potentially due to the 104°F samples for those RSPMs experiencing a more heightened negative consequence from the worse rheology caused by the elevated temperature. Furthermore, MgO-1 exhibited a second exception to the expected order as the MgO-1 samples at 73°F and 50°F did not achieve their terminal pulse velocity over the first 24 hours.

Taking a closer inspection of the UPV results for the PC-based RSPMs, two general observations are made. First is that the 104°F and 73°F samples reached their terminal pulse velocities exceptionally rapidly, generally in less than the first hour after casting due to the set accelerators and low water-to cement ratios of the PC-based RSPMs. One exception to this observation PC-5 did exhibit a longer time to reach terminal pulse velocity at 73 °F, reaching its terminal pulse velocity at approximately five hours after casting. The second major observation is that the 50°F pulse velocity evolution curve provides the most variability between the PC-based RSPMs, as PC-1 reached its terminal pulse velocity as early as 2 hours, whereas PC-5 reached its terminal pulse velocity closer to 8 hours after casting.

For the CAC and CSA-based RSPMs no obvious observable trends were found for each outside of the general trends previously discussed, respectively. This is partially due to the reduced amount of RSPMs for their respective binder type and due to differing mixture proportions and initial rheology of the RSPMs. Further trends could be determined when completing an analysis of more CAC and CSA-based RSPMs.

Lastly, the MgO-based RSPM exhibited the most unique profile, due to their differing setting behavior. As previously discussed, the slower stiffening of the MgO-1 samples matches the isothermal and setting time results where the MgO-based RSPMs set at a much slower rate than the PC, CAC, and CSA-based RSPMs. The most critical issue of these systems is that the 50°F 24-hour pulse velocity is approximately 50% of the 73 and 104°F samples. While the pulse velocity may continue to develop after 24 hours it is unlikely that it will reach the same terminal pulse velocity.



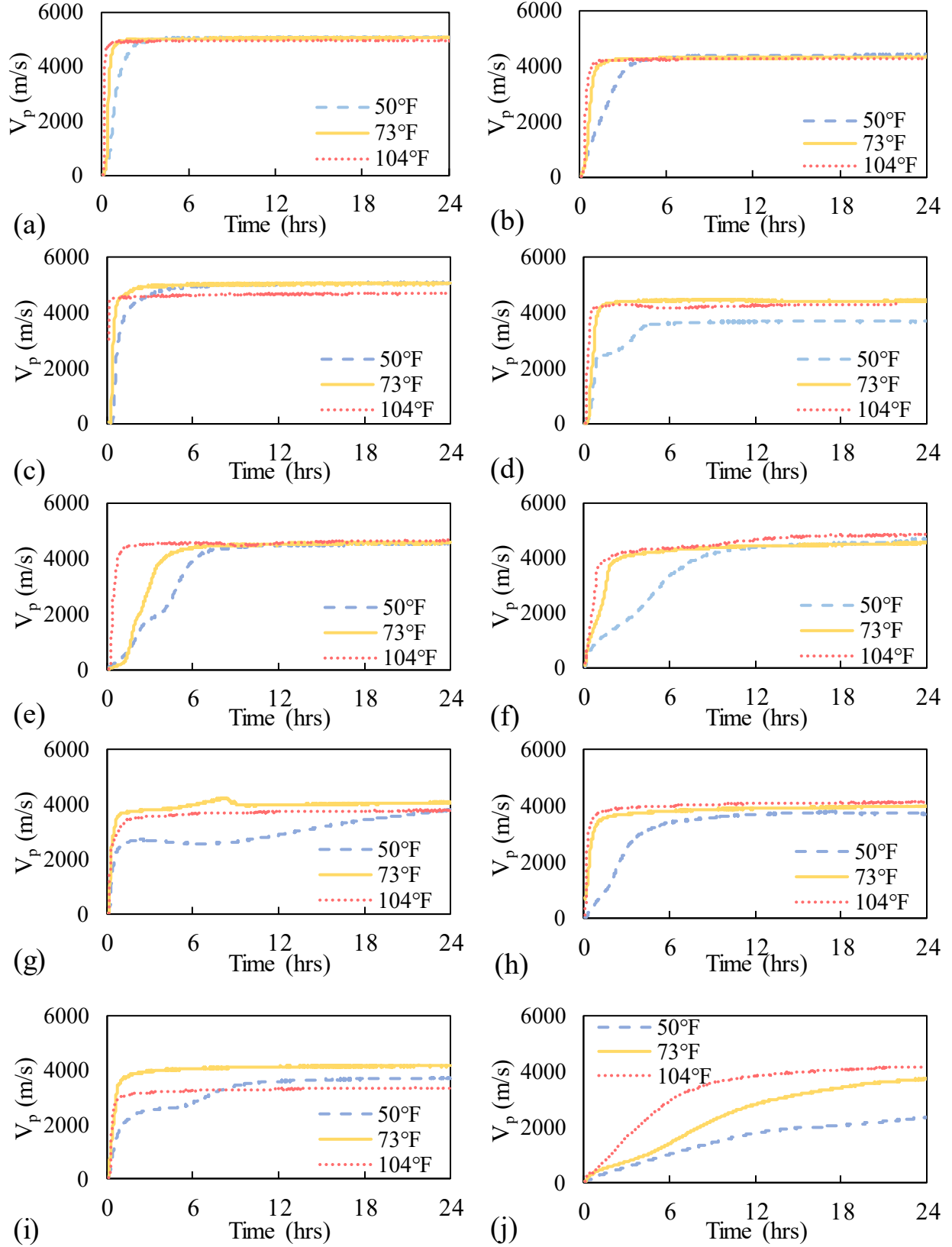


Figure 16: The Influence of Temperature on the Development of the Early Age Ultrasonic Pulse Velocity on (a) PC-1, (b) PC-2, (c) PC-3, (d) PC-4, (e) PC-5, (f) CAC-1, (g) CAC-2, (h) CSA-1, (i) CSA-2, and (j) MgO-I

### 3.3.4. Compressive Strength

The compressive strength of the RSPMs at variable exposure conditions are compared in Figure 18 and Figure 19. The compressive strength was collected at 0.25, 0.5, 1, 3, and 7 days to evaluate the strength evolution of RSPMs at early ages. Importantly, almost all samples at all temperatures exceeded the one-day (2 ksi) and seven-day (4 ksi) compressive strength requirements outlined in ASTM C928-20 for R1 RSPMs, except for MgO-1 one-day results at 50°F (1.4 ksi) and PC-3/CAC-2 at 104°F, which was uncastable and thereby demonstrated no compressive strength. Exceeding the ASTM C928-20 threshold provides ample evidence that the RSPMs evaluated provide sufficient compressive strength under reasonable exposure conditions. An example of an attempt to cast PC-3 is shown in Figure 17.



Figure 17: Influence of Elevated Temperature on RSPM Casting

The 50°F testing of the RSPMs generally resulted in a reduced compressive strength, except for the CSA cement samples, which provide greater strength at lower temperatures due to metastable hydration products not experiencing decomposition. However, PC-4 also experienced a slight compressive strength increase at 50°F indicating that a mineral admixture may be included to improve low temperature performance. For the samples not previously discussed the one-day compressive strength of the RSPMs varied from 70-110% of the compressive strength of the 73°F samples indicating sufficient performance. Similarly, the seven-day compressive strength of the RSPMs varied from 65-105% of the seven-day compressive strength of the 73°F RSPMs. Overall, indicating that low temperature exposure conditions appear to have minimal consequences for the performance of the RSPMs.

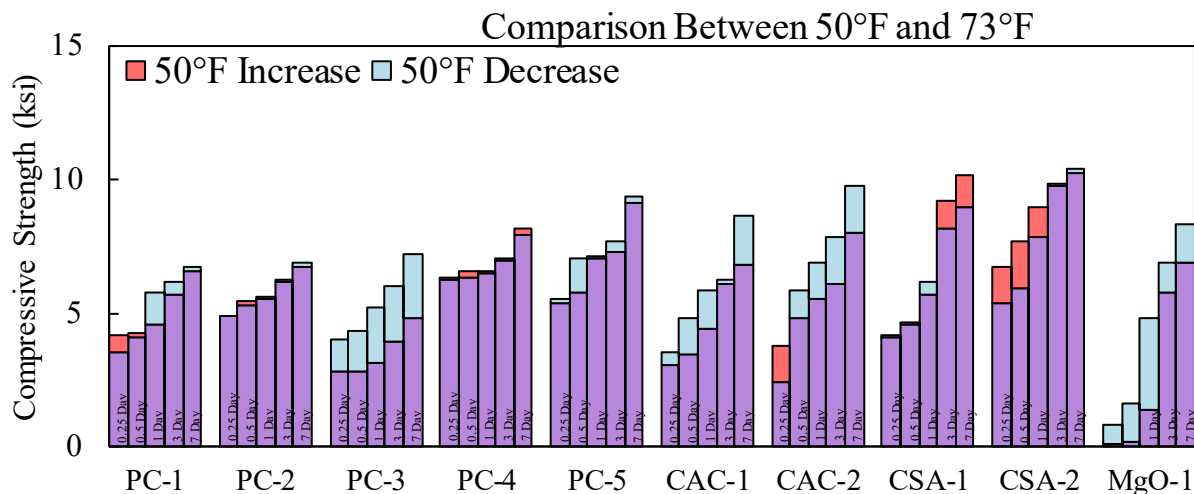


Figure 18: The Compressive Strength at 50°F Compared to the Compressive Strength at 73°F for RSPMs

However, the consequence of elevating temperature has a significantly different effect than that of lowering temperature. While at a temperature of 50°F the variation of performance was minimal with slight increases or slightly larger decreases at 104°F the performance of the RSPMs varies with some RSPMs being uncastable, others seeing substantial decreases in performance relative to the 73°F mixtures, and others seeing only slight deviations from the 73°F mixtures. For PC-3 and CAC-2 the decreased performance is full due to the short setting time (<5 minutes) not allowing for proper mixing or casting. However, for other mixtures, such as CSA-based RSPMs, different mechanisms result in the reduced performance. For the CSA-based RSPMs the metastable phases that at 50°F and 73°F resulted in improved performance are not present, as they have already decomposed resulting in a 20-30% reduction in strength for one-day and 7-day compressive strength samples. However, for all other RSPMs a slight increase in strength at all ages is observed. Specifically, the PC-based, CAC-based, and MgO-based RSPMs all react positively to elevated temperatures. For one-day compressive strength samples this is demonstrated by a 100-125% increase in compressive strength relative to the 73°F samples. Whereas for seven-day compressive strength it is demonstrated in a 98-119% change in compressive strength relative to the 73°F samples. Ultimately, providing better mechanical performance at the cost of reduced workability.

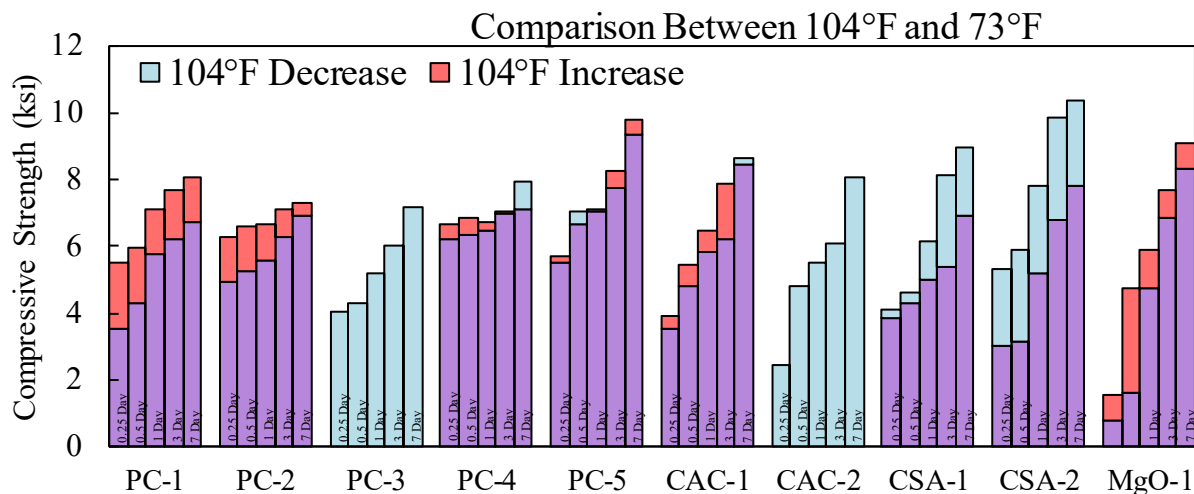


Figure 19: The Compressive Strength at 104°F Compared to the Compressive Strength at 73 °F for RSPMs

### 3.3.5. Shrinkage Ring Test

Supplemental testing of the restrained shrinkage of the RSPMs at 50, 73, and 104°F. For samples at 73°F that failed before five days from casting additional testing was completed at 50°F. For samples that failed after three days of casting or did not fail additional testing was completed at 104°F. However, CAC-1 and CSA-2 did not complete supplemental testing due to material availability issues. The results from the restrained shrinkage ring tests are shown in **Table 12**.

The testing completed at 50°F demonstrated an increased time to crack for PC-1 (19 days), PC-2 (1.25 days), CAC-2 (0.25 days), CSA-1 (>28 Days), and MgO-1 (> 28 Days). However, PC-4 (1 day) did experience an accelerated time to crack at 50°F. This general extension of time to cracking is likely due to the reduced rate of reaction of the RSPMs, which allows for a more organized hydration process that would result in a denser cement matrix and less internal strain. This is further supported by the strain rate data, which indicates that the 50°F samples experienced a lesser strain rate compared to the 73°F samples, 12-50% of the 73°F samples (except for PC-4s rate of 400% compared to its 73°F sample).

The testing at 104°F demonstrated similar results to those experienced by the 50°F samples. The influence of elevating the temperature of the RSPM resulted in an accelerated time to crack and an elevated strain rate. PC-3 (1.9 psi/day), PC-4 (1572 psi/day), and MgO-1 (25 psi/day) all demonstrated elevated strain rates, while PC-5 demonstrated a slightly reduced strain rate. The cause of the increased strain rate for most samples was the increased rate of reaction, which deposits hydration products in an unoptimized fashion resulting in internal stress.

Ultimately, RSPMs provide drastically different performances at varying temperature for restrained shrinkage and the other previously discussed test methods. PC-2, PC-4, CAC-1, and CAC-2 provided insufficient performance at any temperature to resist restrained shrinkage cracking. RSPMs that perform adequately at 50°F by demonstrating long time to crack and low strain rates are PC-1, CSA-1, and MgO-1. In comparison, PC-3, PC-5, and CSA-2 provide

excellent performance at 73°F and could potentially provide adequate performance at 50°F demonstrating times to crack more than 20 days at 73°F. Lastly, PC-3 and PC-5 appear to be the only RSPMs that display sufficient performance to resist restrained shrinkage cracking. Based upon these results it appears possible that some failures of patching materials are due to incorrect material selection for conditions, as no previous SCDOT standard required restrained shrinkage monitoring for RSPMs.

Table 12: Time to Cracking and Strain Rate from Restrained Shrinkage Ring Testing on RSPMs at 50, 73, and 104°F

50°F										
	PC-1	PC-2	PC-3	PC-4	PC-5	CAC-1	CAC-2	CSA-1	CSA-2	MgO-1
Time to Crack (Days)	19	1.25	---	1	---	---	0.25	>28	---	>28
Strain Rate (psi/day)	4.4	73.3	---	82.4	---	---	322.6	1.5	---	2.4
73°F										
Time to Crack (Days)	1.75	0.25	>28	4.25	22.25	1.5	0.1	4.5	>28	4.25
Strain Rate (psi/day)	34.4	142.7	1.3	20.4	4.5	59	990.2	5.2	3.17	10.5
104°F										
Time to Crack (Days)	---	---	>28	0.025	>28	---	---	---	---	1.5
Strain Rate (psi/day)	---	---	1.9	1572	2.1	---	---	---	---	25

## 4. Evaluation of Accelerated Batched Concrete Mixtures

---

### 4.1. Problem Statement

For large-scale pavement distresses the usage of RSPMs is ineffective, as the casting and finishing time greatly exceed the setting time and could result in premature failure. Instead, large-scale repairs utilize accelerated batched concrete mixtures (ABCMs), where a set accelerator is added to an ordinary Portland cement concrete. While the setting time of the ABCMs is longer than the RSPMs it is greatly accelerated compared to ordinary concrete. The accelerated setting time allows for traffic to open sooner, with ABCMs typically opening four to six hours after casting compared to the twelve to seventy-two hours typically required for an ordinary concrete.

ABCMs have become increasingly used to correct major distresses, but the accelerator used has not been properly characterized. The mechanism of set acceleration can be either from a physical or chemical process that influences the rate of reaction differently. For physical accelerators (XS 55 and XS 44) the set is accelerated via the inclusion of nucleation agents that provide additional sites for C-S-H to form. Whereas chemical set accelerators accelerate cement hydration by acting as a catalyst in the cement hydration reaction process accelerating the rate of setting. Furthermore, the chemical set accelerators are further broken down as either chloride (Cl) or non-chloride-based (NCl and NCl-1) set accelerator, as chloride-based set accelerators effective can promote steel corrosion. Ultimately, the variability in chemical composition of set accelerators can result in products under the same designation providing drastically different performances both in terms of early-age properties and hardened performance.

### 4.2. Objective

This study to better understand the hydration kinetics of these set accelerators focuses on the influence that water-to-binder, cement type, temperature (50 and 73°F), and dosage rate have on the early-age properties of the set accelerators. This study does not provide an in-depth investigation of the hardened performance of the ABCMs, as that performance is greatly influenced by the concrete mixture proportions. However, limited testing does explore the change in compressive strength and restrained shrinkage of the ABCMs. The results from these studies allow for the formation of recommendations for when physical and chemical accelerators should be utilized. Additionally, recommendations are made to set bounds for when these set accelerators may provide less than desirable performance.

### 4.3. Results

#### 4.3.1. Setting Time

The initial characterization of setting time of the set accelerators was conducted utilizing at Type I/II and Type III Portland cement at normal consistency at 73°F to provide a baseline for how these set accelerators are designed to perform under ideal construction conditions at their highest and lowest recommended dosage. The results of the tests with Type I/II cement are shown in **Figure 20** and the results for the tests with Type III cement are shown in **Figure 21**. Importantly, the high dosage of the SU accelerator was not completed for the Type I/II cement due to the inability to reach a cohesive mixture. This is potentially due to the high dosage being too great for typical ABCM proportions and the accelerator providing significantly more rapid set acceleration than the other set accelerators chosen.

Testing completed with the Type I/II cement generally showed that the inclusion of the set accelerator resulted in the initial and final setting time being reduced by 50 and 100 minutes, respectively. However, the NCI and SU admixtures were outliers with the NCI admixtures resulting in comparable initial and final setting times at the low and high dosage to the control and the SU admixture completing the initial and final set in 5 and 45 minutes, respectively. The limited change in setting time from the NCI could indicate that the acceleration may not be a hardening, but rather an accelerated heat release, but will be discussed more in the following sections. The full order of the initial and final setting times in ascending order are as follows:

$T_i$  at Low Dosage – *SU* → *CI* → *XS 44* = *XS 55* → *NCI-1* → *Control* → *NCI*

$T_i$  at High Dosage – *CI* → *XS 44* → *NCI-1* → *XS 55* → *NCI* → *Control*

$T_f$  at Low Dosage – *SU* → *XS 44* → *XS 55* → *CI* → *NCI-1* → *NCI* → *Control*

$T_f$  at High Dosage – *CI* → *XS 44* → *NCI-1* → *XS 55* → *NCI* → *Control*

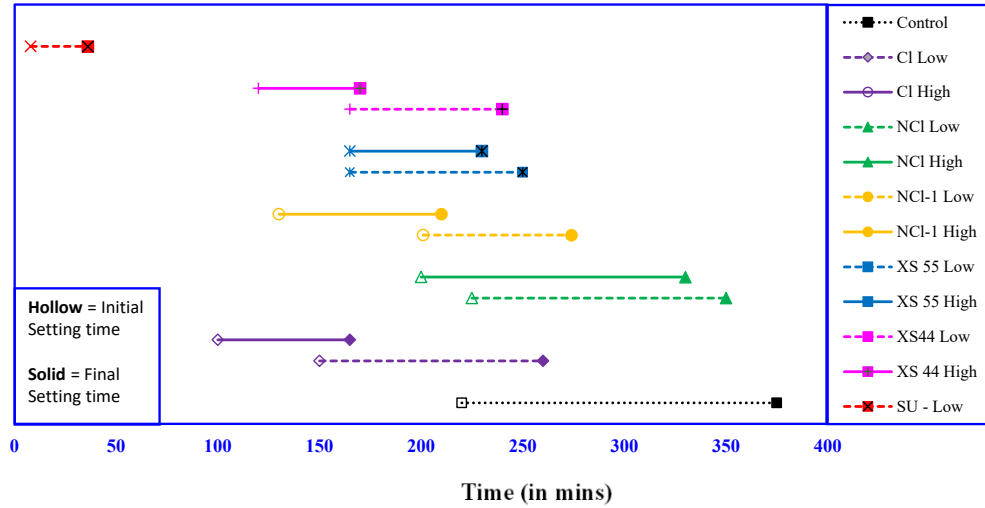


Figure 20: Vicat Needle Setting Time for Type I/II Cement at Normal Consistency at 73 °F

The testing completed with the Type III cement generally showed a reduced acceleration compared to the Type I/II cement, which is potentially due to the rate of reaction already being accelerated by the finer nature of the Type III cement. The time to setting for the control sample was approximately 160 minutes for the initial set and 250 minutes for the final set. On average, the samples containing set accelerators had an initial set between 110-140 minutes and a final set between 150-225 minutes. Which, while faster than the Type I/II samples average, does not provide the same relative acceleration comparing the control to the accelerated samples. Additionally, the Cl low, XS 55 low and high, and XS 44 low demonstrated negligible reductions in setting time. The comparable setting time for XS 55 and XS 44 to the control is potentially due to the physical acceleration mechanism, which provides limited benefit when excess nucleation sites are present. For the chloride-based accelerator the apparent reduced acceleration of the initial and final setting time is potentially due to the maximization of the catalyzation, as the initial and final setting time of the samples tested for the Type I/II and Type III cements deviated by less than five minutes. The full order of the initial and final setting times for the Type III cement is listed in ascending order as follows:

$T_{i \text{ at Low Dosage}} - SU \rightarrow Cl \rightarrow XS\ 44 \rightarrow NCl \rightarrow NCl-I \rightarrow Control \rightarrow XS\ 55$

$T_{i \text{ at High Dosage}} - SU \rightarrow NCl-I \rightarrow XS\ 44 \rightarrow NCl \rightarrow Cl \rightarrow XS\ 55 \rightarrow Control$

$T_{f \text{ at Low Dosage}} - SU \rightarrow NCl-I \rightarrow NCl \rightarrow XS\ 44 \rightarrow XS\ 55 \rightarrow Control \rightarrow Cl$

$T_{f \text{ at High Dosage}} - SU \rightarrow XS\ 44 \rightarrow NCl-I \rightarrow NCl \rightarrow Control \rightarrow XS\ 55 \rightarrow Cl$



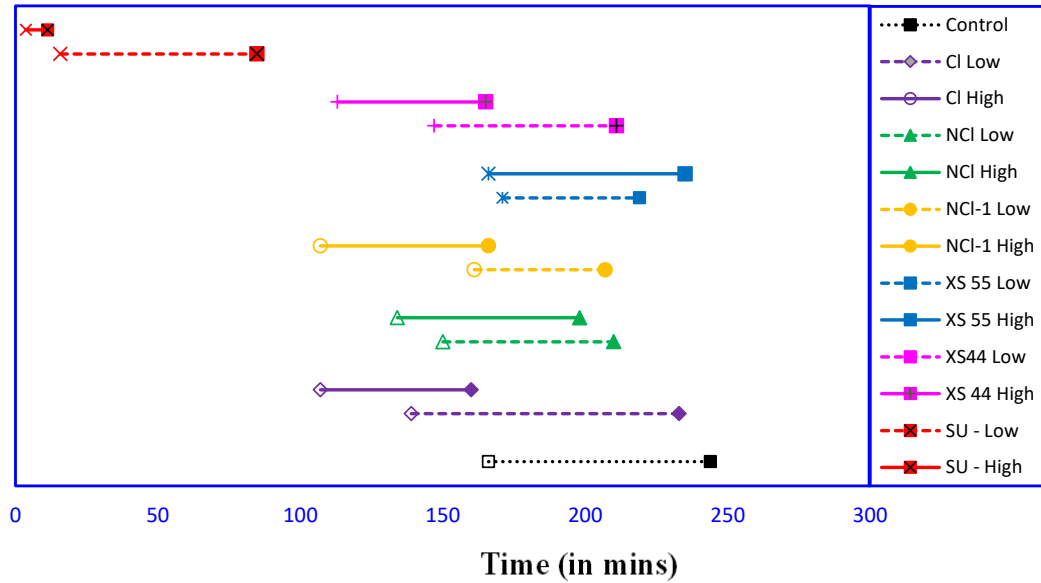


Figure 21: Vicat Needle Setting Time for Type III Cement at Normal Consistency at 73 °F

After identifying baseline performance to the set accelerators, the influence of temperature and water to binder ratio on the setting behavior of ABCMs containing set accelerators was investigated utilizing a Type III cement. The water to binder ratios tested were 0.33, 0.36, and 0.42 at temperatures 50 and 73°F. The results for which are included in **Figure 23** to **Figure 24** and **Table 13** to

Table 15. General trends indicated that as the water-to-cement ratio decreased the setting time decreased and that with decreased temperature the setting time increased, as expected. However, the behavior of the set accelerators provided more variable performance.

**Figure 22** displays the results from testing at 50 and 73 °F at a water-to-cement ratio of 0.33. The initial and final setting time of the 50°F control was approximately 200 and 300 minutes, respectively. Whereas the initial and final setting time of the 73°F control was approximately 165 and 225 minutes, respectively. Except for the SU accelerator, the initial and final setting time for mixtures at both 50 and 73 °F containing set accelerators showed either small decreases or increases in setting time for both low and high dosages of set accelerators. However, the 50 °F samples did experience the retarding effect more heavily than the 73 °F samples with seven of the twelve high and low dosage samples exhibiting a delayed final setting time. The delay in setting time from the inclusion of set accelerators at low water-to-cement ratios is potentially due to the rate of reaction being limited by the availability of water rather than the chemical composition of the pore solution. Additionally, the location of the hydration products that do form may limit further hydration as unhydrated cement is blocked from reacting with the limited water available, but the physical set accelerators also exhibiting the delayed setting time limits this theory. Further testing should investigate the combined effect of accelerators and water reducers to better identify the cause of the delayed setting time, as the better dispersion of the cement may provide an accelerated rate of reaction.

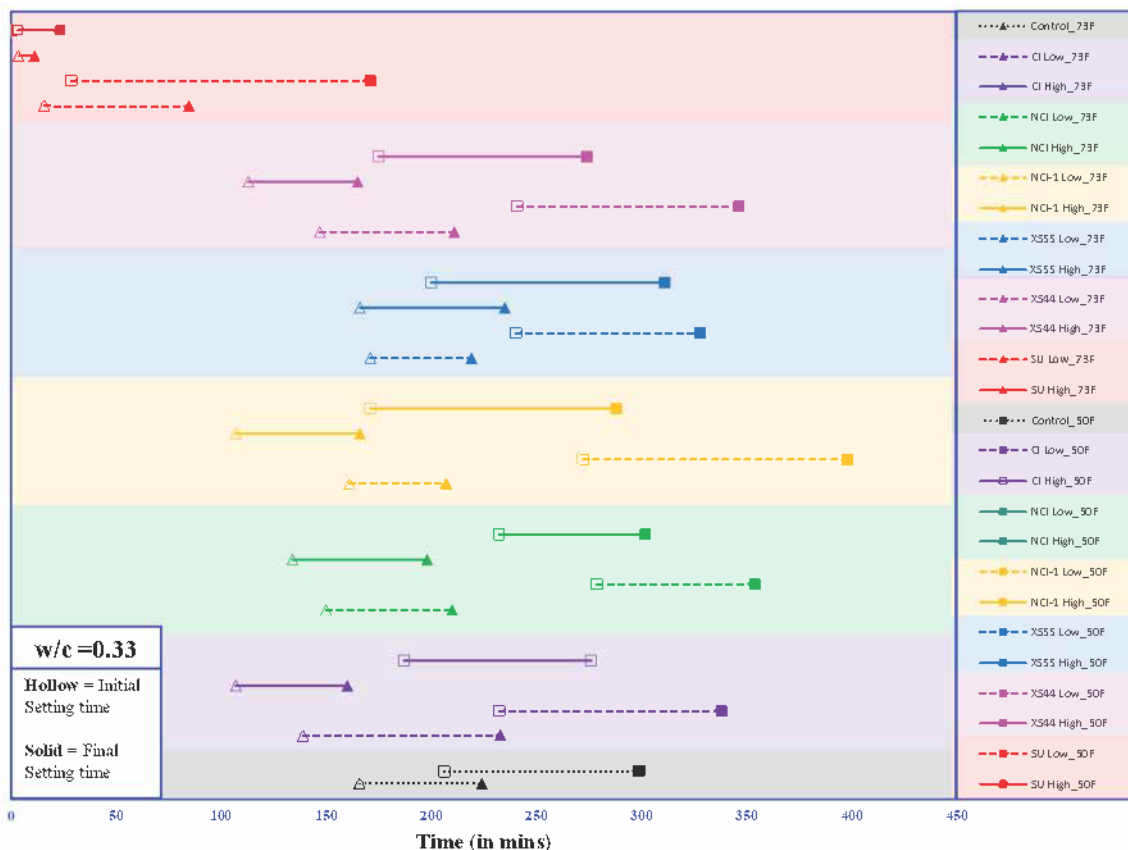


Figure 22: Influence of temperature on setting time of Type III cement at w/c = 0.33

Further analysis on the role of temperature was conducted by calculating the reduction in setting time, reduction in the interval between the initial and final setting time and the apparent activation energy as a function of the temperature increase from 50 to 73 °F. The apparent activation energy ( $E_A$ ) has been calculated for initial and final setting time for two temperatures of 50 °F and 73 °C as [22]:

$$E_A = \frac{-\ln\left(\frac{t_{50}}{t_{73}}\right)R}{\left(\frac{1}{T_{73}} - \frac{1}{T_{50}}\right)}$$

Where,  $E_A$  is the apparent activation energy in kJ/mol,  $t_{50}$  and  $t_{73}$  are the times of setting at 50 and 73 °F and  $T_{50}$  and  $T_{73}$  are the temperature (in K) of 50 °F (283.15 K) and 73 °F (296.15 K) and  $R$  is the universal gas constant (8.314 J/(mol.K)).

The apparent activation energy was determined to identify how the inclusion of set accelerator changes the minimum energy for the cement hydration reactions to occur. The results from this analysis are shown in **Table 13**. Results generally indicated that the setting time was reduced by approximately 40% for all chemical admixtures, apart from SU high which demonstrated an increase in setting time due to test variability and its rapid setting time creating some error. In comparison, the setting time of the control mixture was only reduced by approximately 20% when increasing the temperature from 50 to 73 °F. This discrepancy indicates that the set accelerators are becoming more effective at higher temperatures when utilized at low water-to-cement ratios. This could cause issues for ABCMs if the assumed reduction in setting time is based upon a fixed value and does not account for the effect of temperature. Doing so could potentially result in the premature opening to traffic, as the final setting time is extended and cause unexpected project delays. Further analysis of the apparent activation energies also highlighted the danger of using accelerators at a lower water to binder ratio, as the apparent activation energy was of the control mixture was lower than all the low accelerator dosages and all the high dosage except for NCl. An increase in activation energy corresponds to a reduction in the rate of reaction and would potentially reduce the degree of hydration of concrete. Overall, testing indicates that the usage of set accelerators at low water-to-cement ratios is problematic and could result in increased setting times.

Table 13: Percentage difference in setting time and  $T_i$  to  $T_f$  interval with temperature change from 50 to 73 °F for Type III cement at w/c = 0.33

Mix	Dosage of accelerators	Reduction in Setting time (%) with temperature increase		Reduction in interval between $T_i$ and $T_f$ in %	Apparent activation energy ( $E_A$ ), kJ/mol	
		$T_i$	$T_f$		$T_i$	$T_f$
Control		19	25	38	11.6	15.5
Cl	Low	40	31	11	27.5	20
NCl		46	41	20	27.3	29.2
NCl-1		41	48	63	33.33	28
XS 55		29	33	45	29.4	22.6

XS 44		39	39	39	28.1	35.1
SU		46	50	51	25.1	29.5
CI		43	42	40	18.2	21.7
NCI		42	34	9	10	15
NCI-1	High	37	42	50	26.5	26.5
XS 55		17	24	38	23.5	27.2
XS 44		35	40	47	32.9	37.7
SU		-23	51	63	NA	38.6

**Figure 23** displays the results of testing completed at water-to-cement ratio of 0.36 as a function of temperature and admixture type/dosage. The testing at 73°F saw similar observations to the results from testing at a water-to-cement ratio of 0.33 when comparing the control samples to the samples containing set accelerators, with multiple high and low dosages retarding rather than accelerating the setting time relative to the control. However, the 50°F samples all demonstrated a reduction in the initial and final setting time in comparison to the control. The improved performance of the 50°F accelerator samples relative to their 73°F counterparts further support the hypothesis that the inclusion of set accelerators at low water-to-binder ratios predominately hindering the rate of reaction due to unoptimized deposition of the hydration products, as lower temperatures and slower setting times would allow for a more even deposition.

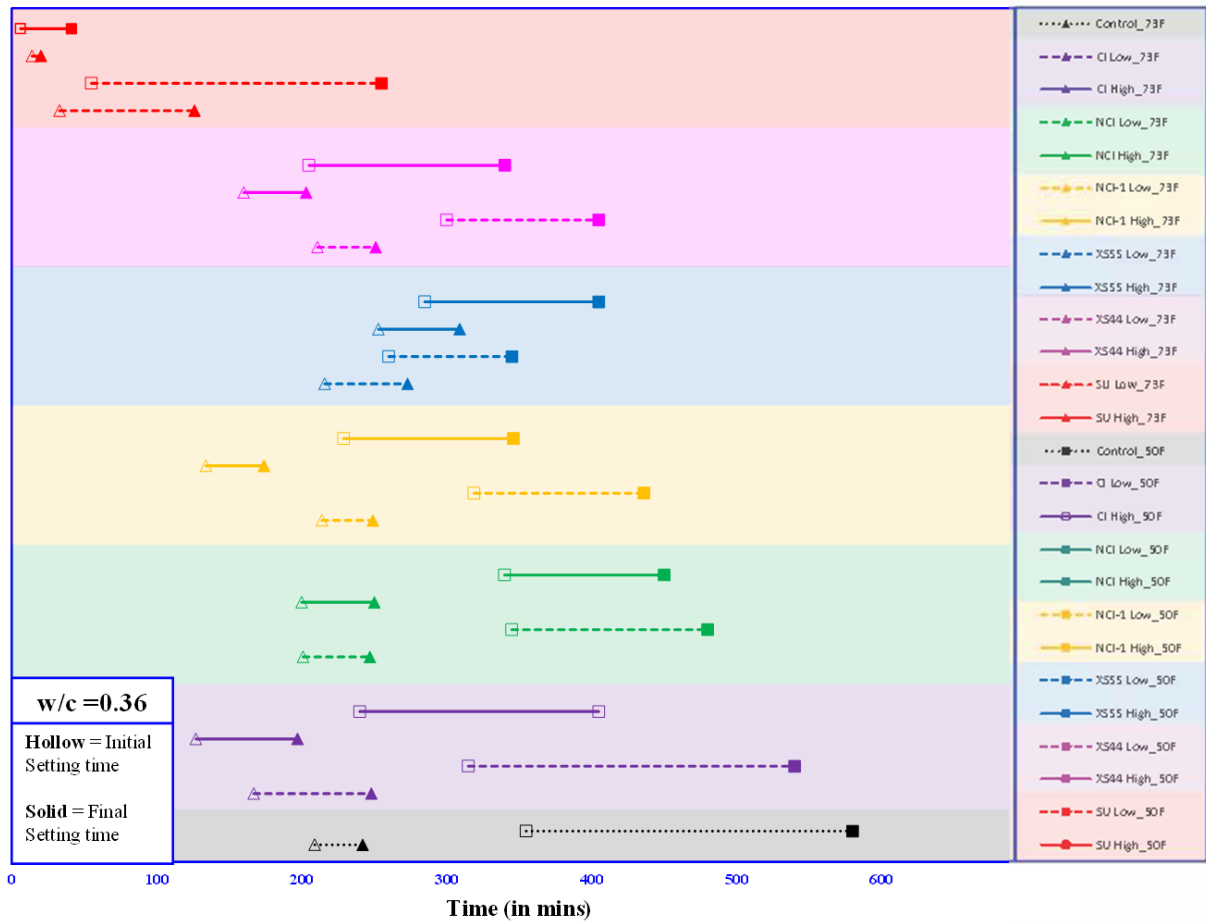


Figure 23: Influence of temperature on setting time of Type III cement at  $w/c = 0.36$

Further analysis of the testing on the water-to-cement of 0.36 samples was conducted to determine the reduction in setting time, reduction in initial and final setting time interval, and the apparent activation energy as a function of increasing temperature (

**Table 14).** Relative to the results discussed for the water-to-cement of 0.33 samples, the percent reduction in initial and final setting was comparable with the reduction in initial setting showing no change and the final setting time showing a slight increase in the percent reduction. This would indicate that the set accelerators are seeing a slight increase in the change in performance as a function of temperature, but not a significant jump. However, the results for the reduction in interval between the initial and final setting time did differ with the increased water-to-cement ratio with the average percent reduction increasing from approximately 35% to 45%, indicating that with increasing water-to-cement ratios the influence of temperature is greater, resulting in it being a more influential parameter for design. Finally, tests results analyzing the apparent activation energy found minimal change in the necessary activation energies at the elevated water-to-binder ratio, indicating that the hydration process is still limited.

Table 14: Percentage difference in setting time and  $T_i$  to  $T_f$  interval with temperature change from 50 °F to 73 °F for Type III cement at w/c = 0.36

Mix	Dosage of accelerators	Reduction in Setting time (%) with temperature increase		Reduction in interval between $T_i$ and $T_f$ in %	Apparent activation energy ( $E_A$ ), kJ/mol	
		$T_i$	$T_f$		$T_i$	$T_f$
Control		41.1	58.3	33	11.6	46.9
CI	Low	47	54.1	81	34	41.7
NCI		41.7	48.5	46	29	35.6
NCI-1		32.9	42.9	35	21.4	30
XS 55		16.9	20.9	37	9.9	12.6
XS 44		29.7	38	40	18.9	25.7
SU		40	50.6	93	27.4	37.7
CI	High	47.1	51.4	70	34.1	38.6
NCI		41.2	44.4	50	28.5	31.5
NCI-1		41.5	49.7	40	28.7	36.9
XS 55		11.2	23.7	56	6.4	14.5
XS 44		22	40.3	43	13.3	27.7
SU		-133.3	51.2	6	45.4	38.5

Testing at a water-to-binder ratio of 0.42 was conducted at 50 and 73°F in a continuation of the study investigating the influence of water-to-cement ratio on the effectiveness of set accelerators. The results for testing at a water-to-cement ratio of 0.42 are shown in **Figure 24**. The testing at 50 and 73°F both began to demonstrate the increase in effectiveness of the set accelerator, with the setting time substantially reduced at low and high dosages for all accelerators, except for NCI-1. This indicates that set accelerators are most effective at high water-to-cement ratios and that their inclusion should be closely monitored.

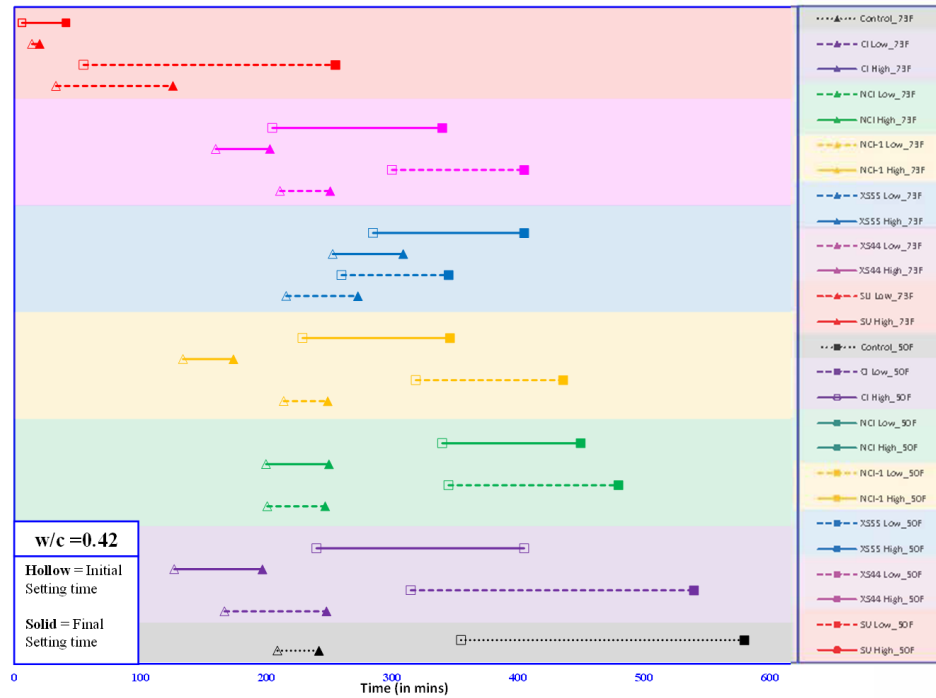


Figure 24: Influence of temperature on setting time of Type III cement at w/c = 0.42

Further analysis of the testing on the water-to-cement of 0.42 samples was conducted to determine the reduction in setting time, reduction in initial and final setting time interval, and the apparent activation energy as a function of increasing temperature (

Table 15). Relative to the control, the percent reduction in initial and final setting was increased for all chemical set accelerators and all high dosage physical set accelerators. However, for the low dosages of physical set accelerators the impact was negative showing little variation as a function of temperature. Finally, tests results analyzing the apparent activation energy found that relative to the control the set accelerator provided equal or lesser required apparent activation energies indicating reduced energy input to achieve the hydration reactions.



Table 15: Percentage difference in setting time and  $T_i$  to  $T_f$  interval with temperature change from 50 to 73 °F for Type III cement at w/c = 0.42

Mix	Dosage of accelerators	Reduction in Setting time (%) with temperature increase		Reduction in interval between $T_i$ and $T_f$ in %	Apparent activation energy ( $E_A$ ), kJ/mol	
		$T_i$	$T_f$		$T_i$	$T_f$
Control		33.2	43.2	37	21.6	30.3
CI	Low	31.3	33.3	100	20.1	21.7
NCI		33.7	44.7	41	22	31.8
NCI-1		37.8	35.3	75	25.4	23.3
XS 55		3.1	15.9	26	1.7	9.3
XS 44		5.1	17.5	36	2.8	10.3
SU		68.1	46.2	105	61.3	33.3
CI	High	18.2	32.3	43	10.7	20.9
NCI		48.2	49.5	73	35.2	36.6
NCI-1		43.1	37.9	99	30.3	25.5
XS 55		0	18.8	33	0	11.2
XS 44		24.7	31.5	50	15.2	20.3
SU		46.2	64.6	21	33.2	5.6

#### 4.3.2. Isothermal Calorimetry

After identifying that the setting behavior of the ABCMs containing set accelerators experienced drastically differing performances as a function of dosage further testing was conducted utilizing isothermal calorimetry to observe the cumulative heat release and early-age heat flow of accelerated mixtures including variable dosage of the chosen set accelerators between the high and low recommended dosages. The dosages utilized are listed in percent by weight of cement added to the paste samples. Testing was completed at 73°F with a Type III cement and a water-to cement ratio of 0.42 to maximize the effectiveness of the set accelerators.

The first analyzed set accelerator was the CI accelerator at dosages of 0 (control), 0.52, 1.44, 2.36, and 3.26% by weight of cement (bwoc). The results for the isothermal calorimetry testing are shown in **Figure 25**. The addition at a lower dosage of 0.52 % bwoc does not change the onset of acceleration stage (length of dormant period), however, the rate of heat flow increases with a higher alite peak as compared to control. As the dosage is increase to 1.44% bwoc and above, the length of dormant period starts to reduce. The reduction of dormant period is a function of dosage, as the dosage increases, the length of dormant period decreases and the rate of hydration acceleration increase. However, the height of main acceleration peak was lower for dosage of 3.26%. In addition to that, as the dosage is increasing the prominence of sulfate depletion peak decreases. At the high dosage of 3.26% bwoc, the sulfate depletion peak is not detected. Additionally, based upon testing an analysis of the HoH plots the addition of accelerator increases the heat of hydration (HoH) at 12-hours by 8.96%, 44.36%, 60.89%, 149.21% as compared to control for dosages of 0.52%, 1.44%, 2.34% and 3.26% bwoc respectively. At 1-day, the increase in HoH is about 4%, 18.8%, 22.95% and 13.6%. At 3-days, the increase is about 1.43%, 13.45%, 15.46% and 8.8%. At 7-days, the increase is about -0.32%, 12.75%, 14.13% and 9.31%. The effect

of low dosage of 0.52% on HoH increase diminishes as the age of samples increases and there is no increase at 7-days as compared to control. For all ages above 12-hours, the data shows that the dosage of 2.34% bwoc shows the highest increase in HoH and any increase in dosage above 2.34% decreases the performance.

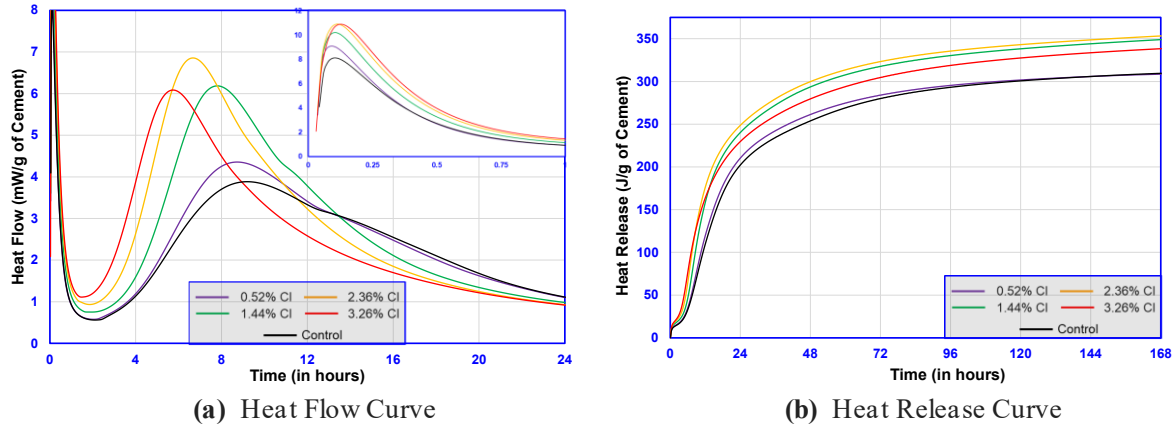
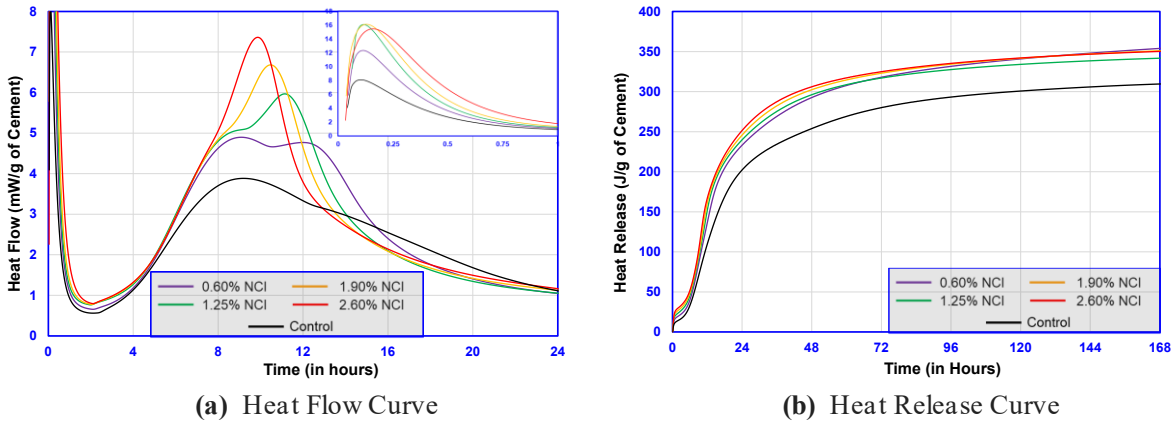


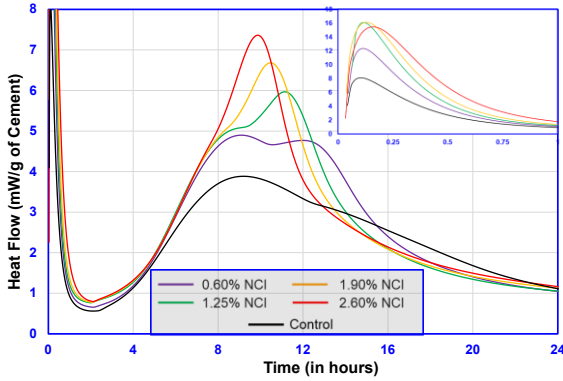
Figure 25: Hydration kinetics for Cl accelerator at 73°C (w/c = 0.42)

For the NCl accelerator testing was conducted at dosage rates of 0 (control), 0.60, 1.25, 1.90, and

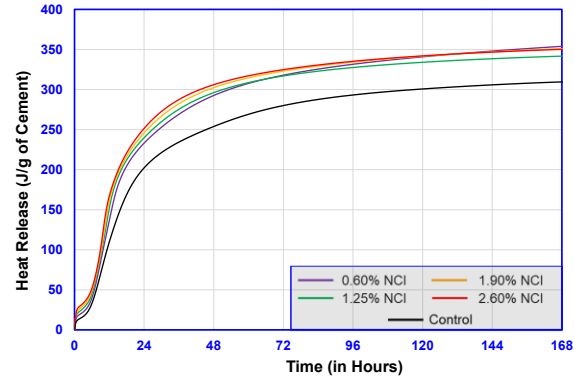


2.60% bwoc. The results for which are shown in Figure 26. The addition of the NCl accelerator at any dosage does not change the length of dormant period. However, the rate of acceleration from the onset of acceleration period is higher as compared to the control. The acceleration period peak increases as the dosage is increased, however, the sulfate depletion peak significantly shows higher heat signature, and the onset of sulfate depletion peak is a function of dosage. Higher the dosage, the faster the onset of sulfate depletion peak. Beyond the dosage of 1.90% bwoc, there is no distinction between alite peak and sulfate depletion/second aluminate peak. The sulfate depletion peak onset time reduces as a function of dosage of the accelerator added to the mix. In addition, the alite peak and sulfate depletion peak start to merge into single peak above the dosage of 1.90% bwoc. Analysis of the heat of hydration plots indicated that at 12- hours, the addition of NCl increases the HoH by 24.32%, 38.58%, 46.46% and 52.04% for dosages of 0.6%, 1.25%, 1.90% and 2.60% respectively. For 1-

day the increase is 15.3%, 18.6%, 21.51% and 24.34%. The influence of presence and dosage of accelerator is significant till 24-hours. At 3-days the effect of increasing dosage diminishes and the increase in HoH is about 13-16% and for 7-days it ranges between 10-14% with highest 7-day HoH recorded for low dosage of 0.6% bwoc. The HoH released at the end of 7-days is



(c) Heat Flow Curve

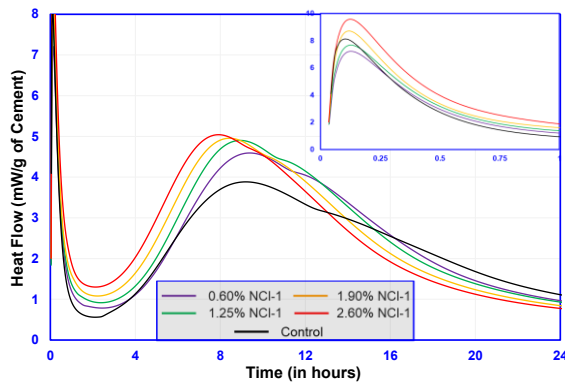


(d) Heat Release Curve

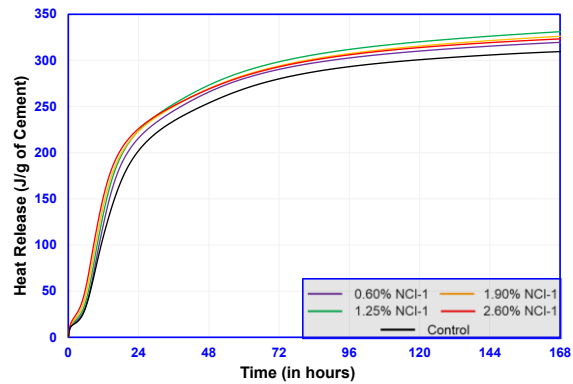
approximately similar.

Figure 26: Hydration kinetics for NCI accelerator at 73°C (w/c = 0.42)

For the NCI-1 accelerator testing was conducted at dosage rates of 0 (control), 0.60, 1.25, 1.90, and 2.60% bwoc. The results for which are shown in **Figure 27**. The addition of 0.60% bwoc does not influence the dormant period, however, as the dosage is increased the length of dormant period reduces. In addition, the addition of accelerator increases rate of acceleration after the onset of acceleration period and the main acceleration peak for alite increases and the dosage is increased. There is no significant effect on the prominence of the sulfate depletion peak. When observing the heat release curves for NCI-1 accelerator with variable dosage as compared to control. The addition of 0.60%, 1.25%, 1.90% and 2.60% bwoc NCI-1 based accelerator increases the HoH by 11.63%, 22.3%, 30.01%, 38.93%, respectively after 12-hours of hydration. However, from 24-hours to 172-hours, the effect of accelerator addition diminished and was in the range of 6-11%, 3-6% and 3-6% at 1-day, 3-day and 7-day respectively.



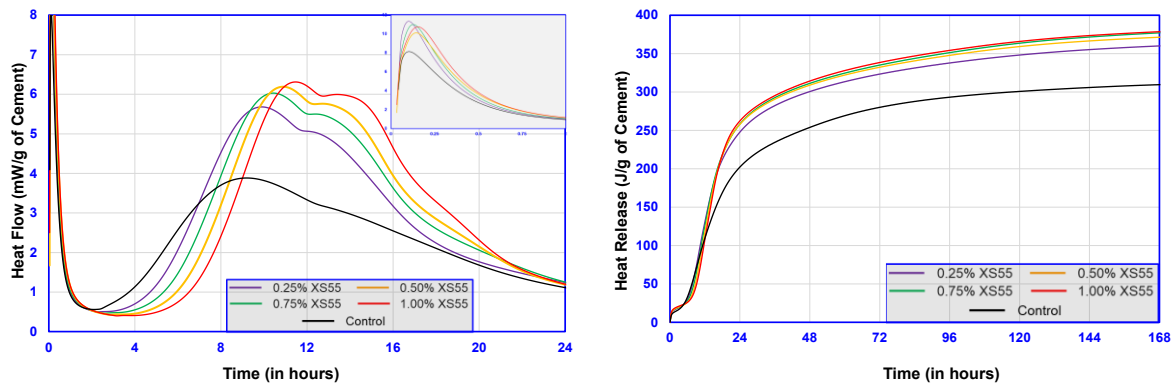
(a) Heat Flow Curve



(b) Heat Release Curve

Figure 27: Hydration kinetics for NCI-1 accelerator at 73°C (w/c = 0.42)

After completing the analysis of the chemical reaction-based set accelerators the physical set accelerators were tested. For the XS-55 accelerator testing was conducted at dosage rates of 0 (control), 0.25, 0.50, 0.75, and 1.00% bwoc. The results from testing of the XS-55 accelerator shown in **Figure 28**. Analysis of the heat flow found that as the dosage of XS 55 is increased, the length of the dormant period increases. This increase in dormant period (retardation of hydration reaction) can be attributed to the presence of polymeric dispersing medium present in the XS 55 or triisopropylamine in the system. The higher dosage of 1 % bwoc shows a retardation of about 2.5 hours. As the dosage of XS-55 is increased, the main hydration peak and sulfate depletion peak/accelerated aluminate reaction is significantly higher than the control. A slight hump is noticed between 16 to 24 hours for 1% and 0.25% bwoc dosages. When analyzing the heat of hydration data, it was found that the addition of 0.25%, 0.50%, 0.75% and 1% XS 55 based accelerator reduces the heat of hydration slightly till 11 hours. However, the addition of XS 55 increases the HoH after 12-hours to 19.2%, 14.8%, 7.1 % for dosages of 0.25%, 0.5% and 0.75%, however, for a dosage of 1 % XS 55, the HoH is still at 1.6% lower as compared to control. As the hydration reaction progresses, the HoH with XS 55 based mixes is significantly higher than control. At the age of 24-hours, the HoH increases by 22.5%, 27.7%, 27.5%, 29.7% as compared to control and at 7-days, the HoH is 16.3%, 21.8%, 20% and 22.3% higher as compared to control at XS 55 dosages of 0.25%, 0.5%, 0.75% and 1% respectively. At 7-days, the increase in HoH is a function of the dosage of XS 55.



(a) Heat Flow Curve (b) Heat Release Curve  
Figure 28: Hydration kinetics for XS-55 accelerator at 73°C (w/c = 0.42)

Further testing of physical set accelerators was conducted on the XS-44 set accelerator at 0 (control), 0.60, 1.25, 1.90, and 2.60% bwoc. The results from this testing are shown in **Figure 29**. As seen in the figure, the addition of XS 44 reduces the length of dormant period as the dosage is increased above 1.25%. For all dosages of XS 44, the rate of reaction (Heat Flow) significantly increases as compared to control. As the XS 44 dosage is increased, the onset and height of sulfate depletion peak is accelerated and higher, respectively. Furthermore, when observing the heat release curves it is observed that the addition of XS 44 increases the HoH at all stages of hydration reaction beyond 12 hours. The lower dosage shows a slight retardation of reaction and the heat of hydration at 6-hours for the dosage of 0.6% XS 44 is 12.3% lower than control, however, for the HoH is

12.6%, 34.5% and 59.6% higher as compared to control for dosages of 1.25%, 1.90% and 2.60% respectively. As the reaction continues, the addition of XS 44 shows a higher HoH for all dosages of XS 44. With HoH increase of 17.6%, 23%, 26.7%, and 29.8% at 24-hours and 9.6%, 11.7%, 11.3% and 11.4% at 7-days as compared to control for dosages of 0.6%, 1.25%, 1.9% and 2.6% respectively. At 7-days, the dosage of 1.25% seems to be the threshold for HoH increase. Beyond the dosage of 1.25% XS 44, no additional increase in HoH is seen.

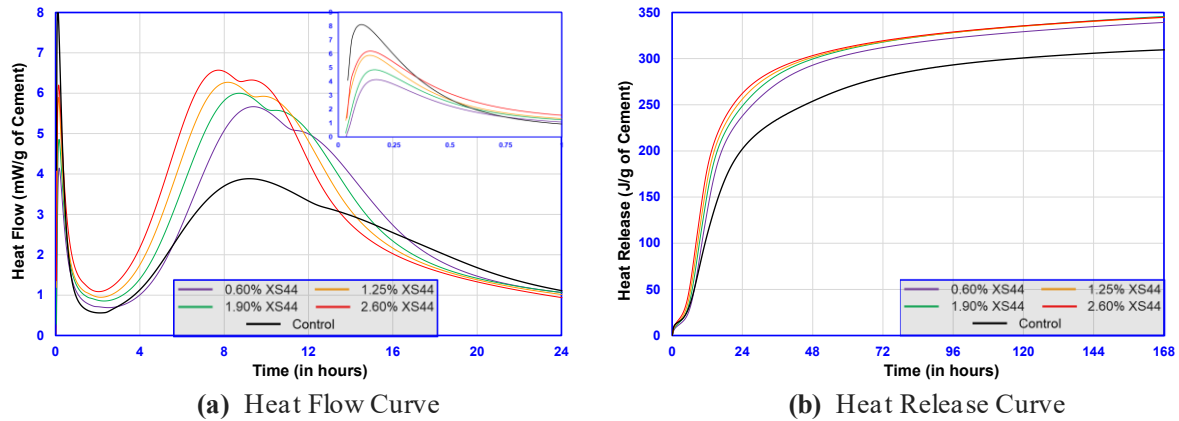


Figure 29: Hydration kinetics for XS-44 accelerator at 73°F (w/c = 0.42)

Finally, testing was completed on the shotcrete accelerator (SU) at dosage rates of 5, 6.66, 8.32, and 10% bwoc, which is significantly greater than the dosages for the other set accelerators. The results from this testing are shown in **Figure 30**. The heat flow is significantly steady (approximately 20 mW/g) for all dosages. However, once the dosage is increased the length of the initial flat peak increases from 15 mins for low dosage and 25 mins for high dosage. The addition of accelerator significantly reduces the length of induction period at all dosages, however, increase in dosage of shorts the onset of acceleration stage further. The rate of heat flow significantly increases in the acceleration period as compared to control. The addition of the accelerator also broadens the main hydration peak such that the main silicate peak and the sulfate depletion peaks are of similar higher at higher dosages. Furthermore, from the heat release plots it is observed that the accelerator addition of 5%, 6.66%, 8.32% and 10% bwoc increases the heat of hydration at 6 hours by 141.4%, 267.6%, 297.2%, 309.6% respectively. For 24 hours and 72 hours the increase in the HoH is 30.7%, 28.5%, 29.5%, 27.5% and 21%, 16.9%, 17.8%, 16.5% respectively. The initial acceleration due to higher dosages diminishes around 16 hours and lower dosage starts to generate heat at a higher rate. The reduction in reaction due to higher dosages can be attributed to the fact that the increased amount of calcium sulfo-aluminate hydrate acts as barrier for the hydration of calcium silicate and the water binding effect of calcium sulfo-aluminate hydrate can lower the water content available for

calcium silicate hydration [23]. At 7-days, the heat evolved as compared to control is 20.2%, 15.4%, 16.8% and 15.6% higher. The low dosage has the highest HoH.

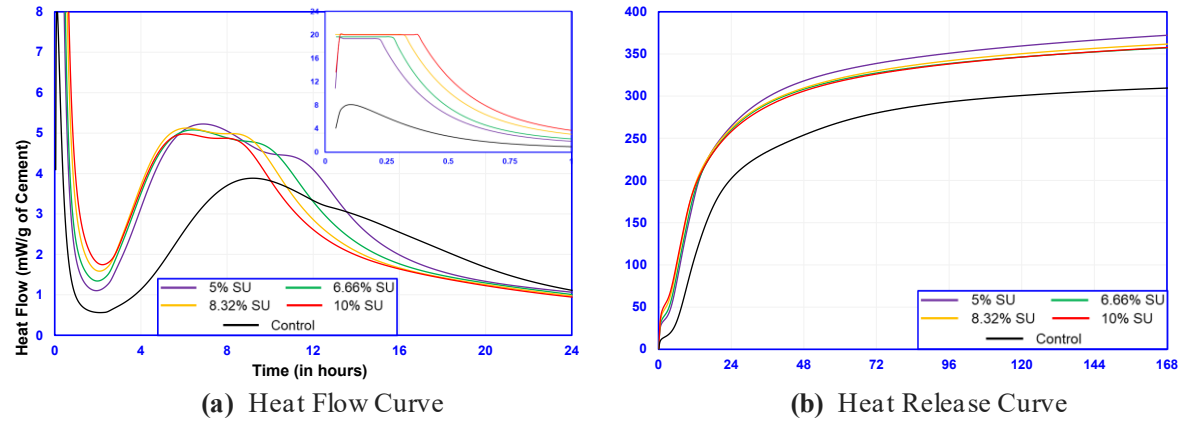


Figure 30: Hydration kinetics for SU accelerator at 73°F (w/c = 0.42)

#### 4.3.3. UPV

In support of the setting time results UPV testing was completed to provide a mechanical mechanism of analysis for the early-age performance of the ABCMs. UPV testing observes the change in stiffness of the cement paste samples and gives critical context to development of the strength and load-bear capacity of the ABCMs. Testing was primarily completed at 73°F at a water-to-cement ratios of 0.33, 0.36, and 0.42 to maximize the effectiveness of the set accelerators. However, testing was also completed at 50°F to monitor the role of temperature on the stiffening of samples containing set accelerators.

**Figure 31** displays the UPV results for testing at a water-to-cement ratio of 0.33. The addition of accelerators at low dosage slightly increases the time for onset of acceleration period for all accelerators except SU. However, the rate of acceleration of all accelerators after the onset of acceleration period is higher compared to control. At 6-hours, the difference in wave velocities of Cl, NCl, NCl-1, XS 55, XS 44 and SU as compared to control is about -2.2%, -5.5%, -8.6%, -7.5%, -5.7%, and 28%, respectively. After a hydration time of 12-hours, the difference in velocities is about -2.5%, 5%, 1.1%, 3%, 0.4%, and 12.3% as compared to control. At 24 hours, the difference is about -1.2%, 3.5%, 1.7%, 3%, 1.3% and 4.8 % for Cl, NCl, NCl-1, XS 55, XS 44 and SU as compared to control, respectively. All the accelerators at low dosage show a slight increase in 24-hour wave velocity except Cl, which has a wave velocity less than control by 1.2%. Based on the acceleration data plots the order for onset of acceleration period for low dosages is as follows:

$$\text{Control} > \text{Cl} > \text{XS 44} = \text{NCl} > \text{NCl-1} = \text{XS 55}$$

The addition of the high dosages (except NCl and XS 55) decreased the length of the dormant period. The dormant period for NCl is similar to that of control, however, the addition of XS 55 significantly increases the length of dormant period. At 6-hours, the difference in wave velocities of Cl, NCl, NCl-1, XS 55, XS 44 and SU as compared to control is about 25.5%, 1.3%, 10.4%, -15.3%, 0.5%, and 34.9% respectively. After a hydration time of 12-hours, the difference in

velocities is about -0.4%, 11.4%, 5%, 1.9%, 6.2%, and 9.6%. At 24-hours, the difference is about -4.8%, 3.9%, 2.1%, 2.1%, 4.4% and -1.7% for CI, NCI, NCI-1, XS 55, XS 44 and SU as compared to control respectively. At hydration time of 24-hours, all the accelerators except SU and CI show higher wave velocity as compared to control. Based on the acceleration data plots the order for onset of acceleration period for low dosages is as follows:

$$CI > NCI-1 > XS44 > NCI = Control > XS 55$$

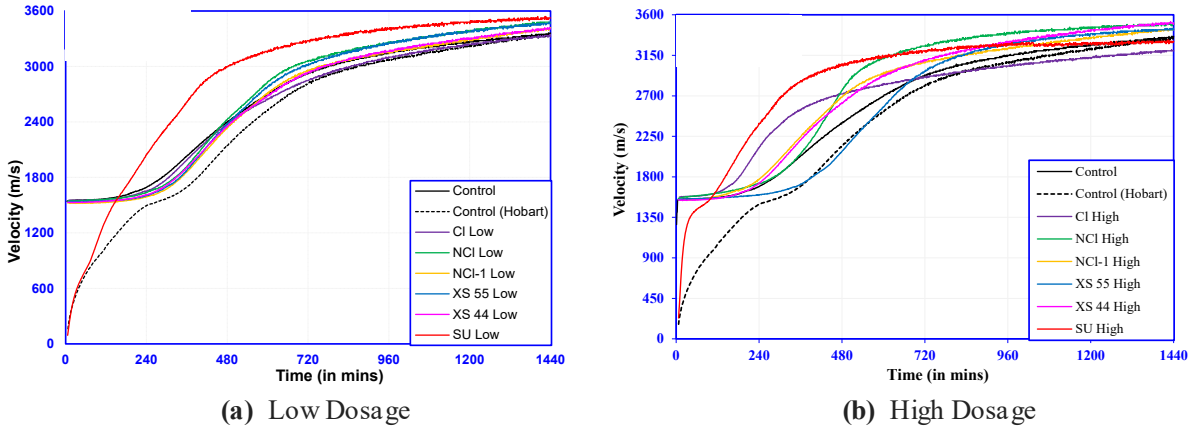


Figure 31: Ultrasonic wave velocity for different accelerators at w/c = 0.33 (73 °F)

The results for UPV testing at a water-to-cement ratio of 0.36 are shown in **Figure 32**. The addition of all accelerators except SU slightly reduces the length of dormant period, however, in case of SU, the reduction in length of dormant period is significant. At 6-hours, the difference in wave velocities of CI, NCI, NCI-1, XS 55, XS 44 and SU as compared to control is 5%, 4.8%, 2%, 2.7%, 2.4% and 39.8% respectively. After 12 hours the difference is about -2%, 3.5%, 0.7%, 2.5%, 1% and 14.1%, respectively. The difference in wave velocity as compared to control is about -2.4%, 0.8%, -0.4%, 2.1%, 1.1% and 4.7% for CI, NCI, NCI-1, XS 55, XS 44 and SU, respectively. Based on the ultrasonic wave velocity measurement, there is no significant difference between wave velocities and behavior as compared to control). However, the difference between control and SU at 6-hours, 12-hour and 24-hours was about 45%, 16% and 6% respectively. For first 80 mins, the control and SU do not show any deviation in the  $V_p - t$  curve, however, after 80 mins, SU based mix accelerates rapidly. Based on the data a very clear distinction on order based on length of dormant period cannot be identified.

The addition of different accelerators at high dosage reduced the length of dormant period for all accelerators except XS 55, where there is an increase in the length of dormant period. After the onset of acceleration period, the rate of velocity gain is higher in all accelerators as compared to control excluding CI-based mix, where the rate is similar to the control. In addition to that, the steady state period develops significantly early for CI-based mix as compared to control. At 6-hours, the difference in wave velocities of CI, NCI, NCI-1, XS 55, XS 44 and SU as compared to



control is 34.9%, 7.7%, 20.7%, -5.3%, 16.8% and 59.2% respectively. After 12 hours the difference is about 4.3%, 11.9%, 8.6%, 1.4%, 6.2% and 14.5% respectively. The difference in wave velocity at 24-hours as compared to control is about -2.8%, 3.4%, 2.1%, 3.4%, 2.5%, and 1.7% for Cl, NCl, NCl-1, XS 55, XS 44 and SU respectively. Except Cl, all other accelerators show a higher wave velocity as compared to control at 24-hours. Based on the length of dormant period, the order of onset of acceleration period, hence, setting is as follows:

$$SU > Cl > NCl-1 > XS\ 44 > NCl > Control > XS\ 55$$

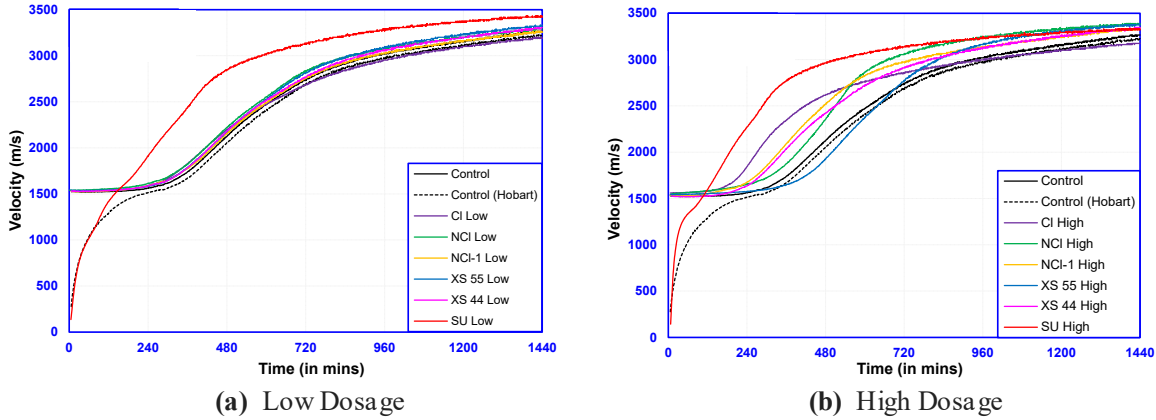


Figure 32: Ultrasonic wave velocity for different accelerators at w/c = 0.36 (73 °F)

The results for UPV testing at a water-to-cement ratio of 0.36 are shown in **Figure 33**. The addition of accelerators reduces the dormant period for all accelerators slightly and significantly for SU as compared to control. After the onset of acceleration period the rate of wave velocity increase is higher for all accelerators as compared to control. After a hydration time of 6-hours, the difference in wave velocities of Cl, NCl, NCl-1, XS 55, XS 44 and SU as compared to control is about 2.1%, 11.7%, 2.7%, 1%, 0.2% and 26.2% respectively. After 12 hours the difference as compared to control is about 7.1%, 8.4%, 12.8%, 9.7%, 8.7% and 26.1% respectively. The difference in wave velocity at 24 hours as compared to control is about 3.3%, 5.6%, 7.7%, 7.3%, 5.6% and 11.1% for Cl, NCl, NCl-1, XS 55, XS 44 and SU respectively. Based on the length of dormant period, the order of onset of acceleration period, hence, setting is as follows:

$$SU > Cl = NCl-1 > XS\ 55 = NCl = XS\ 44 > Control$$

The high dosage test results at a w/c ratio of 0.42 showed a significant effect on the onset of the acceleration period for all accelerators except XS 55 as compared to control. There is a retardation in onset of acceleration period for mixes with XS 55. However, after the onset of acceleration period, the rate of increase in wave velocity for all accelerators is high as compared to control. After a hydration time of 6-hours, the difference in wave velocities of Cl, NCl, NCl-1, XS 55, XS 44 and SU as compared to control is about 23.7%, 4.7%, 15.8%, 2.4%, 12.1% and 53.4%



respectively. After 12 hours the difference as compared to control is about 18.7%, 23.1%, 21.9%, 6.5%, 21.5% and 34.6% respectively. The difference in wave velocity at 24-hours as compared to control is about 4.5%, 10.2%, 8.9%, 8.9%, 10.6% and 12.9% for CI, NCI, NCI-1, XS 55, XS 44 and SU respectively. Based on the length of dormant period, the order of onset of acceleration period, hence, setting is as follows:

$$SU > CI > NCI-1 > XS44 > NCI > Control > XS 55$$

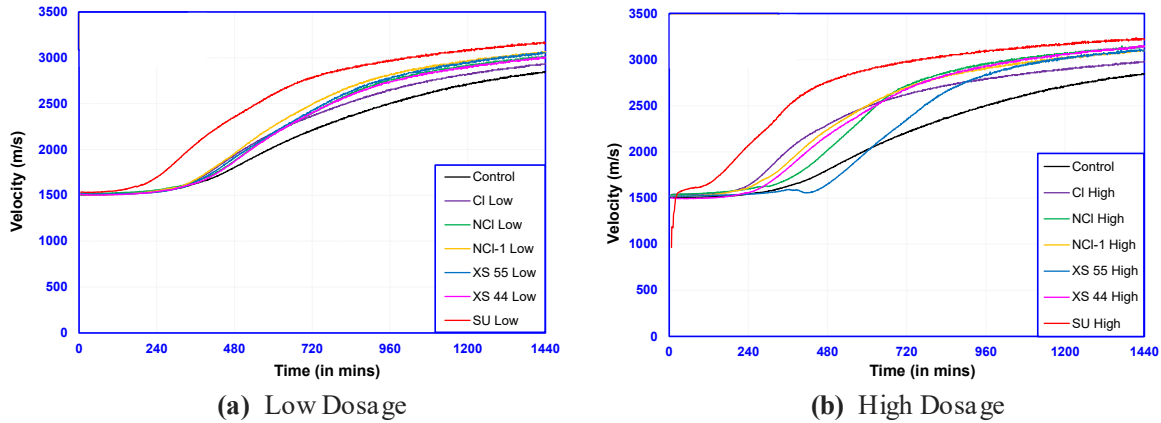


Figure 33: Ultrasonic wave velocity for different accelerators at w/c = 0.42 (73 °F)

The influence of temperature on the ultrasonic wave propagation for cementitious systems with two dosages each (low and high) of different accelerators was studied at 50 °F and the results are compared to the mixes at 73 °F. The study was carried out using ASTM Type III cement with a water-to-cement ratio of 0.42 for 48 hours of hydration as compared to 73 °F where hydration was studied for 24 hours only. The difference in time is due to the mixes at lower temperatures taking more time to reach the steady-stage period.

**Figure 34** show the ultrasonic wave velocities for Type III cement at 50 °F at low and high dosages of different accelerators respectively. The initial ultrasonic wave velocity for all mixes including control is about 1490-1510 m/s and any increase in the velocity corresponds to development of hydrated microstructure in the cementitious matrix. For the low dosage of accelerators only SU and CI-based accelerators show a notable effect on acceleration of wave velocity from initial value as compared to control with SU being most effective. All other accelerators show either a slight acceleration or slight retardation in the onset of acceleration period. For high dosage, all accelerators except XS 55 reduce the length of dormant period in the following order:

$$SU > CI > NCI-1 > XS 44 > NCI > Control > XS55$$

The addition of XS 55 at high dosage causes retardation and hence increases the length of the dormant period. The ultrasonic pulse velocities measured for low dosage of mixes based on CI, NCI, NCI-1, XS 55, XS 44 and SU at 24-hours is about 8.3%, 7%, 7%, 0%, 2.7% and 12% higher

as compared to control and at 48-hours is about 2.4%, 1.6%, 0.8%, 0.8%, -0.8% and -0.4% different than the control respectively. For mixes at high dosage at 24-hours, the velocities are higher as compared to control by 17.4%, 17.8%, 15%, -8.7%, 16.6% and 17.7% for mixes with Cl, NCl, NCl-1, XS 55, XS 44 and SU respectively and at 48-hours, the difference in velocities as compared to control, is around 1.6%, 4%, 0.8%, 1.6%, 2.4% and 6.6%.

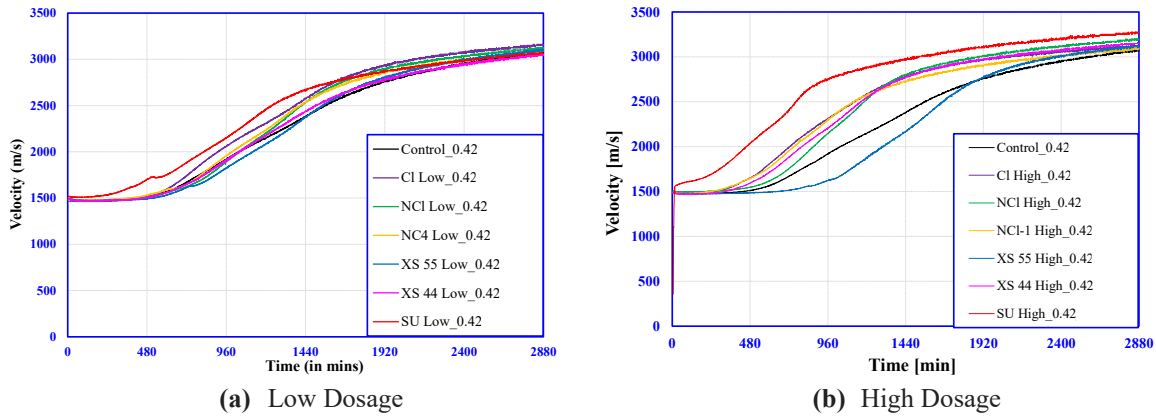
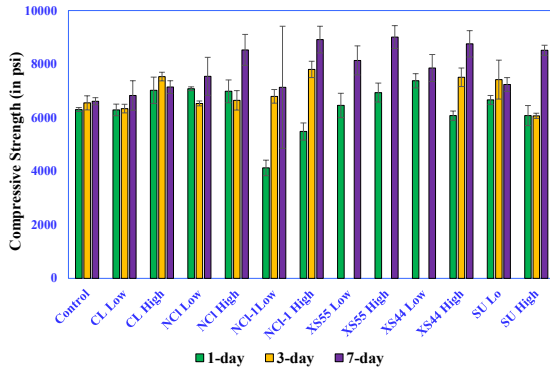


Figure 34: Ultrasonic wave velocity for different accelerators at 50 °F (w/c = 0.42)

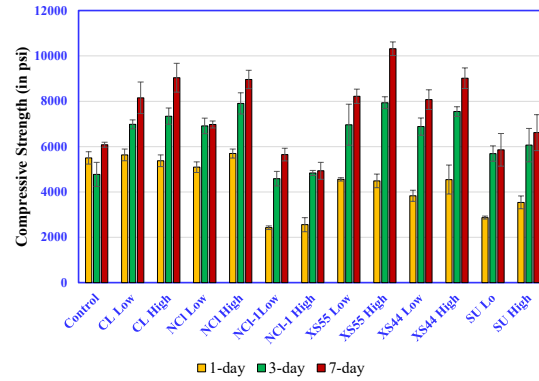
#### 4.3.4. Compressive Strength

To provide context on the mechanical performance of the ABCMs compressive strength testing was completed at one, three, and seven-days after casting to monitor the influence of the set accelerators on compressive strength development. Testing predominately focused on the role of set accelerator dosage, cement type, and temperature on the change in strength development rate, due to their significant role in the early-age performance as indicated in the setting time, isothermal, and UPV results discussed previously.

**Figure 35** displays the results of 1, 3, and 7-day compressive strength testing of cement paste samples utilizing Type III and Type I/II cement at a water-to-cement ratio of 0.42 and sand-to-cement ratio of 1.5. The one-day compressive strength of the Type III cement samples generally exceeded the compressive strength of the Type I/II cement samples. However, for three and seven day tests the gap decreased with the best performing Type I/II cement samples providing higher compressive strength than the Type III cement samples. Granted, the performance was variable with the Type I/II NCl-1 low and high dosage providing the lowest compressive strength at seven days at 5900 and 5000 psi, respectively. Testing generally indicated that the inclusion of set retarders improved the compressive strength of all samples, except for NCl-1. On average the compressive strength at seven days was increased by approximately 30% for both Type I/II and Type III cements, with the Type I/II cement demonstrating a greater variability in percent change in compressive strength.



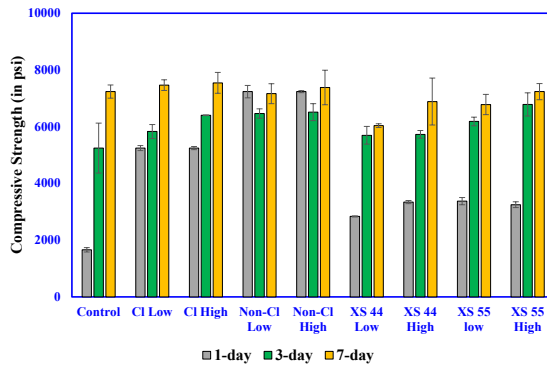
(a) ASTM Type III Cement



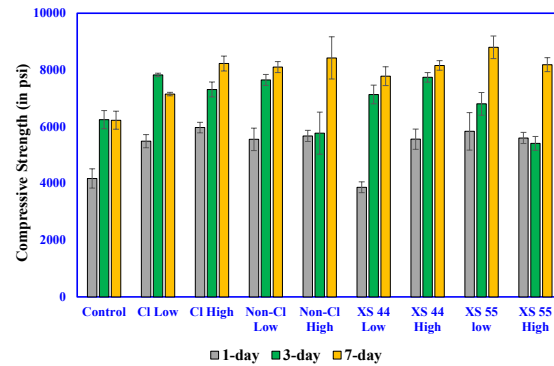
(b) ASTM Type I/II Cement

Figure 35: Compressive strength of cement pastes at a temperature of 73 °F and w/c = 0.42 (S/C=1.5)

Testing was also completed at 50 °F to investigate the temperature dependency of set accelerators. The results for compressive strength testing at 50 and 73 °F are shown in **Figure 36**. Compared to the control, the set accelerators provided a greater percentage increase in compressive strength at 50 rather than 73 °F at early ages with the compressive strength more than doubling on average. Importantly, the chemical accelerators (150-200% increase) provided a markedly higher one-day compressive strength compared to the physical accelerators (50-75% increase). However, at later ages the benefit of including the set accelerator was less pronounced, as the compressive strength was approximately equal to the control for all admixtures at both low and high dosages at seven days. Testing generally indicates that the inclusion of set accelerators is beneficial at lower temperatures to increase the early-age strength without sacrificing the later-age strength.



(a) Temperature = 50 °F



(b) Temperature = 73 °F

Figure 36: Compressive strength of cement mortar at a temperature of 50 and 73 °F and w/c = 0.42 (S/C = 1.5)

#### 4.3.5. Shrinkage Ring Test

Lastly, to provide some context for the durability of ABCMs restrained shrinkage ring testing was completed utilizing dosage rate and temperature as the two primary variables. Testing does not provide an absolute effectiveness of the set accelerators as the RSPM restrained shrinkage ring testing provided, because the aggregate and other additive contents are not optimized for service conditions as was done for the RSPMs. Instead, these results provide a relative comparison into the shrinkage and tensile strain capacity development of the mortar mixtures containing set

accelerators. Importantly, the NCI-1 and SU admixtures were not tested for their restrained shrinkage performance due to the depletion of the cement batch used for the plurality of testing.

The results for testing at 73 °F at a water-to-cement ratio of 0.42 and a sand-to-cement ratio of 1.5 are shown in **Figure 37**. Test results generally indicated that the mortar mixtures containing set accelerators demonstrated a reduced time to crack and a lower ultimate strain at cracking. Furthermore, testing indicated that the high dosage for each accelerator demonstrated a lower ultimate strain at cracking and earlier time to cracking relative to their low dosage counterparts. These results indicate that the usage of the set accelerators while accelerating the rate of reaction are not accelerating the rate of tensile strain capacity gain, which therefore results in the earlier failure of the mortar samples. This claim is further supported when analyzing the heat of hydration and time to crack results concurrently, where it was found that the heat of hydration at the time to cracking was comparable for all accelerators and the control. For low dosages and control the average heat of hydration at cracking is about 268 J/g of cement with a standard deviation of 3.2 J/g of cement and for high dosages and control, the heat of hydration at cracking time is about 258 J/g of cement with a standard deviation of 9.35 J/g of cement and coefficient of variation of about 3.48%. In practice, these results highlight the increased potential for cracking in ABCMs containing set accelerators if the repaired sections are not properly jointed.

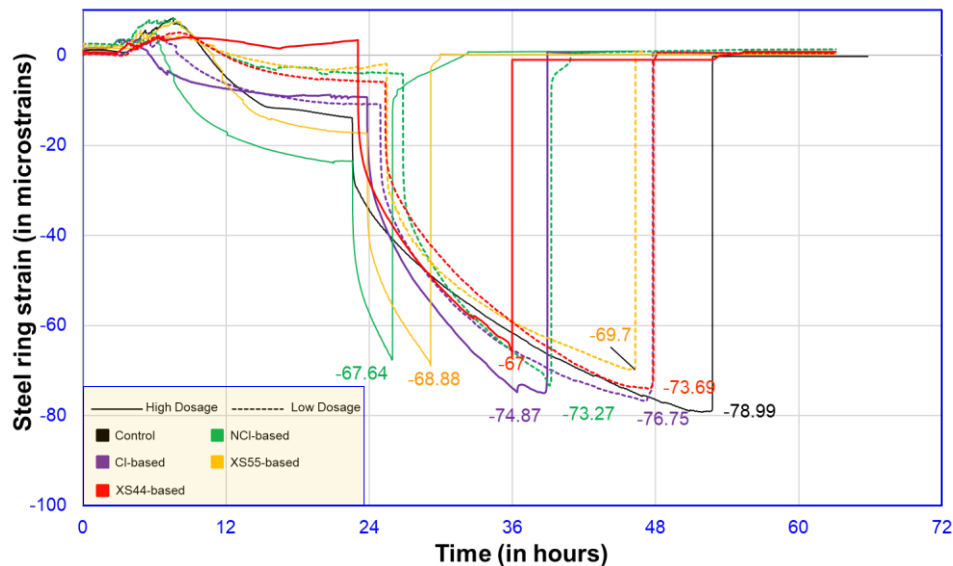


Figure 37: Influence of accelerator type and dosage on the restrained shrinkage and cracking time of mortar with S/C = 1.5 at 73 °F (w/c = 0.42)

Testing on the role of environmental temperature on the restrained shrinkage of ABCMs is shown in **Figure 38**. Testing was completed at 50 °F utilizing the same water-to-cement and sand-to-cement ratios, to compare against the previously conducted 73 °F restrained shrinkage ring tests. Chemical accelerators experienced shorter times to crack at 50 °F relative to the physical set accelerators. The CI accelerated experienced a comparable time to cracking and ultimate strain values at both 50 and 73 °F for the low and high dosage. However, the other chemical accelerator,

NCI, demonstrated a slight retardation increasing the time to crack by approximately 12 hours for both the high and low dosage. In comparison the XS-44 and XS-55 accelerators demonstrated an increase in time to crack approximately 24 hours for both the low and high dosages. These observations correlate well to the previously discussed heat of hydration data analyzed in the isothermal calorimetry section, as the heat of hydration data for 50 °F paste samples found an average heat of hydration at the time of cracking of 238 J/g of cement with a standard deviation of 18% and a coefficient of variation of about 7.63%.

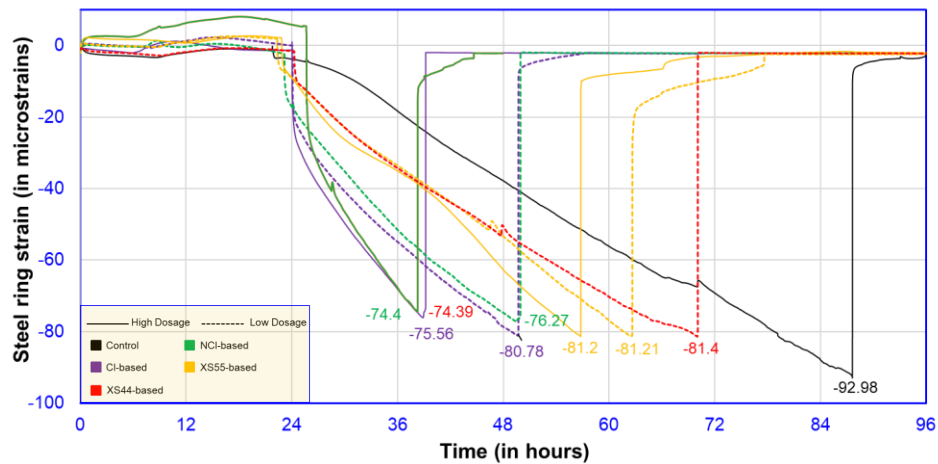


Figure 38: Influence of accelerator type and dosage on the restrained shrinkage and cracking time of mortar with S/C = 1.5 at 50 °F (w/c = 0.42)

## 5. Conclusions and Recommendations

---

### 5.1. Conclusions

Based upon the experimental testing on the RSPMs the following conclusions were drawn regarding the effectiveness and usage of RSPMs:

- The performance of PC, CSA, and CAC-based RSPMs was comparable across the full range of testing and did not indicate that one binder type was preferable. However, testing on the MgO-based RSPM did demonstrate that the early-age performance of MgO-based RSPMs should be closely monitored, due to the slower rate of reaction.
- The setting time of RSPMs is highly dependent upon environmental temperature, as only one RSPM was within the allowed setting window at all of 50°F, 73°F, and 104°F (PC-2).
- The compressive strength of most RSPMs decreased when cured at 50°F as compared to 73°F compressive strength test results, except for the CSA-based RSPMs which exhibit an increased compressive strength due to the formation of metastable hydration phases.
- The compressive strength of most RSPMs was higher at 104°F relative to the 73°F compressive strength results, except for PC-3 and CAC-2 which experienced significantly accelerated setting times resulting in the cylinder being uncastable and the CSA-based RSPMs due to the decomposition of the previously mentioned metastable hydration products.
- The slant-shear bond strength of most RSPMs was higher when utilizing a dry substrate instead of an SSD substrate. This is potentially caused by the reduction in macro/microtexture due to surface moisture and/or lack of sufficient interaction between the hydration products of repair materials with substrate concrete in shear.
- The pull-off bond strength of most RSPMs was higher when utilizing an SSD substrate instead of a dry substrate, this is potentially caused by a lower degree of hydration as moisture is being taken to saturate the substrate.
- Restrained shrinkage ring testing indicated that several RSPMs are not suited for restrained conditions due to the shrinkage exceeding the tensile strain capacity at early ages.
- Restrained shrinkage testing at 50°F and 104°F indicated that suitability for casting under restrained conditions is dependent on environmental temperature, as changes in the environmental temperature resulted in drastically different times to crack and strain rates.
- Durability testing focused on the coefficient of thermal expansion, dynamic modules of elasticity, and Poisson's ratio indicated that all mature RSPMs are mechanically suitable for their exposure conditions and should not result in incompatibility-related distress.
- Testing on the electrical resistivity and chloride migration coefficients indicated that while most RSPMs provide adequate compatibility with OPC concrete, some RSPMs provide insufficient resistance to chloride ingress while others provide excessive resistance both of which could potentially result in future deterioration.

Based upon the experimental testing on the ABCMs the following conclusions were drawn regarding the effectiveness and usage of accelerated concrete mixtures:

- The inclusion of both chemical and physical set accelerators significantly decreases the setting time of ABCMs, for both Type I/II and Type III cement. However, the set is more accelerated for Type I/II cements than for Type III cements.
- The water-to-cement ratio is critical to the performance of ABCMs containing set accelerators. Low water-to-cement ratios (0.33) cause set accelerators to demonstrate minimal to negative acceleration in the setting time. Whereas high water-to-cement ratios (0.42) result in all set accelerators demonstrating a reduced setting time.
- The role of ambient environmental temperature is key to the performance of ABCMs containing set accelerators. Low temperatures cause set accelerators to demonstrate greater set acceleration at high water-to-cement ratios and lesser acceleration at lower water-to-cement ratios.
- The increase in set accelerator dosage results in an increased heat flow during the acceleration period relative to lower dosages but does not provide a significant increase in the final heat of hydration relative to other dosages of set accelerators, excluding the control.
- The inclusion of chemical set accelerators typically results in no change or a decrease in the dormant period duration, whereas the inclusion of physical set accelerators typically results in no change or an increase in the dormant period duration.
- The inclusion of set accelerators results in no change to the ultimate pulse velocity of ABCMs but does influence the rate of change in velocity after the dormant period. For low dosages the change is negligible, but for high dosages of set accelerators the change in velocity is pronounced.
- The influence of set accelerators on the compressive strength of ABCMs is heavily dependent on temperature. For low temperatures the influence on the ultimate compressive strength is negligible, however for higher temperatures the ultimate compressive strength is increased.
- The inclusion of set accelerators in ABCMs results in an accelerated time to crack and a lowering of the ultimate strain capacity when tested in restrained shrinkage. The inclusion of set accelerators increases the risk of cracking due to the improperly timed cutting of joints in concrete pavements.
- Environmental temperature is key to the effectiveness of set accelerators in ABCMs under restrained shrinkage. At lower temperatures the time to crack is delayed for chemical set accelerators and substantially delayed for physical set accelerators.
- The heat of hydration at the time of cracking is highly consistent at both 50 and 73°F, indicating that the degree of hydration is critical to a sample failing under restrained shrinkage.

## 5.2. Recommendations

Based upon experimental testing on the RSPMs the following recommendations were drawn regarding the selection and usage of RSPMs:

- RSPMs should be prequalified at multiple environmental temperatures to ensure that the product will have a sufficient setting window to allow for the proper mixing and consolidation of the RSPM or repair personnel should be trained to ensure that the RSPM must meet temperature requirements before placement to ensure a durable repair.
- The geometry of the section requiring patching should be considered when selecting a RSPM for repair. Roadway patches that may provide restraint on the RSPMs should require patching materials that display low shrinkage or high strain capacity.
- Roadway patches should be prepared with surface preparation prior to installation and the reinforcement should be cleaned of corrosion to ensure a durable and well-bonded repair.
- The patch surface should be prepared either under SSD or dry condition based upon the bond strength test results collected for a given RSPM. For RSPMs that perform better under SSD condition care should be taken to ensure water is not puddled when casting.
- The electrical resistivity/chloride migration coefficient of the RSPM should be similar to the electrical resistivity/chloride migration coefficient of the substrate concrete. Electrical resistivities greater than the substrate could result in microcell corrosion, whereas electrical resistivities less than the substrate could result in accelerated chloride ingress into the concrete.
- The coefficient of thermal expansion, modulus of elasticity, and Poisson's ratio of RSPMs should be monitored, but preliminary testing indicates most RSPMs are compatible with ordinary Portland cement concrete substrates.

Based upon experimental testing on the ABCMs the following recommendations were drawn regarding the selection and usage of accelerated concrete mixtures:

- The inclusion of set accelerators into ABCMs is of limited effectiveness at low water-to-cement ratios without high range water reducers. Further testing is needed to determine if low water-to-cement ratios with high range water reducers experience similar limited performance.
- Ambient environmental temperature is critical to the effectiveness of set accelerators in ABCMs, as low temperatures can result in the extension of setting time at lower water-to-cement ratio and results in the ABCMs demonstrating no change in compressive strength, whereas testing at higher temperature demonstrated a strength increase.
- The inclusion of chemical set accelerators will either result in no change or a decrease in the dormant period duration, whereas the inclusion of physical set accelerators will result in no change or an increase in the dormant period duration.



- The inclusion of set accelerators provides minimal change in the final stiffness of ABCMs but does provide some change in the rate of stiffness development at higher dosages of set accelerators. The increased rate of stiffening would allow for the earlier opening of repaired pavement sections to traffic, assuming the strength of the concrete is sufficient.
- The inclusion of set accelerators decreases the time to crack for ABCMs under restrained conditions. This highlights the importance of ensuring that concrete sections are patched quickly for ABCMs and that the window for jointing is understood before casting the repaired section of pavement.

## References

---

- [1] FHWA, Performance of Concrete Highway Bridge Decks using Nationwide Condition Data, 2018.
- [2] E. and M. National Academies of Science, Concrete Bridge Deck Performance, Transportation Research Board, Washington, D.C., 2004. <https://doi.org/10.17226/17608>.
- [3] N.M. Cervo, A.J. Schokker, Bridge Deck Patching Materials, 2008. [www.pti.psu.edu](http://www.pti.psu.edu).
- [4] N.K. Emberson, G.C. Mays, Significance of property mismatch in the patch repair of structural concrete Part 1: Properties of repair systems, Magazine of Concrete Research 42 (1990) 147–160.
- [5] P. Ram, J. Olek, J. Jain, Field Trials of Rapid-Setting Repair Materials, West Lafayette, IN, 2016. <https://doi.org/10.5703/1288284315185>.
- [6] N. Su, L. Lou, A. Amirkhanian, S.N. Amirkhanian, F. Xiao, Assessment of effective patching material for concrete bridge deck -A review, Constr Build Mater 293 (2021). <https://doi.org/10.1016/j.conbuildmat.2021.123520>.
- [7] P. Rangaraju, R.R. Pattnaik, Evaluation of Rapid Set Patching Materials for PCC Applications, 2008.
- [8] SCDOT, SCDOT: Strategic 10-year Asset Management Plan, Columbia, SC, 2022. [www.scdot.org](http://www.scdot.org).
- [9] Federal Highway Administration, LTBP InfoBridge: Data, (2018). Accessed December 2021.
- [10] P.H. Emmons, A.M. Vaysburd, Factors affecting the durability of concrete repair: the contractor's viewpoint, Constr Build Mater 8 (1993) 5–16. [https://doi.org/10.1016/0950-0618\(94\)90003-5](https://doi.org/10.1016/0950-0618(94)90003-5).
- [11] S. Soltesz, Cementitious Materials for Thin Patches, 2001. Oregon Department of Transportation.
- [12] K.E. Hassan, J.J. Brooks, L. Al-Alawi, Compatibility of repair mortars with concrete in a hot-dry environment, n.d. [www.elsevier.com/locate/cemconcomp](http://www.elsevier.com/locate/cemconcomp).
- [13] P.S. Mangat, F.J. O'flaherty, Influence of elastic modulus on stress redistribution and cracking in repair patches, 2000.
- [14] S. Asayesh, A.A. Shirzadi Javid, H. Ziari, B. Mehri, Evaluating fresh state, hardened State, thermal expansion and bond properties of geopolymers for the repairing of concrete

- pavements under restrained conditions, *Constr Build Mater* 292 (2021). <https://doi.org/10.1016/j.conbuildmat.2021.123398>.
- [15] M. Sánchez, P. Faria, L. Ferrara, E. Horszczaruk, H.M. Jonkers, A. Kwiecień, J. Mosa, A. Peled, A.S. Pereira, D. Snoeck, M. Stefanidou, T. Stryzewska, B. Zając, External treatments for the preventive repair of existing constructions: A review, *Constr Build Mater* 193 (2018) 435–452. <https://doi.org/10.1016/j.conbuildmat.2018.10.173>.
  - [16] P.J. Robins, S.A. Austin, A unified failure envelope from the evaluation of concrete repair bond tests, *Magazine of Concrete Research* 47 (1995) 57–68. <https://doi.org/10.1680/mac.1995.47.170.57>.
  - [17] P. Winker, ICRI Technical Guideline NO. 310.2R-2013, Selecting and Specifying Concrete Surface Preparation for Sealers, Coatings, Polymer Overlays, and Concrete Repair, *Concrete Repair Bulletin*, May/June, 2013.
  - [18] P.H. Perkins, *Repair, Protection and Waterproofing of Concrete Structures*, 3rd ed., Taylor & Francis Group, 1997. <http://www.thomson.com>.
  - [19] J. Bensted and P. Barnes, *Structure and Performance of Cements*, CRC Press, 2002.
  - [20] Y. Guan, Y. Gao, R. Sun, M.C. Won, Z. Ge, Experimental study and field application of calcium sulfoaluminate cement for rapid repair of concrete pavements, *Frontiers of Structural and Civil Engineering* 11 (2017) 338–345. <https://doi.org/10.1007/s11709-017-0411-0>.
  - [21] Q. Yang, Zhu, B., and X. Wu, Characteristics and durability test of magnesium phosphate cement-based material for rapid repair of concrete, *Mat. Struct.* 33, 229-234, 2000, <https://doi.org/10.1007/BF02479332>
  - [22] D.P. Bentz, Activation energies of high-volume fly ash ternary blends: Hydration and setting, *Cement and Concrete Composites* 53 (2014) 214–223. <https://doi.org/10.1016/j.cemconcomp.2014.06.018>.
  - [23] J. Han, K. Wang, J. Shi, Y. Wang, Mechanism of triethanolamine on Portland cement hydration process and microstructure characteristics, *Constr. Build. Mater.* 93 (2015) 457–462. <https://doi.org/10.1016/j.conbuildmat.2015.06.018>.

## Appendix A: RSPM Summary Sheets

The tables below present an overview of the experimental testing regime and experimental results for each RSPM for the differing testing temperatures and against the OPC control. These tables provide a summary of relevant experimental results to aid the material selection process to better understand how these materials behave under variable environmental exposure conditions. The framework of the summary sheet is shown in **Table A-1**. The completed summary sheets are shown in **Table A-2** to **Table A-11**.

Table A-1: Framework of RSPM Summary Sheets

Rapid Setting Patching Material ID/Name						
Compressive Strength (psi)	Time (Days)	50°F	73°F	104°F	Shrinkage Ring (73°F)	
	0.25				Crack Time (Days)	Strain Rate (in/in/day)
	0.50					
	1					
	3				COTE (in/in/°F)	
	7					
Setting Time (min)	Initial Set (min)				Electrical Resistivity (kΩ*cm)	
					Bulk	Surface
	Final Set (min)				Chloride Migration Coefficient (m <sup>2</sup> /s)	
	Initial – Final (min)					
UPV (m/s)	Time (hrs.)				Pull-off Bond Strength	
	1				SSD	Dry
	3					
	6				Slant-Shear Bond Str.	
	24				SSD	Dry
Optimal Environment:						
					Dynamic Elastic Modulus	
					Dynamic Shear Modulus	
Potential Concerns:						
					Poisson's Ratio (-)	
					Specific Gravity (-)	

Table A-2: PC-1 Summary Sheet




PC-1						
Compressive Strength (psi)	Time (Days)	50°F	73°F	104°F	Shrinkage Ring (73°F)	
	0.25	4166	3533	5502	Crack Time (Days)	Strain Rate (in/in/day)
	0.50	4285	4063	5965		
	1	4588	5767	7103	1.75	34.4
	3	5686	6200	7702	COTE (in/in/°F)	
	7	6584	6747	8051	6.88*10 <sup>-7</sup>	
Setting Time (min)	Initial Set (min)	59	10	10	Electrical Resistivity (kΩ*cm)	
					Bulk	Surface
	Final Set (min)	96	13	11	78.5	70.9
					Chloride Migration Coefficient (m <sup>2</sup> /s)	
	Initial – Final (min)	37	3	1	1.1*10 <sup>-9</sup>	
UPV (m/s)	Time (hrs.)				Pull-off Bond Strength	
	1	3089	4819	4908	SSD	Dry
	3	4938	5000	4938	571 psi	457 psi
	6	5031	5031	4938	Slant-Shear Bond Str.	
	24	5063	5063	4969	SSD	Dry
Optimal Environment: This patching material is best utilized at 73 or 104°F on a low restraint and SSD substrate. Batches should be small to account for the shorter casting window. Provides higher bond strength relative to other RSPMs.					3207 psi	2942 psi
					Dynamic Elastic Modulus	
					7.16*10 <sup>6</sup> psi	
					Dynamic Shear Modulus	
					3.12*10 <sup>6</sup> psi	
Potential Concerns:					Poisson's (-)	
					0.15	
					Specific Gravity (-)	
					2.34	

Table A-3: PC-2 Summary Sheet

PC-2						
Compressive Strength (psi)	Time (Days)	50°F	73°F	104°F	Shrinkage Ring (73°F)	
	0.25	4927	4927	6272	Crack Time (Days)	Strain Rate (in/in/day)
	0.50	5412	5248	6566		
	1	5557	5554	6658	1.5	59.0
	3	6.193	6248	7101	COTE (in/in/°F)	
	7	6.584	6923	7316	6.9*10 <sup>-7</sup>	
Setting Time (min)	Initial Set (min)	20	18	11	Electrical Resistivity (kΩ*cm)	
					Bulk	Surface
	Final Set (min)	22	32	17	44.1	33.4
					Chloride Migration Coefficient (m <sup>2</sup> /s)	
	Initial-Final (min)	2	14	6	3.1*10 <sup>-9</sup>	
UPV (m/s)	Time (hrs.)	<del>                    </del>	<del>                    </del>	<del>                    </del>	Pull-off Bond Strength	
	1	1498	3687	4082	SSD	Dry
	3	3791	4255	4233	339 psi	234 psi
	6	4324	4301	2355	Slant-Shear Bond Str.	
	24	4444	4324	4301	SSD	Dry
Optimal Environment: This patching material is best used on a low restraint substrate with surface preparation and an SSD substrate. This RSPM casting window has a low temperature dependency and is suitable in most environments.					2822 psi	1656 psi
					Dynamic Elastic Modulus	
					6.51*10 <sup>6</sup> psi	
					Dynamic Shear Modulus	
Potential Concerns:					3.12*10 <sup>6</sup> psi	
					Poisson's Ratio (-)	
					0.20	
					Specific Gravity (-)	
					2.34	

Table A-4: PC-3 Summary Sheet


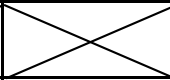
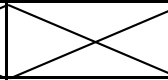
PC-3						
Compressive Strength (psi)	Time (Days)	50°F	73°F	104°F	Shrinkage Ring (73°F)	
	0.25	2803	4045	N/A	Crack Time (Days)	Strain Rate (in/in/day)
	0.50	2842	4309	N/A		
	1	3135	5220	N/A	>28	1.3
	3	3948	5988	N/A	COTE (in/in/°F)	
	7	4841	7172	N/A	6.5*10 <sup>-7</sup>	
Setting Time (min)	Initial Set (min)	29	21	1	Electrical Resistivity (kΩ*cm)	
	Final Set (min)	35	24	2	Bulk	Surface
					76.2	87.3
					Chloride Migration Coefficient (m²/s)	
	Initial– Final (min)	6	3	1	7.7*10 <sup>-10</sup>	
UPV (m/s)	Time (hrs.)				Pull-off Bond Strength (psi)	
	1	3540	4571	4571	SSD	Dry
	3	4678	4908	4571	N/A	N/A
	6	4938	5031	4624	Slant-Shear Bond Str. (psi)	
	24	5063	5063	4706	SSD	Dry
Optimal Environment: This patching material is best used at 50 or 73°F with surface preparation and a dry substrate. This RSPM demonstrated a low risk of cracking, making it useful for patches of irregular geometry.					1655	2201
					Dynamic Elastic Modulus	
					6.15*10 <sup>6</sup> psi	
					Dynamic Shear Modulus	
Potential Concerns: <ul style="list-style-type: none"><li>Significantly accelerated setting time at high temperatures</li><li>Low bond strength</li></ul>					2.56*10 <sup>6</sup> psi	
					Poisson’s Ratio (-)	
					0.20	
					Specific Gravity (-)	
					2.15	

Table A-5: PC-4 Summary Sheet

PC-4						
Compressive Strength (psi)	Time (Days)	50°F	73°F	104°F	Shrinkage Ring (73°F)	
	0.25	6302	6220	6662	Crack Time (Days)	Strain Rate (in/in/day)
	0.50	6528	6336	6869		
	1	6534	6475	6730	4.25	20.4
	3	7059	6947	7012	COTE (in/in/°F)	
	7	8151	7945	7125	6.2*10 <sup>-6</sup>	
Setting Time (min)	Initial Set (min)	21	16	6	Electrical Resistivity (kΩ*cm)	
					Bulk	Surface
	Final Set (min)	24	17	6	10.5	6.6
	Initial – Final (min)	3	1	0	Chloride Migration Coefficient (m <sup>2</sup> /s)	
					1.5*10 <sup>-9</sup>	
UPV (m/s)	Time (hrs.)				Pull-off Bond Strength (psi)	
	1	2439	3980	4211	SSD	Dry
	3	2847	4420	4255	505	283
	6				Slant-Shear Bond Str. (psi)	
	24	3620	4444	4167		
Optimal Environment: This patching material is best used at 50 or 73°F on a low restraint substrate with surface preparation and an SSD substrate. This patching material provides a very high initial strength gain relative to other RSPMs.					3670	4420
					4301	
					SSD	Dry
					2933	3061
					Dynamic Elastic Modulus	
Potential Concerns:					6.46*10 <sup>6</sup> psi	
					Dynamic Shear Modulus	
					2.67*10 <sup>6</sup> psi	
					Poisson's Ratio (-)	
					0.21	
					Specific Gravity (-)	
					2.31	



Table A-6: PC-5 Summary Sheet

PC-5						
Compressive Strength (psi)	Time (Days)	50°F	73°F	104°F	Shrinkage Ring (73°F)	
	0.25	5353	5515	5729	Crack Time (Days)	Strain Rate (in/in/day)
	0.50	5759	7055	6645		
	1	7055	7100	7055	22.25	4.5
	3	7298	716	8249	COTE (in/in/°F)	
	7	9110	9350	9760	6.9*10 <sup>-6</sup>	
Setting Time (min)	Initial Set (min)	64	25	10	Electrical Resistivity (kΩ*cm)	
					Bulk	Surface
	Final Set (min)	72	29	11	>1000	>1000
	Initial – Final (min)	8	4	1	Chloride Migration Coefficient (m <sup>2</sup> /s)	
					1.8*10 <sup>-13</sup>	
UPV (m/s)	Time (hrs.)				Pull-off Bond Strength (psi)	
	1	408	233	4301	SSD	Dry
	3	1835	3101	4545	378	242
	6				Slant-Shear Bond Str. (psi)	
	24	3941	4420	4571		
Optimal Environment: This patching material is best used at 73 or 104°F on a substrate with surface preparation. This patching material provides a very high chloride permeability relative to other RSPMs.					4571	4651
					SSD	Dry
					1509	3275
					Dynamic Elastic Modulus	
					6.42*10 <sup>6</sup> psi	
Potential Concerns:					Dynamic Shear Modulus	
					2.67*10 <sup>6</sup> psi	
					Poisson's Ratio (-)	
					0.20	
					Specific Gravity (-)	
					2.31	

Table A-7: CAC-1 Summary Sheet

CAC-1						
Compressive Strength (psi)	Time (Days)	50°F	73°F	104°F	Shrinkage Ring (73°F)	
	0.25	3066	3553	3919	Crack Time (Days)	Strain Rate (in/in/day)
	0.50	3488	4827	5434		
	1	4435	5824	6465	1.5	59
	3	6105	6223	7854	COTE (in/in/°F)	
	7	6800	8648	8465	6.9*10 <sup>-7</sup>	
Setting Time (min)	Initial Set (min)	48	17	11	Electrical Resistivity (kΩ*cm)	
					Bulk	Surface
	Final Set (min)	68	28	15	104.2	47.9
	Initial – Final (min)	20	11	4	Chloride Migration Coefficient (m <sup>2</sup> /s)	
					2.3*10 <sup>-10</sup>	
UPV (m/s)	Time (hrs.)				Pull-off Bond Strength (psi)	
	1	980	1826	4082	SSD	Dry
	3	1728	4061	4233	453	230
	6	3333	4278	4255	Slant-Shear Bond Str. (psi)	
	24	4678	4571	4301	SSD	Dry
Optimal Environment: This patching material is best used at 73 or 104°F on a low restraint substrate under SSD conditions. This patching material provides good chloride permeability resistance.					2058	3465
					Dynamic Elastic Modulus	
					7.44*10 <sup>6</sup> psi	
					Dynamic Shear Modulus	
Potential Concerns:					3.23*10 <sup>6</sup> psi	
					Poisson's Ratio (-)	
					0.15	
					Specific Gravity (-)	
					2.35	

Table A-8: CAC-2 Summary Sheet

CAC-2						
Compressive Strength (psi)	Time (Days)	50°F	73°F	104°F	Shrinkage Ring (73°F)	
	0.25	3775	2429	N/A	Crack Time (Days)	Strain Rate (in/in/day)
	0.50	3791	803	N/A		
	1	4131	5494	N/A	0.1	990.2
	3	4360	6107	N/A	COTE (in/in/°F)	
	7	6332	8042	N/A	$7.7 \times 10^{-7}$	
Setting Time (min)	Initial Set (min)	25	5	3	Electrical Resistivity (kΩ*cm)	
	Final Set (min)	33	6	5	Bulk	Surface
	Initial – Final (min)	8	1	2	>1000	536.3
					Chloride Migration Coefficient (m <sup>2</sup> /s)	
					$6.7 \times 10^{-11}$	
UPV (m/s)	Time (hrs.)				Pull-off Bond Strength (psi)	
	1	2492	3653	3200	SSD	Dry
	3	2685	3791	3540	101	152
	6	2572	3980	3636	Slant-Shear Bond Str. (psi)	
	24	3774	4082	3774	SSD	Dry
Optimal Environment: This patching material is best used at 50°F on a low restraint substrate with surface preparation and under SSD condition. This patching material provides a very high chloride permeability relative to other RSPMs.					2064	2818
					Dynamic Elastic Modulus	
					$5.85 \times 10^6$ psi	
					Dynamic Shear Modulus	
Potential Concerns:					$2.46 \times 10^6$ psi	
					Poisson's Ratio (-)	
					0.19	
					Specific Gravity (-)	
					2.26	

Table A-9: CSA-1 Summary Sheet

CSA-1						
Compressive Strength (psi)	Time (Days)	50°F	73°F	104°F	Shrinkage Ring (73°F)	
	0.25	4075	4125	3876	Crack Time (Days)	Strain Rate (in/in/day)
	0.50	4600	4635	4284		
	1	5681	6164	4968	4.5	5.2
	3	9194	8144	5381	COTE (in/in/°F)	
	7	10194	8989	6921	6.2*10 <sup>-7</sup>	
Setting Time (min)	Initial Set (min)	48	16	1	Electrical Resistivity (kΩ*cm)	
	Final Set (min)	55	24	2	Bulk	Surface
					12.2	5.2
	Initial – Final (min)	7	8	1	Chloride Migration Coefficient (m <sup>2</sup> /s)	
					1.5*10 <sup>-9</sup>	
UPV (m/s)	Time (hrs.)				Pull-off Bond Strength (psi)	
	1	637	3376	3704	SSD	Dry
	3	2462	3687	3902	226	222
	6	3376	3791	3980	Slant-Shear Bond Str. (psi)	
	24	3704	3960	4124	SSD	Dry
Optimal Environment: This patching material is best used at 73 °F on a low restraint substrate with surface preparation. This RSPM provides an elevated compressive strength at lower temperatures compared to other RSPMs.					1078	1030
					Dynamic Elastic Modulus	
					3.55*10 <sup>6</sup> psi	
					Dynamic Shear Modulus	
Potential Concerns:					1.53*10 <sup>6</sup> psi	
					Poisson's Ratio (-)	
					0.16	
					Specific Gravity (-)	
					2.15	

Table A-10: CSA-2 Summary Sheet

CSA-2						
Compressive Strength (psi)	Time (Days)	50°F	73°F	104°F	Shrinkage Ring (73°F)	
	0.25	6729	5347	3009	Crack Time (Days)	Strain Rate (in/in/day)
	0.50	7716	5916	3149		
	1	8974	7805	5219	>28	3.2
	3	9739	9855	6785	COTE (in/in/°F)	
	7	10275	10383	7823	6.9*10 <sup>-7</sup>	
Setting Time (min)	Initial Set (min)	18	3	1	Electrical Resistivity (kΩ*cm)	
					Bulk	Surface
	Final Set (min)	25	5	7	18.2	20.1
	Initial – Final (min)	6	3	6	Chloride Migration Coefficient (m <sup>2</sup> /s)	
					4.1*10 <sup>-10</sup>	
UPV (m/s)	Time (hrs.)				Pull-off Bond Strength (psi)	
	1	1942	3604	3019	SSD	Dry
	3	2540	3960	3175	389	431
	6	2797	4040	3226	Slant-Shear Bond Str. (psi)	
	24	3704	4167	3333	SSD	Dry
Optimal Environment: This patching material is best used at 50°F and is suitable for restrained substrates. This RSPM provides an elevated compressive strength at lower temperatures relative to other RSPMs.					4063	4847
					Dynamic Elastic Modulus	
					5.66*10 <sup>6</sup> psi	
					Dynamic Shear Modulus	
Potential Concerns: <ul style="list-style-type: none"> <li>Significantly accelerated setting time at high temperatures</li> </ul>					2.31*10 <sup>6</sup> psi	
					Poisson's Ratio (-)	
					0.23	
					Specific Gravity (-)	
					2.25	

Table A-11: MgO-1 Summary Sheet

MgO-1						
Compressive Strength (psi)	Time (Days)	50°F	73°F	104°F	Shrinkage Ring (73°F)	
	0.25	100	800	1538	Crack Time (Days)	Strain Rate (in/in/day)
	0.50	163	1586	4740		
	1	1398	4768	5908	4.25	10.5
	3	5741	6864	7.682	COTE (in/in/°F)	
	7	6881	8308	9104	7.6*10 <sup>-7</sup>	
Setting Time (min)	Initial Set (min)	396	188	96	Electrical Resistivity (kΩ*cm)	
	Final Set (min)	523	193	107	Bulk	Surface
					31.7	33.0
					Chloride Migration Coefficient (m²/s)	
	Initial– Final (min)	127	5	11	2.1*10 <sup>-9</sup>	
UPV (m/s)	Time (hrs.)				Pull-off Bond Strength (psi)	
	1	237	421	552	SSD	Dry
	3	54	751	161	507	342
	6	1019	1446	23	Slant-Shear Bond Str. (psi)	
	24	2353	3721	4145	SSD	Dry
Optimal Environment: This patching material is best used at 73 or 104°F on a low restraint substrate with surface preparation under SSD conditions. This patching material should also receive an extended delay before reopening to traffic to account for the slowed setting and strength gain.					1536	1149
					Dynamic Elastic Modulus	
					4.83*10 <sup>6</sup> psi	
					Dynamic Shear Modulus	
Potential Concerns: <ul style="list-style-type: none"><li>Significantly slower setting time than other RSPMs</li><li>Does not perform well under restrained conditions</li></ul>					2.00*10 <sup>6</sup> psi	
					Poisson’s Ratio (-)	
					0.21	
					Specific Gravity (-)	
					2.14	

## Appendix B: Field Visits

---

The images and subsequent descriptions found below discuss the various field/site visits taken to different districts located in South Carolina. As a part of the project background investigation, bridges in various states of deterioration were observed and analyzed to determine possible causes and rates of deterioration based on the provided background knowledge of the bridge's construction and possible prior repairs. The findings from the field visits are separated based on the seven SCDOT districts.

### *District One – Columbia, SC*

#### **I-77 NB and SB Bridge Deck Repair Job**

Access to an on-going repair and rehabilitation job was granted by the SCDOT for seven different bridges across I-77 NB and SB. Unfortunately, an initial field visit to the various bridges prior to hydro-demolition was not permitted and therefore, initial deterioration inspections were not able to be performed. However, contractors and engineers described the initial conditions of the several bridges as various states of deterioration, such as surface cracking of the prior overlay, failed repair sites and presence of corrosion related damages. During the bridge deck visit, various NDE tests such as surface resistivity measurements were performed to test compatibility of the various substrate and patching materials. Additionally, hydro-timer tests and high-resolution laser texture scans were performed on the various surface preparation methods and unprepped decks to compare the differences in surface profiles. As seen in **Figure B-1**, there are multiple spots on the bridge decks littered with various patching materials with different stages of deterioration. Most of the materials had large differences in surface resistivity values, indicating that there is some difference in the physio-chemical properties of the materials. Additionally, some of the exposed rebar that traveled through these different repair materials, were experiencing various stages of corrosion. This could be a direct result of the incompatibility of the materials used in prior repair jobs.



**(a)**



**(b)**



**(c)**



**(d)**



**(e)**



**(f)**

Figure B-1: The exposed surface of deteriorating patching materials (a) patch 1 (b) patch 2 (c) patch 3 (d) patch 3 (e) patch 5 (f) patch 6



*District Three – Greenville/Spartanburg*  
**US 25N@276 (34°56'50.1"N 82°26'17.7"W)**

The bridge located on US 25N over 276 (**Figure B-2a** and **Figure B-2b**) was in poor condition with large alligator cracking present across the pavement surface and some of the repaired areas. Based upon observations it was theorized that the presence of a structural deficiency or sagging in the middle beams caused the roadway surface and repair deterioration. Based upon the severity of the alligator cracking transmission of chlorides and water to the reinforcing steel is possible allowing for corrosion and further rapid deterioration. Additionally, the thermal differences between the patched area and the roadway surface demonstrate a significant difference between the repair materials and the existing substrate increasing the risk of cracking caused by thermal incompatibility (**Figure B-2c** and **Figure B-2d**).

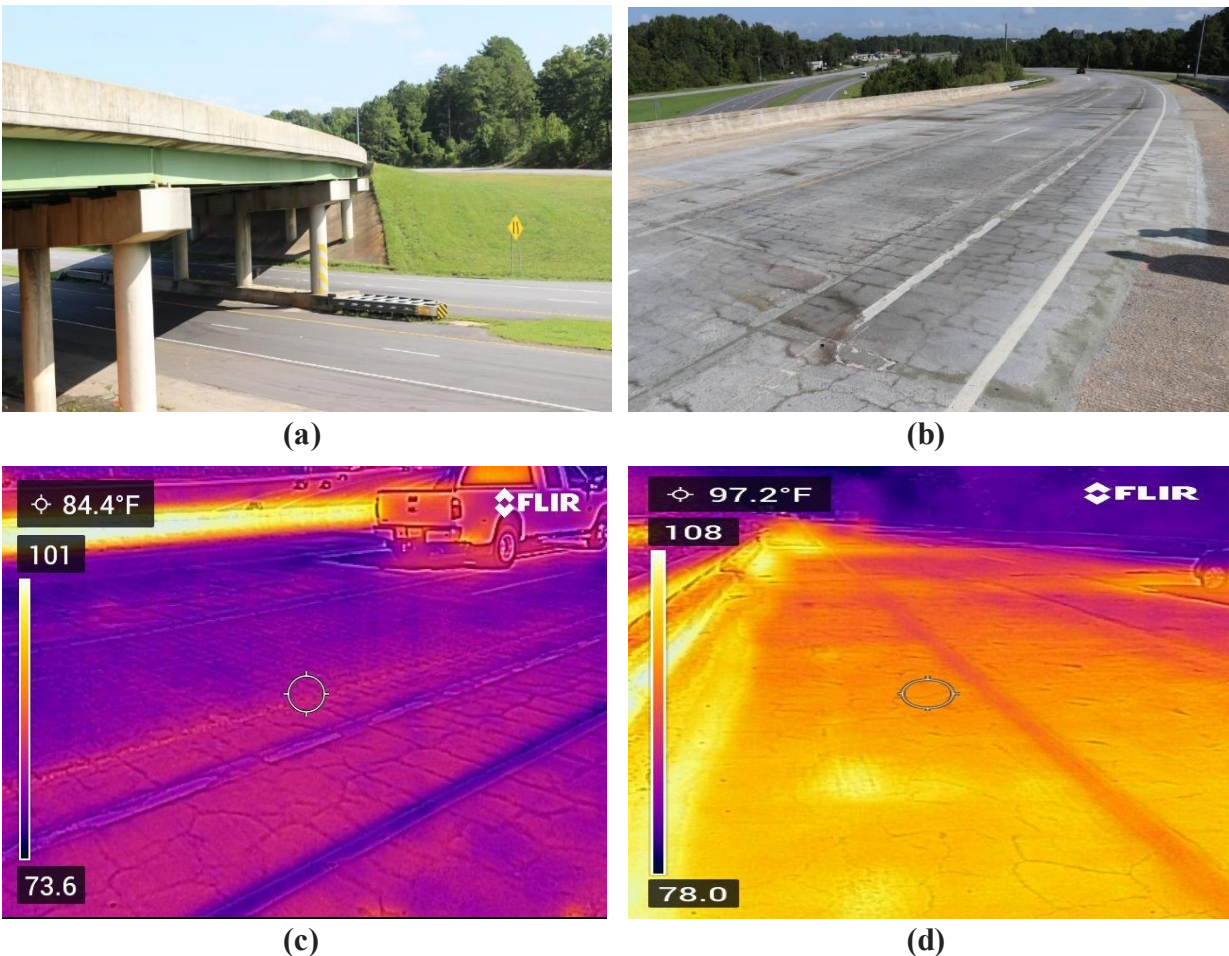


Figure B-2: (a) Bridge Substructure and Supports (b) Bridge Pavement Surface with Alligator Cracking (c) Thermal Gradient of Pavement Surface in the Morning (d) Thermal Gradient of Pavement Surface in the Evening

### **Bryant Road Bridge over I-85 Business (35°00'10.2"N 81°55'32.1"W)**

Observations from the Bryant Road Bridge (Figure B- 3) located over I-85 were almost identical to those found on the US 25N Bridge described previously. However, the severity of the alligator cracking was less than the US 25N Bridge. This may be due to the age difference in the repairs or could be the result of greater compatibility between the RSPM and asphalt surface.



Figure B- 3: Pavement Surface of the Bryant Road Bridge over I-85

### **I-26 over Lake Bowen (35°06'28.0"N 82°04'54.7"W)**

Similar observations were found on I-26 over Lake Bowen (Figure B-4a). Both the substrate and previous repairs had deteriorated substantially with alligator cracking across the patch and subsidence across the most trafficked portions of the patch. Thermal imaging indicated thermal differences across the patch that could have contributed to the deterioration of the patch (Figure B-4b).

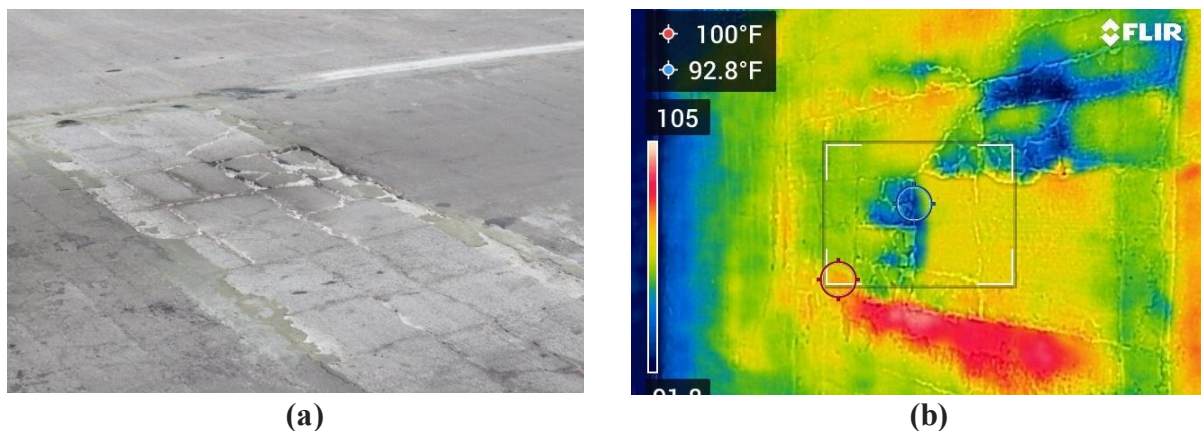


Figure B-4: (a) Deteriorated Patch on I-26 over Lake Bowen (b) Thermal Imaging of Deteriorated Patch on I-26 over Lake Bowen



### FairForest Road Bridge Over I-85 Business (34°58'12.5"N 81°59'56.5"W)

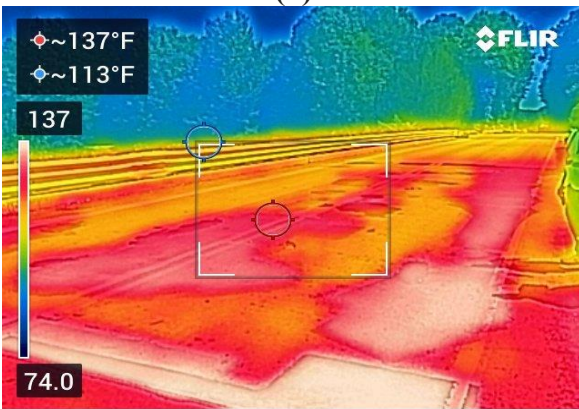
Substantial deterioration and improper patches were observed on FairForest Road bridge in District 3 (**Figure B-5a**). The transition to the bridge deck was predominately covered in small asphalt patches, potentially due to potholes or subsidence. These asphalt patches being irregular shapes increases the potential for debonding and stress concentration (**Figure B-5b**). Thermal imaging showed that the patched areas were 10-20°F warmer than the unpatched areas (**Figure B-5c**). With the combined irregular geometry and temperature gradient there is a high likelihood of thermal incompatibility related distresses in the future. Furthermore, the unpatched areas along the shoulder of the pavement surface showed clear signs of distress with visible corrosion deposits on the surface. This would indicate either chloride intrusion or insufficient cover depth above the rebar.



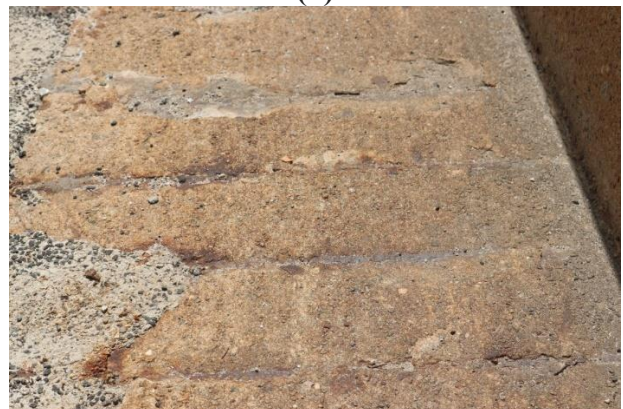
(a)



(b)



(c)



(d)

Figure B-5: (a) Pavement Surface on Fairforest Bridge Road (b) Side Profile of Patching (c) Thermal Imaging of Pavement Surface (d) Deteriorated Shoulder with Corrosion

*District Five – Florence/Myrtle Beach*

**SC 22 over 501sc (33°55'06.5"N 79°09'08.3"W)**

Visits to SC 22 over Highway 501 located in District 5 demonstrated multiple types of failure along the pavement surface. The bridge deck had multiple sections of map cracking and corrosion/reinforcement visible on the surface (**Figure B-6a** and **Figure B-6b**). The deterioration of the substrate could be due to design choices or improper construction. Also present on the pavement surface were several repairs with varying size and repair material. The repairs themselves are in various states of deterioration likely due to incompatibility of the repair and the substrate concrete. **Figure B-6c** displays an incompatible RSPM, as corrosion staining is visible across the surface. This could either be due to the differing resistivity/pH of the patching material and substrate or due to the improper cleaning of the reinforcement allowing corrosion to continue after repair. **Figure B-6d** displays a RSPM that was potentially cast outside of the recommended temperature window or some time after mixing, as the surface appears uneven with cracking and defects along the surface. It is probable that better QA/QC could have resulted in a better patch by either casting early, reducing the temperature of the mix, or selecting a different patching material.

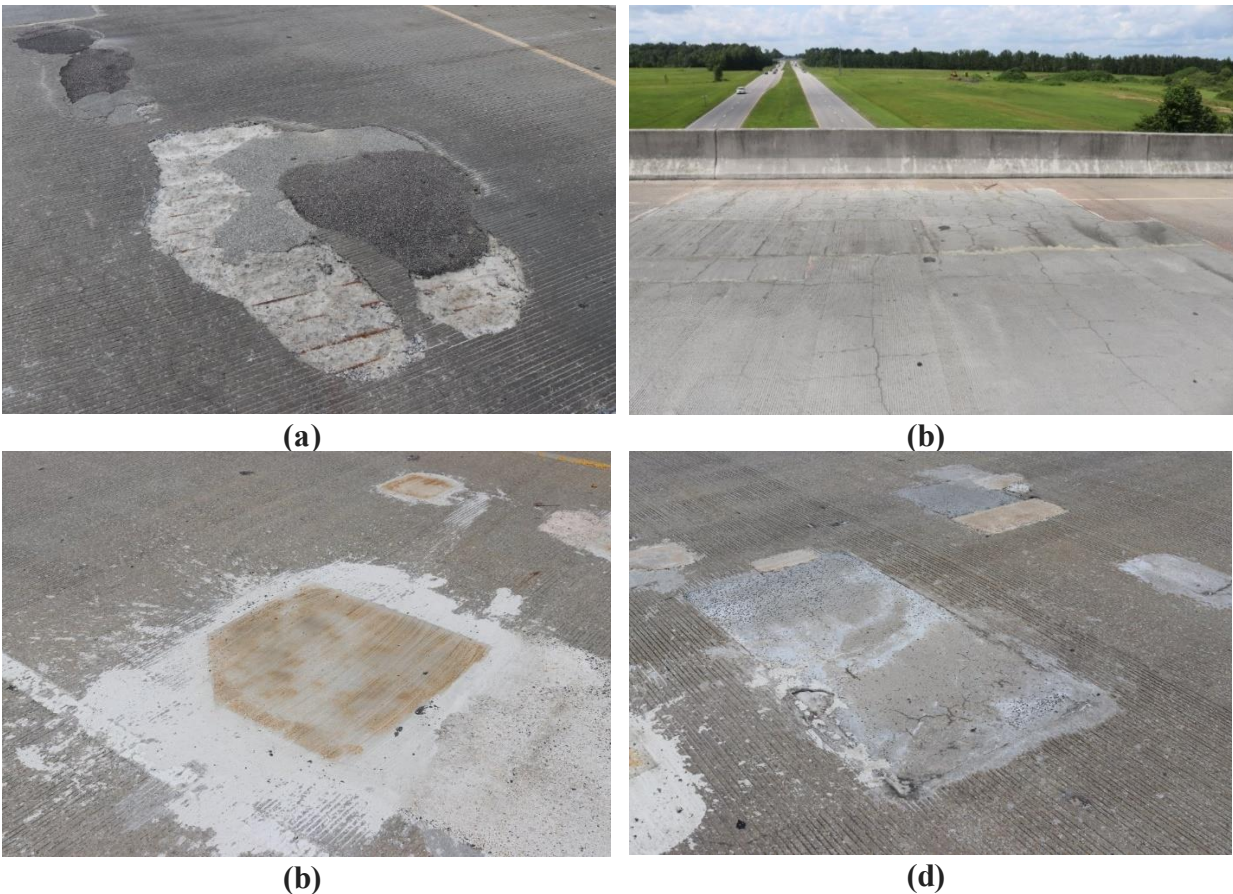


Figure B-6: (a) Patched Pavement Section with Corrosion (b) Alligator Cracking along Patched Area (c) Patched Section with Corrosion Staining (d) Uneven and Cracked Patch



### **I95 South over SC 9 (34°26'33.4"N 79°22'22.5"W)**

The bridge on I95 S over SC 9 had several instances of corrosion present on the deck and around new patches. As seen in **Figure B-7a** and **Figure B-7b**, corrosion products are leaching through the surface of the substrate concrete directly beside a bitumen based asphalt repair material. This was likely due to an improper substrate preparation before patching, where little regard was taken to clean the reinforcement and ensure substrate compatibility performance. **Figure B-7c** shows that the reinforcement is at an insufficient cover depth allowing for the earlier initiation of corrosion, which increases the importance of completing a proper repair. Instruction and training of maintenance personnel could allow for a reduction in patches with insufficient cover depth being filled with improper patching materials.

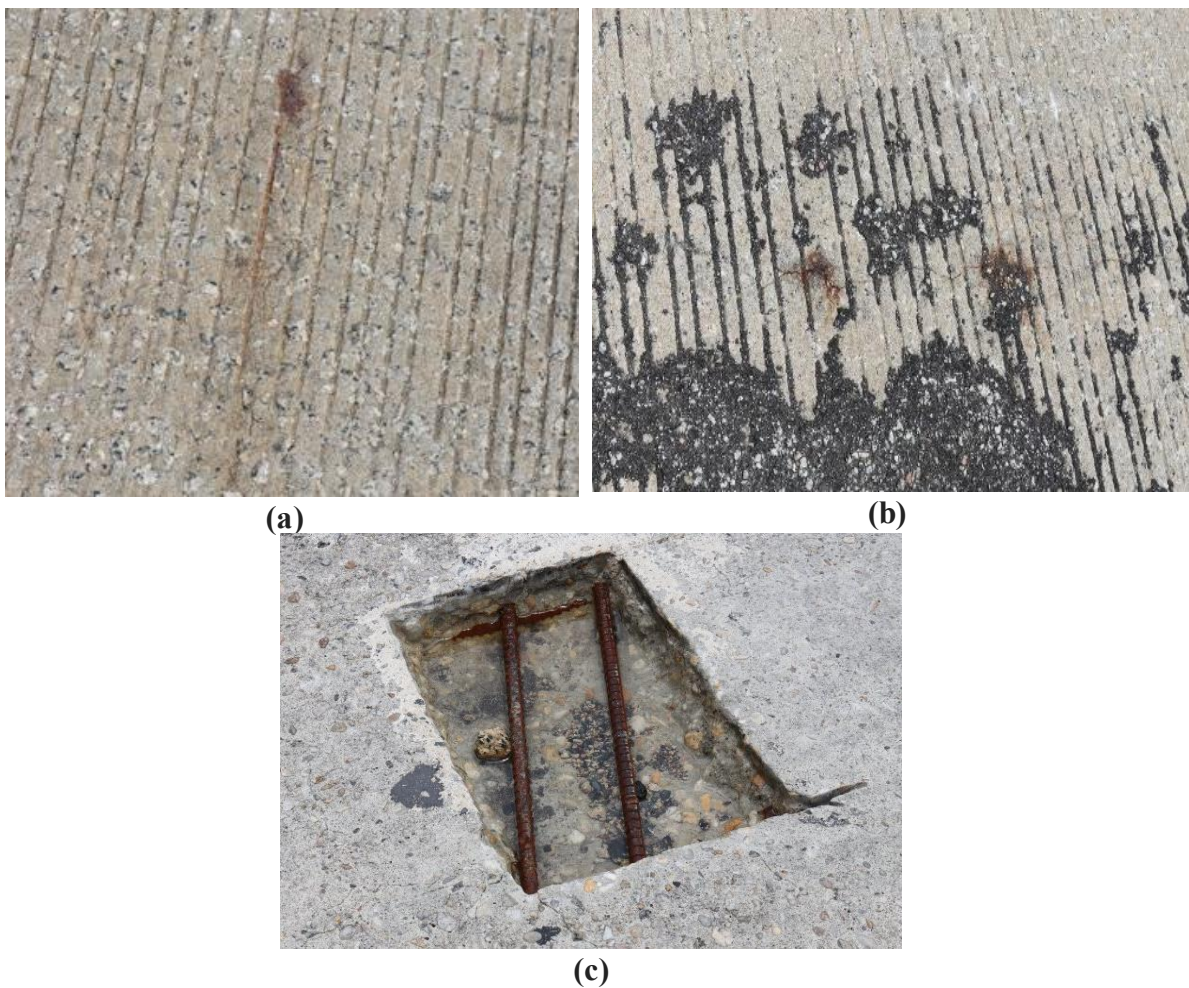


Figure B-7: (a) Corrosion through Pavement Surface (b) Corrosion Adjacent to Patched Section (c) Section to Expose Corroded Rebar

### US 17 over Sampit River (33°22'00.5"N 79°15'56.0"W)

The bridge located on US 17 over Sampit River (**Figure B-8a**), was in fair condition compared to others but had several small repairs. Besides pavement surface cracking, the most concerning observation was several repairs, all in direct contact with one another. Based upon the discoloration present on one of the patches a galvanic corrosion cell (due to RSPM incompatibility) is present corroding the rebar (**Figure B-8b**). Over time this will result in further deterioration and the need for further patching over a larger surface area. To alleviate the galvanic cell a removal of the original patch is necessary and the cleaning of the rebar to reduce the risk of reinitiating corrosion. Maintenance personnel should be cautious when placing a repair directly next to another patch, as it potentially indicates a larger problem.



Figure B-8: (a) Pavement Surface of US 17 over Sampit River (b) Potential RSPM Incompatibility with Subsequent Repairs

# Appendix C: Provisional Specification for Qualifying Cementitious Rapid Set Patching Materials

---

## SUPPLEMENTAL PROVISION

### CEMENTITIOUS RAPID-SET PATCHING MATERIALS FOR BRIDGE DECK REPAIRS

---

#### 1. GENERAL

This supplemental specification outlines the criteria for selecting and utilizing Rapid-Set Cementitious Patching Materials for rapid repairs of hardened Portland cement concrete in bridge decks (i.e., horizontal surfaces). It should be noted that this special provision does not address the needs of repair for overhead patching or vertical members. The rapid-set patching materials considered in this provision shall meet the Standard Specifications for materials designated as R2 and/or R3 per ASTM C928, unless as specified in this document. The rapid set patching materials shall be based on hydrating cementitious-based materials that react with plain water at ambient temperature and can be cured using traditional curing agents. These materials shall be formulated to deliver high early-age strength, long-term durability, and be compatible with existing concrete substrates to not cause any distress such as mass loss, cracking or delamination, due to dissimilar shrinkage behavior, dissimilar modulus of elasticity and/or coefficient of thermal expansion. This provision serves to augment the requirements for rapid set patching materials per ASTM C928 and standard specifications for bridge deck repair practices such as achieving adequate surface preparation in terms of minimum patch depth, minimum surface roughness and sufficient moisture saturation of the substrate concrete.

#### 2. MATERIAL REQUIREMENTS

All rapid-set patching materials must meet the following criteria:

- **Composition:** The primary component of the rapid-set patching materials shall be based on one of the active binder systems, such as Portland cement, Portland Limestone cement, calcium sulfo-aluminate cement and calcium aluminate cement. These binders could be used with or without other chemical admixtures to control the workability (flow), setting, shrinkage, and compressive strength of these mixtures. Combinations of active binder materials are also allowed as long

as the necessary fresh and hardened properties are met. The properties of the materials listed below are based on extended mixtures, unless otherwise indicated.

- **Compressive Strength (AASHTO T22):** The rapid-set patching materials designated as R2 shall meet a minimum compressive strength of **1, 000 psi (6.89 MPa)** at 3 hours, **3,000 psi (21 MPa)** at 1 day and **4000 psi (28 MPa)** at 7 days. Patching materials designated as R3 shall meet a minimum compressive strength of **3, 000 psi (21 MPa)** at 3 hours, **5,000 psi (35 MPa)** at 1 day.
- **Bond Strength (ASTM C1583):** The bond strength of the rapid set patching materials with a substrate concrete shall be determined using the direct tension (pull-off) test method per ASTM C1583. The pull-off bond strength shall be conducted on a representative substrate concrete section with a similar surface texture/roughness as required in the field. The surface roughness of the substrate concrete shall be equivalent to the roughness as represented by a Concrete Surface Profile scale of CSP 5-6 per the ICRI guidance. A **minimum pull-off bond strength of 250 psi (1.72 MPa)** at 28 days shall be considered meeting the requirement. Bond strength as measured by the slant shear bond strength test per ASTM C882, is not recommended, due to variability in the test results and the sensitivity of test method to conditioning of the substrate concrete in terms of surface roughness and moisture condition.
- **Shrinkage (AASHTO T160):** Relative to the initial length of the test specimen at 3 hours, the percent change in length shall not be more than 0.05% when continuously dried in a 50% relative humidity air.
- **Freeze-Thaw Durability (AASHTO T161):** The rapid set patching materials shall achieve a minimum durability factor of 90% based on dynamic modulus of elasticity when tested in accordance with **Procedure A** in **AASHTO T161** test for 300 freeze-thaw cycles.
- **Total Chloride Content (AASHTO T260):** The total chloride content of rapid set patching materials shall not exceed 0.60 lb./yd<sup>3</sup> (~0.40 kg/m<sup>3</sup>).
- **Chloride Ion Diffusion Coefficient (ASTM C1556):** The apparent chloride ion diffusion coefficient of rapid set patching materials cured for 28 days shall not exceed  $5 \times 10^{-12}$  m/s.
- **Electrical Surface Resistivity of Concrete (AASHTO T358):** The electrical surface resistivity of rapid set patching material cured for 28-days in a saturated condition shall not be less than 30 kΩ-cm when tested according to AASHTO T358.



- **Workability (ASTM C1437):** Materials designated as R2 and R3 shall achieve and maintain a flow of 100% (mortars) and a slump of 3 inches (concrete) at 15 minutes after mixing with water.
- **Setting Time (AASHTO T131, ASTM C403):** The minimum initial setting time of rapid set patching materials (AASHTO T131 for neat pastes and ASTM C403 for extended mixtures) shall be 15 minutes at 73°F ± 2°F. When the anticipated temperature in the field deviates from the 73°F ± 2°F, the temperature of the rapid set patching mixture shall be suitably adjusted using the provisions in ACI 305 (Guide to Hot Weather Concreting) or ACI 306 (Guide to Cold Weather Concreting) to maintain between 70°F and 80°F. The temperature of the substrate should be reasonably maintained to match the temperature of the repair material.

### 3. SURFACE PREPARATION

Prior to placement of the patching material, the bridge deck surface must be:

- **Clean and free** of loose debris, dust, oil, and contaminants.
- **Saturated Surface Dry (SSD)**, unless otherwise specified by the manufacturer.
- **Mechanically prepared** using hydro-demolition, scarification, or shot-blasting techniques to ensure proper bonding. The surface roughness shall meet the Concrete Surface Profile rating of CSP 5-6, per the ICRI guidelines.
- **Thickness** of the repair material to be placed in the partial depth repair section shall be no less than 1.5 inches. The maximum size of extender aggregate used in the rapid set patching material shall be no more than 1/3<sup>rd</sup> of the thickness of the patching depth.

### 4. MIXING AND PLACEMENT

- Mix per **manufacturer's instructions** ensuring uniform consistency.
- Maintain and document **recommended water-to-cement ratio** for the inspector to verify and approve..
- Place material within the **specified working time** to maintain optimal adhesion.
- Ensure proper **curing methods** (e.g., wet curing, curing compounds) to achieve maximum strength gain.

### 5. CURING AND QUALITY CONTROL

- Use appropriate **curing methods** to prevent premature drying and cracking.

- Conduct **quality control tests** for compressive strength, bond strength, and shrinkage compliance.
- Follow **manufacturer's guidelines** and standard testing procedures to ensure compliance.

## **6. ACCEPTANCE AND FINAL INSPECTION**

- All repairs must undergo visual and structural inspection prior to final acceptance.
- The patched areas shall exhibit **uniform texture, bond integrity, and no visible cracking**, and shall maintain a gray color as close as possible to the color of the substrate concrete.
- Final approval shall be based on compliance with **compressive strength, bond performance, and durability criteria**.